Spring 5-22-2020

Modeling of Distributary Channels Formed by a Large Sediment Diversion in Broken Marshland

Dylan Blaskey
University of New Orleans, New Orleans, djblaske@uno.edu

Modeling of Distributary Channels Formed by a Large Sediment Diversion in Broken Marshland

A Thesis

Submitted to the Graduate Faculty of the
University of New Orleans
in partial fulfillment of the
requirements for the degree of

Master of Science
in
Engineering
Civil and Environmental Engineering

by

Dylan Blaskey

B.S. University of Minnesota, 2015

May, 2020

Acknowledgements

I would like to thank Dr. John Alex McCorquodale for the constant guidance as we worked through the many difficulties that occur during a master's program. Your continued support and incredible patience has taught me so much about the field of engineering and the process of researching. None of this would be possible without you.

In addition, I would like to extend my gratitude to Dr. Malay Ghose Hajra for guiding me through the process of being a master student and always checking in with me to make sure I was on track. I really appreciate you accommodating me when I was trying to finish my research quickly and then working on a plan to extend my timeline as my life circumstances changed.

Finally, I would like to thank Dr. Ioannis Georgiou for asking me the tough questions when I was developing the model and making me think critically about the results. I still remember you telling me to fully understand my results before you start to draw conclusion. This is a lesson I learned the hard way but it will be with me as I continue on as a researcher.

Table of Contents

List of Figures

List of Tables

List of Acronyms

BWW	Barataria Waterway
CPRA	Coastal Protection and Restoration Authority
ESLR	Eustatic Sea Level Rise
GIWW	Gulf Intracoastal Waterway
NAVD88	North American Vertical Datum 1988
NCDC	National Climatic Data Center
NOAA	National Oceanic and Atmospheric Administration
RM	River Mile
RMSE	Root Mean Square Error
RSLR	Relative Sea Level Rise
SLR	Sea Level Rise
TWIG	The Water Institute of the Gulf
USACE	United States Army Corps of Engineers
USGS	United States Geological Survey
UTM	Universal Transverse Mercator

Abstract

A 2-D DELFT3D model was developed to address the morphological response of Barataria Bay, the sediment deposition rate in the receiving basin, and the impact on the existing distributary channels within the broken marsh system due to the proposed Mid-Barataria Sediment Diversion. The model had a mesh size sufficient to accurately represent the development of the distributary channels, localized flooding, erosion, and salinity in the basin. The model predicts that the receiving basin will experience extensive erosion during the first year the diversion is open creating three major distributary pathways which flood much of the basin in freshwater. Most locations experience peak flood stage when the diversion reaches its peak capacity after which flood stage tends to decrease. The area of open water near the diversion opening will experience higher suspended sediment concentrations than those in the diversion due to the erosion of the receiving basin.

Keywords: Mid-Barataria Sediment Diversion, hydrodynamic modeling, distributary channel formation, marsh flooding

Chapter 1: Introduction

1.1 Introduction

Deltas across the world are some of the most sensitive features on the planet due to the large populations, vast agricultural resources, and their proximity to the sea. They rely on a constant inflow of sediment to maintain their elevation to counteract sea level rise, storm surge and wave attack, salt water intrusion, and human activities that erode them. Sea level rise is accelerating and is expected to eliminate 22% of the world's coastal wetlands by 2100 (Nicholls et al., 1999) although this varies by region (Michener et al. 1997).

The Mississippi River Delta has a large economic, cultural, and natural value to southern Louisiana and the United States as a whole (Batker et al., 2014). The Lower Mississippi River corridor contains wetlands, bayous, shallow estuaries, and emerged ridges formed through delta progradation during the late Holocene (Coleman et al., 1998) Annual floods developed natural levees and the low marshes surrounding the main channels of the river. Lobe switching carved new channels to the gulf, connected marshes systems to form interwoven deltaic wetlands (Russell, 1936; Russell, 1939; Russell, 1940; Fisk 1944; Kolb and Van Lopik, 1966). The delta is characterized as sediment supply dominated with low wave and tidal energy (Roberts, 1997)

Prior to the 20th century long term land loss was balanced with the land building driven by the Mississippi River (Frazier, 1967; Penland et al., 1988; Paola et al. 2011). Since then, the human impact on these areas accelerated through increasing fertilizer usage, dams and levees, deforestation, and other land use changes (Bianchi and Allison, 2009). Whereas soil erosion rates have been accelerating due to human activities, the amount of water and sediment penetrating these areas has decreased (Syvitski, Kettner, Correggiari, & Nelson, 2005; Vörösmarty & Meybeck, 2004).

Coastal Louisiana is experiencing some of the highest rates of wetlands loss on earth (Gagliano et al., 1981; Day et al., 2000). The causes of these losses are vest including subsidence, saltwater intrusion, sediment toxicity, artificial channel cutting leading to expansion, pond creation, urbanization, and oil and gas withdrawal (Britsch and Kemp, 1990; Penland et al., 2005; Turner, 1997; Day et al., 2000, 2007; Reed, 2002; Morton et al., 2003, 2006; Barras, 2006). These are continually eroding the coastline while hurricanes are periodic events in the geologic record that account for significant wetland loss. Hurricane Katrina and Rita in 2005 destroyed a combined 562 km2 of land in South Louisiana; (Barras, 2006). Due to these numerous factors, more than 1800 square miles of land has been lost to the Gulf of Mexico since the 1930s (Couvillion et al., 2017).

The wetlands of Louisiana are built of layers of uncompact peat and mud due to the yearly floods. Over time, the peat at the lower depths are dewatered and compacted by the weight of the overlaying soil (Morton et al., 2002). Vertical accretion of both mineral sediment and organic matter must be sufficient to offset this subsidence and sea level rise for these wetlands to survive (Mossa and Roberts, 1990; Conner et al., 1997; Simas et al., 2001; Van Wijnen and Bakker, 2001; Lane et al., 2006; Paola et al., 2011; Delaune et al., 1983; Nyman et al., 1990; Cahoon and

Reed, 1995). Mineral deposits come from suspended sediment particles composed mainly of clay and silt which are trapped during high flow events. When the flow is slowed by bed friction and above ground structures (stems, trunks, pneumatophores, burrows, etc.) the particles flocculate and settle out (Wolanski and Gibbs, 1995; Young and Harvey, 1996). Without the addition of sediment from the Mississippi River, these wetlands become sediment starved (Baumann et al., 1984; Boesch et al., 1994; Penland and Ramsey, 1990) and not able to outpace relative sea level rise (Blum and Roberts, 2009) 80% of which is subsidence (Dokka, 2006). As the sea rises, the marshes become inundated allowing salt water to penetrate further into the back basin (DeLaune and White 2012). This is a positive feedback loop that is accelerating wetland loss.

Climate change will bring increases in precipitation amount and intensity, rates of sea level rise, and frequency of hurricanes inundating more of these coastal wetlands. In coastal Louisiana, sea level rise will be a major factor in wetland survivability (Simas et al., 2001; Van Wijnen and Bakker, 2001; Day et al., 2008). Accelerated eustatic sea level rise, which is estimated by the IPCC to be between 40 to 120 cm by 2100 (IPPC, 2013; Horton et al, 2014), will lead to longer inundation periods, increase erosion and saltwater intrusions affecting the proliferation of vegetation leading to wetland loss (Day et al., 2005; Blankespoor et al., 2012). Hurricane intensity is expected to increase due to increased sea surface temperature (Mendelsohn et al. 2012; Donnelly et al. 2015; Knutson et al. 2010). However, there are still limitations in scientific understanding of the divers of hurricane frequency and intensity (Zwiers et al. 2013), so specific increases are hard to predict and model. It is unknown whether coastal wetlands will be able to survive more frequent and severe storms (Michener et al. 1997, Day et al. 2008, Knutson et al. 2010, Leonardi et al. 2016).

Many of the solutions to these problems focus on moving sediment from the Mississippi River into the coastal marshland. However, human interventions, such as dams and bank protection, around the river basin have reduced the sediment load of the lower Mississippi by more than 50% (Kesel, 1988; Meade and Moody, 2010; Horowitz, 2010). In the delta, long, interconnected levee systems put in place after the great flood of 1927 to protect New Orleans and the surrounding populations have prevented the river from overflowing its banks and replenishing the sediment in the surrounding marshes (Baumann et al., 1984; Walker et al., 1987). This annual flooding would also resupply the marshes with fresh water preventing saltwater intrusion (Walker et al., 1987; Boesch et al., 1994; Day et al., 2000). Other causes of water and sediment loss include dredging for navigational channels, removal of water for industrial and agricultural use, and flood protection outflows like the Bonnet Carré Spillway, which has a maximum design capacity of 250,000 cfs, and an overflow weir near Bohemia at river mile 38.6.

This study focuses on Barataria Basin which is nestled between the Mississippi and the Atchafalaya River. The Atchafalaya River has been known as a distributary channel of the Mississippi River since as early as the 1500s (Fisk, 1952). The river steadily increased its volume during the first half of the 20th century and would have captured the entire discharge of the Mississippi River if not for the Old River Control Structure. This was built in 1963 and was updated after a high flood in 1973 damaged the structure. To this day, the structure allows 30% of the flow of the Mississippi River to enter the Atchafalaya River, which is further supplied by the Red River creating a flow that is fairly equal to the Mississippi River (Roberts, 1998)

Today, Barataria Basin loses around 1300 acres of coastal wetlands each year (Couvillion et al., 2017) leaving Plaquemines and Lafourche Parish even more susceptible to storms. Yet, over 100 million tons of sediment pass down the Mississippi River adjacent to the Barataria Basin each year (Allison et al., 2012). To combat this problem, the State of Louisiana has planned a sediment diversion into the basin (CPRA, 2017). A sediment diversion is a control structure built through the levees of the Mississippi River to allow the river water, sediment, and nutrients to flow into the broken distributary channels remaining in the wetlands. These diversions are anticipated reduce the rate of land loss and possibly build land, restore freshwater habitats, and improve the overall health of the Gulf (Paola et al., 2011; Gagliano et al., 1970; Kim et al., 2009; Gagliano et al., 1973).

A sediment diversion reintroduces sediment rich river water into the wetland by maximizing the sediment to water ratio in the diversion (Meselhe et al., 2012) and retaining this sediment in the receiving area by mimicking the natural effects of crevasse splay, which is an integral part in the evolution of deltas (Snedden et al., 2007; Day et al., 2009, 2012; Kim et al., 2009; Allison and Meselhe, 2010; Paola et al., 2011; Meselhe et al., 2012; Wang et al., 2014). Increasing the sediment ratio particularly of sand and coarse silt is controlled by the angular orientation and elevation at the intake of the diversion (Gaweesh and Meselhe, 2016; Yuill et al., 2016) and the proximity to bank margin lateral or point bars. These are significant sources of bed load material (Ramirez and Allison, 2013; Allison et al., 2014). Sediment capture in the receiving basin is a function of concentration, grain size, and flow. Coarse sediment, such as sand, is easier to capture in the receiving area due to its faster settling velocities and resistance to resuspension. Sand has limited consolidation and forms a substrate allowing for initial subaerial emergence. Once these are established with vegetation, silts become important for sustaining them through vertical accretion (Peyronnin et al., 2017). The orientation of these sediment accretions help to develop splay island channels by resisting local flow and shielding existing wetlands from waves (Wellner et al., 2005; Esposito et al., 2013). Inundation of saline marshes will account for about 40% of future land loss but 10% comes from salt water intrusion (Reed et al., 2019). Both freshwater and sediment diversion establish salinity gradients acceptable for sustaining fish species, maintain wetlands stability, and reducing hypoxia in the Gulf of Mexico (Day et al., 1997, 2009; LaPeyre et al., 2009; Rivera-Monroy et al., 2013; White et al., 2019).

Sediment diversions are critical to restoring the Louisiana Coastline (DeLaune et al., 2003; Lane et al., 2006; Day et al., 2009; Allison and Meselhe, 2010; Paola et al., 2011; Meselhe et al., 2012; Teal et al., 2012), so the CPRA is planning to build two along the Mississippi River: Mid-Barataria and Mid-Brenton. Together these will cost over $2.2 billion to help accomplish the ambitious goals set forward in Louisiana's Coastal Master Plan, which aims to create 800 square miles of land over the next 50 years (CPRA, 2012; CPRA, 2017). The Mid-Barataria Diversion will be constructed just north of Myrtle Gove, LA at river mile 60.7 with a flow of approximately 2100 m^3/s (Meselhe et al., 2012). The location of the diversion is placed just below a sandbar in the river to maximize sediment being transported through the diversion. The first of its kind project has been planned for decades which has allowed plenty of time for it to be modeled but construction is still a few years off (CPRA, 2012; CPRA, 2017; Meselhe et al., 2012) so there is no hard data yet. While there are currently no large scale sediment diversions to base the Mid Barataria Diversion models, there are numerous other diversions of the Mississippi

River that provide a scientific basis for modeling this diversion (CPRA, 2017; Peyronnin et al., 2017).

1.2 Caernarvon and Davis Pond

Caernarvon and Davis Pond are freshwater diversions on the Mississippi River intended to reduce salt water intrusion in the receiving basins. Caernarvon is a gated structure that allows a maximum flow of 8000 cfs into the Brenton Estuary since it began operation in 1991 (Allison and Meselhe, 2010). It is a box culvert with five vertical lift gates that adjust the flow based on the Mississippi River discharge. A minimum river stage of 4 ft is needed to operate the diversion. On average the diversion has a flow of 1200 cfs and is open 60% of the year (CPRA, 2003). The goal of the diversion is to keep the average salinity at 15 ppt near Stone Island by operating the diversion December through May with a minimum flow of 500 cfs and a maximum of 7500 cfs (CPRA, 2020). Most of the flow (one half to two third) from the diversion travels east and south to Lake Leary while the rest travels to Oak River (DNR, 1991; USACOE, 1993).

The Caernarvon Diversion was built on a historic crevasse that opened up in the early 1900s and was active during the Great Flood of 1927. This provided the first data of what a diversion like this would do. Deposition during this event was at least 22 mm/month, with a capture efficiency of 55% to 75% of suspended sediment concentrations that flowed in from the river. This crevasse deposition event shows how sediment and freshwater capture efficiencies can be enhanced through pulsed flooding (Day et al., 2016).

The modern day diversion, however, was designed to introduce freshwater and were not designed to maximize sediment capture, yet they have still built land. Soil accumulation is a byproduct of this diversion and not the main goal. The Caernarvon Diversion has built 700 acres of new land and developed a sizable subdelta in and around Big Mar Pond (Baker et al., 2011, Lopez et al., 2014b). Sediment availability differs throughout the year. The TSS of water entering the Brenton Sound through the diversion ranged from 40 to 252 mg/L, with the lowest concentrations occurring in the summer and fall and the highest concentrations during the winter and spring. This sediment reached 10-15 km into the sound (Lane, 2007). This land building takes time. From 1992 to 2005, Caernarvon had almost no land change before and after the diversion opening. Then Hurricane Katrina came and dramatically reduced the land cover in the receiving basin (Turner, 2019). Vegetation coverage around Caernarvon declined by 142 km^2 or about 33% following the hurricane and the marshland near the outlets of the diversion lost more vegetation than further away (Kearney, 2011). Some studies show that nutrient influx from the diversion leads to more erodible soils which contributed to the large land loss after Hurricane Katrina (Howes et al., 2010). In fact, six major hurricanes have affected Louisiana since the opening of Caernarvon and the land has recovered from all of them but possibly not because of the diversion. Turner (2019) found that no significant land changes between the diversion opening and 2010 as compared to a control marsh.

Davis Pond showed similar results. Davis Pond Diversion is located at river mile 118 above Head of Passes on the west bank of the river that has been operational since 2002. The diversion is made up of four gated reinforced concrete 14 by 14 ft culverts with inflow and outflow channels and a 570 cfs pumping station that has a maximum capacity of 10,670 cfs. The goal of the project is to preserve 33,000 acres of wetlands and benefit 777,000 acres of marshes over its

50 year lifespan (Allison and Meselhe, 2010; Das et al., 2012). However, there was no significant changes in land before and after the diversion was opened with a slight decrease of land in the flow path (Turner, 2019). DeLaune et al. (2013) researched the marsh soil accretion at 12 locations around the northern Barataria Basin in both fresh and brackish marshes. He found that soil accretion ranged from ranged from 0.59 to 1.03 cm/yr. This vast majority of this accumulation was organic matter rather than mineral soil. This organic matter had void ratios over 0.9. He determined that this type of soil was more fragile than a mineral based marsh soil when subjected to saltwater intrusion and storm surge, but accretion of this material is helping to slow down and in some areas prevent the drowning the northern Barataria Basin which is experiencing a local subsidence of 1 cm/yr. This is consistent with the findings of Nyman et al., (1993) and Turner et al., (2000) that found vertical accretion is correlated with in situ organic accumulation.

Yet a lot of sediment is making it into the receiving basin. During a period from November 2014 to April 2015, the time of highest discharge through the diversion that year, Davis Pond received over 100,000 metric tons of sediment, 44% of which is retained within the basin. The mean flow velocity during this time was 0.21 m/s. For the summer through fall of 2015, less flood water flowed through the diversion. During this period, 36,000 metric tons of sediment enter the receiving basin and 81% of that is retained due to a mean velocity of only 0.10 m/s. This shows that while the high velocity brought and retained more sediment, the capture efficiently was cut in half. This is likely due to increased turbulence and bed shear stress in higher velocity currents and less capacity for deposition. The retention rate of Davis Pond is one of the highest in the area due to the enclosed geometry of the receiving basin (Keogh et al., 2019). Much of this sediment is building up subaqueous which would not be captured in aerial imagery used by Turner (2019) (Day et al., 2016; Keogh et al., 2019)

Das et al (2012) studied Davis Pond and determined that this diversion has a limited effect on the salinity of the upper and lower estuary. The upper estuary was already influenced heavily by other freshwater sources such as the Inner Coastal Water Way, rainfall and lock exchange flows limiting the effect of the large volume of fresh water from Davis Pond. The lower estuary's salinity levels are controlled by marine processes limiting the effect of the diversion. The central estuary is heavily influenced by Davis Pond causing salinity levels to fluctuate by 10 ppt depending on the flow.

Unlike Davis Pond, Caernarvon does not have a large source of freshwater near it but is a much smaller estuary of $2x10^8$ m^3 compared to $4.7x10^8$ m^3. Lane et al. (2007) found that the diversion was able to keep the upper estuary fresh throughout the year while spring pulses could cause the entire estuary to become fresh for less than a month. Lane also observed that there was a two week lag time between discharge and salinity changes in the lower estuary.

From these findings future diversions should target a moderate water discharge and flow velocities to maximize sediment deposition and retention, while adding enough fresh water to maintain salinity gradients without flooding the wetlands.

1.3 Bohemia Spillway/Mardi Gras Pass

Mardi Gras Pass is located within the Bohemia Spillway at river mile 43.7 on the east descending bank. This pass developed during the Mississippi River flood in 2011 through an overbank flow that developed into channelized flow over the natural levee, which eventually breached creating a new channel. Headwater erosion across a bar stabilized by trees allowed this pass to breach the Mississippi River completely in early 2012. This pass is now freely flowing distributary of the Mississippi River. Mardi Gras Pass is part of the larger Bohemia Spillway which encompasses almost a 12 mile reach of the river and has been active since the Great Flood of 1927 (Lopez et al., 2013). Today, Mardi Gras Pass can be defined as the four channels (two developed and two pre-existing canals) that extend 0.85 miles to the Back Levee Canal. This pass is significant because it is extremely rare for a new distributary channel to form along the Mississippi River due to the extensive levee system. Research on this pass that discharges freshwater, sediment, and nutrients is used to further understanding of our large scale sediment diversions but is still limited.

Basin wide understanding of the effects of Mardi Gras Pass is hard to determine. The pass started at approximately 2000 cfs but grew to over 13,000 cfs in capacity in just 5 years however this is still much smaller than the Fort Saint Phillip breach that now has a flow of about 160,000 cfs. What is noticeable is that during the time since Mardi Gras Pass has opened, salinity levels in Breton Sound have decreased. Mardi Gras Pass and the Bohemia spillway also deliver significant fluvial sediment to the receiving basin with annual sediment loads around 0.3 MT per year (Allison et al., 2012). While this loading rate was found over just a couple years, if it were constant since the opening of the Bohemia Spillway then 62% of the annual sediment accumulation in the receiving basin is due to this diversion. Downstream almost 20 MT per year of sediment reaches the Breton Sound through eight additional river outlets. This sediment can be moved higher into the basin through tides, cold fronts, and hurricanes (Smith et al., 2015).

Lopez et al. (2014) found the Bohemia Spillway has infilled some canals and prevented indirect wetland loss due to erosion and sea level rise with the canals. The Bohemia wetlands seem to be more resilient than the ones created by Caernarvon since land loss has been negligible around the spillway when net negative at Caernarvon. This led him to hypothesize that diversions should have high discharges and high sediment concentrations early in their operation followed by lower discharges for maintenance of the created wetlands. Numerous studies have shown that marshes that receive a constant supply of sediment are stable and growing more resilient compared to marshes that are saltier with no river inputs (Amer et al., 2017; Smith et al., 2015). They can accrete 1-5 cm of sediment during a seasonal flood, which offsets relative sea level rise at current rates (Kolker, 2012; Esposito et al., 2013)

1.4 West Bay

In 1839, a crevasse opened on the extreme southern tip of the Mississippi River. During the first century this crevasse was open, West Bay developed 297 km^2 of land but then sea level rise, storms, and reduced sediment deposition lead to land loss exceeding land gain (Wells and Coleman, 1987). By the 1980s, West Bay returned to mainly open water (Barras et al., 2009). In 2003, a two-hundred-yard crevasse cut into the bank on the Mississippi River, at river mile 4.7 above Head of Passes, LA to mimic the natural crevasse that used to be there. It consists of an uncontrolled conveyance channel that has a designed capacity of 50,000 cfs at 50 percent

duration stage of the river. The location was chosen to optimize bed material concentration in the diverted water and the channel was built at a 120 degree angle from downstream to enhance this sediment capture. Originally, the channel was 7.6 m deep but increased to 15.2 m with depths in some areas exceeding 20 m by 2009. This change corresponds to an increase in the cross-sectional area from around 800 m^2 to 1600 m^2. In 2009, an island was constructed in West Bay in order to slow flow into the basin and retain more sediment. This decreased the predicted flow velocities within the base and promoted a backwater effect that reduced sediment transport. Local areas of sediment accumulation and erosion show that the diversion was continuing to evolve during this time (Barras et al., 2009). By 2014, erosion around the diversion stopped indicating that after 10 years of development the diversion finally stabilized (Yuill, 2016). Since then the diversion of uncontrolled discharges ranged from negative flow to 70,000 cfs, averaging around 27,000 cfs (Plitsch, 2017). During high flow this diversion fits Allison and Meselhe's (2010) definition of a "large" diversion.

Initially sediment deposition rates were equal or slightly greater than relative sea level rise but the bay has an average depth of 2-4 m meaning only infilling took place of the first few years and no large areas of new land were created (Andrus, 2007; Plitsch, 2017). Then the marsh began to accumulate sediment at a rate of 3 cm per year which exceeded relative sea level (Kolker et al., 2012). This has caused shoaling in the basin and splay islands have become emergent (USACE, 2012) following the floods of 2011 (Khan et al., 2013).

Sediment for this diversion has distributed over a 13.5 km area with the maximum deposition on the seaward side of the receiving basin. This could be due to the silt deposition downstream instead of closest to the riverbank. However, most sediment is retained in the nearshore zone with a capture efficiency of near 70% (Kolker et al., 2012). Allison (2017) broke this down into different types of sediment retention over two weeks of low Mississippi River discharge. He found that silt retention in the basin was 60% but dropped to 4% by the end of the study while sand retention dropped from 100% to 40%.

This shear strength of this soil was found to be 0.2 Pa (Xu, 2016). Sha (2018) followed up on Xu's experiment and found that critical shear stress for resuspension was dependent on the time since deposition. Two months after deposition the sediment had a critical shear stress of 0.2 Pa but that increased to 0.45 Pa after 4 months of consolidation. They also showed that the enclosed basin with low salinity and minimal disturbances all favor mud deposition and retention. Allison (2017) demonstrated that tides, wind generated currents, and waves also have an effect on sand transport within the bay.

1.5 Wax Lake Delta

The Wax Lake Delta is one of the only areas in Louisiana that is gaining land. In 1942, the Army Corps of Engineers dredged the Wax Lake Outlet to reduce flooding in Morgan City (Latimer and Schweitzer, 1951; Fisk, 1952). This outlet was 40 km long, 8 km wide, 3 m deep channel that connected the Atchafalaya River to Atchafalaya Bay which is exposed to the open waters of the Gulf of Mexico.

At first, all sands were removed in the channel allowing only clay and silt to enter Atchafalaya Bay. As the channel filled with these sandy deposits, a long sandbar developed separating the

Wax Lake Outlet from the Atchafalaya River. By 1973, Grand Lake had filled with deposits which allowed more sand to be transported through the Wax Lake Outlet (Roberts et al., 1980; Tye and Coleman, 1989). This early sand transport built the first subaerially exposed deposits in the Wax Lake Delta (Roberts et al., 1980).

Initial channel development began to occur around 1970 (Roberts et al. 1980). These channels incised into the pre-delta substrate (Roberts et al., 1997; Wellner et al., 2005). Just like the West Bay diversion, over the years the channels in the Wax Lake Delta have gotten deeper and wider. From 1973 to 1999, the channels eroded up to 40% of modern flow depth. From 1991 to 2009, the channels widened by 11%. This forces a downstream migration of islands. During spring floods almost all available grains sizes are transported in suspension. Many of the current channels beds are almost entirely made of consolidated clay covered in alluvial sands, which can be eroded easily by sand rich water scouring the bedrock causing the particles to be entrained (Shaw et al., 2013). Adjustments in these channel networks are important to understand the stability of the distributary networks (Smart and Moruzzi, 1971). Changes in channel width force the migration of channel banks and island shorelines (Johnson et al., 1985; Visser et al., 1998; Viparelli et al., 2011). This causes the islands to migrate laterally downstream (Shaw et al., 2013).

When the flow changes from confined within the channel system and unconfined in the islands much of the flow is lost laterally before reaching the receiving basin (Hiatt and Passalacqua, 2017). Only 25-50% of the flow will reach the island system (Hiatt and Passalacqua, 2015). The variation is driven by vegetation roughness within models and not river flow due to backwater control of the subcritical flow. Vegetation on the islands increases velocities within the channels after significant lateral flow has occurred. Areas upstream of this lateral flow vegetation decreases velocities due to increased water levels and a higher cross-section. The gradient between these channels and islands develops a lateral flow to occur which influences the flow and deposition in the backwater (Hiatt and Passalacqua, 2017).

The splay islands created by this diversion has influenced the sediment retention efficiency of the receiving basin (Roberts, 1998; Shaw and Mohrig, 2014; Shaw et al., 2016). These islands resist local currents to shield inland waters from waves to encourage more deposition and less uptakes (Wellner et al., 2005; Esposito et al., 2013) Travel times through these islands is three times longer than the channels at roughly 4 days. These islands are subject to tides and wind which can cause flow reversal that increases travel time allowing even more deposition to occur (Hiatt and Passalacqua, 2015).

The channels reach 2-6 km beyond the sub-aerial emergent delta with bifurcations into similarly sized bifurcation channels with an average width of 150 m. These distributary channels develop through erosion of the foreset deposit. High river flow and high sand supply aggrade the bed inside and outside the channel. Erosion occurs at the sandy shoals along the sidewalls of the bifurcate channels to create a single primary channel. Low flow causes erosion at the channel tips and the beds of the subaqueous channels leading to a lengthening of the channels towards the bay. This process is mainly driven by tidal cycles that support sand suspension in the channels during the ebb tide. Very little sand is supplied from upstream (Shaw and Morhig, 2014; Shaw et al., 2016)

The delta has gone through multiple bifurcations until the modern delta was formed with five main channels. This transition resulted in a 66% reduction in characteristic flow depth and a 33% reduction in flow velocity. The channels maintain 86% of the flow from the feeder channel with 14% of the flow being lost to shallow overland flow over weakly emergent islands. Characteristic channel depths and velocities remain fairly consistent even with channel widths varying by a factor of two. Velocity is maintained around 0.2 m/s (Buttles et al., 2007)

Today, the delta receives around 30 Mt per year of sediment of which roughly 18% is sand (Kim et al., 2009). The large percentage of sand allows the delta to prograde into the bay at a rate of 270 m/yr with 5 km^2/yr of land built to or above mean sea level between 1980 and 2002 (Parker and Sequeiros, 2006). Composition of this new land is made of 67% sand (Roberts et al., 1997).

The vegetation in the Wax Lake Delta has increased in area and vegetation index (NDVI) from 1984 to 2011. This accounts of major storms like Hurricanes Lili (2002), Katrina and Rita (2005) and Ike (2008) where NDVI decreased significantly due to saltwater intrusion brought on by storm surge but recovered quickly and show an increase over the long term trend. This shows that the freshwater marshes within the delta are becoming more productive as the delta matures and are resilient to coastal storm disturbance (Carle and Sasser, 2016; Couvillion et al., 2017).

In 2011, the large flood of the Mississippi River which pushes more sediment and freshwater into the marsh but has the potential to damage plants. Carle et al. (2015) showed that there was a net growth of 6.5 km^2 of land at mean water level and 4.9 km^2 at mean seal level. Almost 32% of the area accreted during the flood and started to transition to higher-elevation species. Most of this came in the transition from fully submerged aquatic vegetation: 55% remained unchanged while 13% converted to lower vegetation. This is a good model for large scale pulsed river diversions. Bevington and Twilley (2018) found that systems can change rapidly in a matter of months due to large river floods. High levels of organic matter also correlates to high elevation in marshes. This shows that organic matter production and accretion play into an important positive feedback loop in wetland development.

Cold fronts can also play a role in vertical accretion of the marsh outside the sand rich delta. When cold fronts approach the Atchafalaya Bay water levels can elevate up to 1 m reversing discharge into the bay. This causes overbank flow into the coastal plain marshes building these up at over 1 cm per year (Roberts et al., 2015).

1.6 Bonnet Carré Spillway

The Bonnet Carré spillway is an existing gated water diversion of the Mississippi with a capacity of 250,000 cfs used to divert water around the city of New Orleans while the river is in flood stage. It differs from both freshwater and sediment diversions due to its sporadic openings (river flow must exceed 1.25 million cfs before it is opened) and it is not intended to help restore sediment (Only the top 10-15% of the water column is skimmed into the floodway (Nittrouer et al. 2012)) or fresh water to the receiving basin. During the flood of 2011, 10-20% of the river was diverted into the spillway but 31-46% of the total sand load in the Mississippi River was diverted into the spillway. Local river condition and the high flow during the flood led to high concentrations of suspended sand load. This is important in the planning of future diversions.

Meselhe et al. (2016) found that reductions in stream flow caused by large diversion such as the Bonnet Carré Spillway can result in aggradation of sand near the diversion and downstream of it. The quantity of this aggregation depends on the capture efficiency of the diversion and the quantity of the water captured. Invert elevation and the placement of diversions near lateral or point bars and the curvature of the river also play into these deposits. However, silt and clay capture are a function of the river hydrograph and not these other factors.

1.7 Proposed Mid-Barataria Sediment Diversion

The closest resemblance to what the Mid-Barataria will look like is West Bay Diversion and the Wax Lake Outlet (Peyronnin et al., 2017). Both of these are deliver sediment and freshwater to a receiving basin that has depths of 1 to 3 m (Kolker et al., 2012; Shaw and Mohrig, 2014). The difference is that the Mid-Barataria sediment diversion will be located farther upstream. This diversion will be located just north of Ironton on the west bank of the Mississippi River at river mile 61. The diversion will have an invert elevation of -40 ft, a width of 1,600 ft, and the conveyance channel will be 2 miles long. This will be a controlled diversion with a capacity of 75,000 cfs that will be conveyed into the broken marshland and areas of shallow open water (CPRA, 2017). From there it will make its way to Barataria Bay which is only 2 m deep (Wilson et al., 2008). The receiving area does not currently have defined distributary channels to convey the amount of water that will flow through the diversion (Shaw and Mohrig, 2014). This could cause temporary flooding of the marshland posing a risk to local communities until the flow develops these distributary channels (Lopez et al., 2014; Lacey, 1929; Cao and Knight, 2002). These channels could take 5 to 10 years to develop before the flow could operate at full capacity (Lopez et al., 2014).

The vegetation in the receiving basin is already flood stressed (Snedden and Steyer, 2013; Snedden et al., 2015) and could die due to limited adaption time once the diversion is opened this in the short term increasing wetland loss (Snedden et al., 2015; Visser and Sandy, 2009). Fish and wildlife species may be affected as well. These effects could be limited if the operation is completed during the non-growing season for the first few years (Peyronnin et al., 2017). However, the proposal has the diversion opening whenever the river reaches 17000 m^3/s (CPRA, 2012). In recent years, this would have the diversion remaining open into late spring or early summer (USGS, 2019).

Another problem that arises is the flooding at the mouth of the diversion. If it was to operate at full capacity on Day 1, the water could surge through these broken distributaries endangering users and scouring the point where the diversion channel meets the receiving basin (Wellner et al., 2005; Wright, 1977). Erosion of the marsh outside of the distributary channels could occur if velocities are greater than 20-50 cm/s but most of this material will eventually be trapped in the downstream wetlands. A gradual operational strategy of the first 10 years should reduce this erosion (Peyronnin et al., 2017). This will also help to build the emergent land area at the mouth of the diversion, which help with the suspended sediment capture (CPRA, 2017).

Under future climate change scenarios, there will be a possible increase in discharge in the basin. Tao et al. (2014) determined that an additional −100 to +450 km^3/yr of water will flow through the lower Mississippi. But this will not be evenly spread through the season. The spring floods will see increased discharge and then late summer droughts will decrease the flow (Nakaegawa

et al., 2013). Climate change literature predicts an increase in both floods and droughts across the Mississippi River watershed (Tao et al., 2014; Melillo et al., 2014) so future hydrographs are hard to predict (Falloon and Betts, 2006). Peyronnin et al. (2017) suggests that the operation of the sediment diversion should be adjusted to correspond with future river discharge patterns.

1.8 Previous Models of Barataria Basin

Georgiou et al. (2010) developed a multidimensional model to study the Barataria Basin's response to multiple diversion of the Mississippi River. This was accomplished through two different models: A one-dimensional link-node model used for simulations over 20 years, and a higher resolutions FVCOM model for shorter timespans. Both models predict that during high flood years, diversions can increase water levels from 0.4 m in the upper part of the receiving basin to 0.05 m in Barataria Bay. Locally at the diversion water levels were shown to reach more than 1 m if flows were high enough. Both high and low flow diversion scenarios had a significant effect of salinities in the basin. The upper Basin was converted to freshwater lakes and ponds with salinities below 0.5 ppt. Diversions dropped the salinity in the middle of the Basin around Little Lake about 5 ppt but with high variability. The lower part of the Basin also drops around 10 ppt. From the model it was determined that the Basin had three distinct parts. The first part, a region north of the GIWW, is primarily freshwater and receives mostly freshwater runoff. The central region is very dynamic since tide, waves, and the diversions will all act in this area and will be the first to show a response to diversions. The lower region is dominated by the exchange with the Gulf of Mexico making it very dynamic but the diversions have less of an impact here.

The Water Institute developed a similar model in DELFT3D to connect the Barataria Basin and the Mississippi River through the Mid-Barataria Sediment Diversion in a single model. This is a depth average 2D model to reduce computation time since velocity and water levels are the most important factors in sediment transport. This model accounts for scour and the movement of sediment which changes downstream geometry and water surface elevation. Parameters from West Bay Sediment Diversion were used in this model. A spread of 0.1 to 1.0 Pa was used as the critical shear stress that resulted in significant variation in sediment deposition and land building capabilities (Meselhe et al., 2015).

The most recent Louisiana Coastal Master Plan used an Integrated Compartment Model to study this diversion. This is a coast wide mass balance model used for a large number of 50-year simulation. This a large scale model so resolutions of the model is small enough to collect valid sediment transport data making projections at a 30 m by 30 m grid cell resolution of the wetland area (Brown et al., 2017). The settling velocity of these particles were calculated using Stokes' Law. The representative particle diameters for the sand, silt, and clay was determined using existing calibration datasets. A critical shear stress of 0.1 Pa was used for sediment suspension (McCorquodale et al., 2017). Data for riverine inflow was calculated using years from 1964 to 2014 at Tarbert Landing truncating at 1.25 million cfs, since the Bonnet Carré Spillway would divert all flow above that level. Tide data came from across the region with the closest station to the Barataria Basin at Caillou Bay. Gridded wind data was obtained from NCDC's North American Regional Reanalysis. This model was run over 50 years with limited analysis taking place of the developing distributary channels during year one (Brown et al., 2017).

Brown et al. (2017) used an AdH model validated against surface elevation, discharge, and salinity to study the land building capability of the diversion. This model shows that there is net land gain in the near vicinity of the diversion outlets and net land loss farther away from them over the project's 50 year lifespan. This loss occurs where there is significant inundation without substantial sediment deposition. Overall they found that there was no net land gain due to this inundation. However, if the diversion operation was optimized there could be near net zero land change. One limitation of this study was that their vegetation growth model only used one variable to predict growth: inundation depth. The CPRA and Water Institute models have much more complex vegetation models. This model found that water freshens significantly during the diversion operation and when the diversion operation is ceased, recovery depends on prevailing offshore conditions rather than the minimal flow they simulated traveling through the diversion. They did note that salinity levels in Southwestern Barataria Bay were minimally affected by the diversion operation.

On the other hand, Lezina and Barth (2019) found that the Mid-Barataria Sediment Diversion could benefit as much as 47 square miles of land over its 50 year lifespan. This model shows that salinity changes will occur over the lifetime of the project whether or not the diversion is built. Their model assumes a year round 5000 cfs of water. When the river reaches 450,000 cfs at Belle Chasse the diversion gates will open allowing 35,000 cfs of water into the bay. When the flow reaches 1 million cfs the diversion will allow 75,000 cfs into the bay. The model showed that the maximum water height during the diversion's operation will be half a foot at Lafitte and about a food at Grand Bayou. Wilkinson Canal water heights could increase by just under three feet.

1.9 Objectives of the Research

The primary objective of this study was to investigate the evolution of a distributary system when a large sediment laden diversion is introduced into a broken marsh.

A secondary objective is to determine the impacts on flooding throughout the receiving waters of the diversion while the distributary is developing.

1.10 Methodology in General

The following approach will be used to address the primary and secondary objectives:

a) The purposed 75,000 cfs Mid-Barataria Diversion into Barataria Basin will be used as a test case for considering the evolution of a distributary system.

b) The flood risk at the Grand Bayou Community will be used to examine flood risk and flood risk changes during the development of the distributary system.

c) A numerical model will be calibrated to physical observation in the Basin and applied to study the introduction of the large diversion.

d) The impacts will be considered by comparing the 'no diversion' and 'diversion' results for normal and high flood years on the Mississippi River.

Chapter 2: Methods

2.1 Model Selection

Delft3D-FLOW is a multi-dimensional program that calculates unsteady flow based on tidal and hydrological/meteorological forcing over the grid. Delft3D-FLOW is designed to solve the Navier Stokes equations for incompressible flow over a structured grid using appropriate initial and boundary conditions (Deltares, 2011).

The program Delft3D was chosen because it includes the relevant physical process involved in hydrodynamics and morphology of distributary development in the receiving area of a large diversion and meets the following criteria: uses the finite volume method, available to non-commercial researchers, free to registered users, open source code, structured curvilinear grid system, salinity module, wind module, a robust sediment module, a large users group and pre/post processing tools. Multiple studies of Barataria and Breton Basins, Pontchartrain Estuary, Lower Mississippi River and the surrounding coast have used Delft3D (Sadid et al., 2018, Brown et al., 2019; McCorquodale et al., 2017; Amini, 2014). The previous work on this domain was also done in Delft3D so a continuation was beneficial to prevent conversion errors.

2.2 Domain

The model covers the Barataria Basin in southern Louisiana, extending from The Pen in the north to the barrier islands on the southern end, and Bayou Lafourche to the Mississippi River shown in Figure 2.1. This domain was selected to include the Mid-Barataria sediment diversion's entire drainage area. To reduce computational time, the geographic location of Lake Salvador was not included in the bathymetry but its storage was included due to a manipulation of the grid. The Coriolis Effect was set to be the same over the entire grid and is estimated using 29 degrees north latitude.

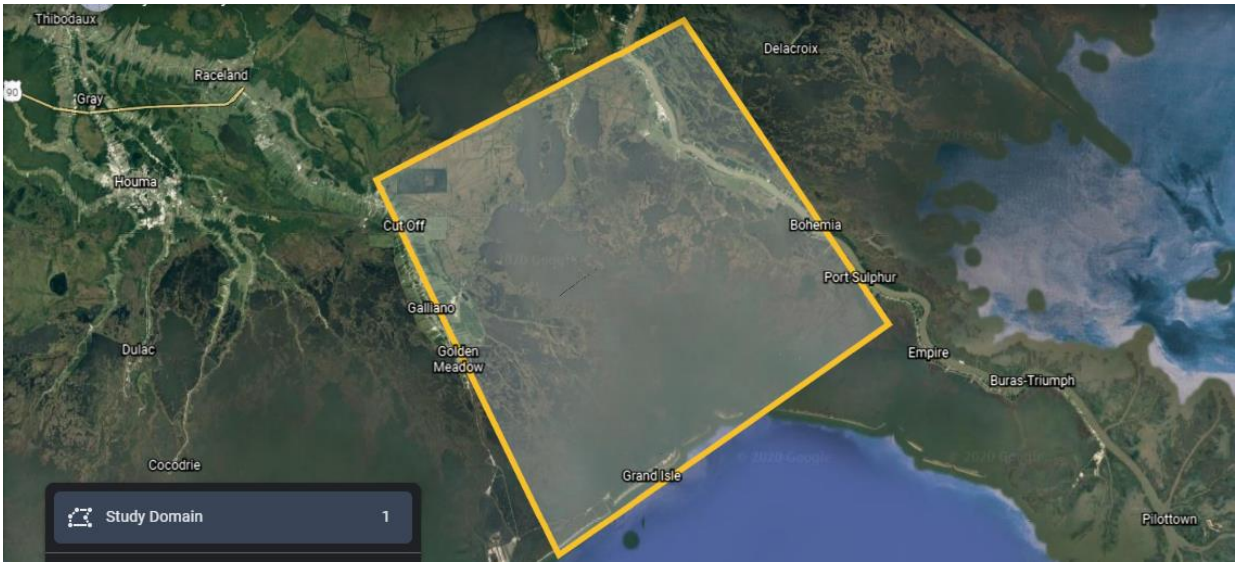

Figure 2.1 Modeling domain of the Barataria Basin excluding Lake Salvador (Google Earth).

2.3 Grid Design

Bathymetric (NOAA/CPRA) data were interpolated onto the grid in Delft3D. The horizontal coordinates are in Universal Trans-Mercator zone 15R in meters, while the vertical coordinate system is in North American Vertical Datum of 1988 (NAVD88) also in meters. A total of 561 longitudinal nodes and 901 lateral nodes were assigned to discretize the domain into a grid. These nodes created 505,461 cells with a maximum size of 10000 m^2 and a minimum size of 400 m^2. A portion of the grid is shown in Figure 2.2. To properly account for some of the changes around the mouth of the diversion and immediately south of it, the smallest mesh was used in this location with cells as small as 400 m^2. After initial calibrations which were not producing adequate results, the top row (northerly portion) of the grid was extended to account for the storage of Lake Salvador without adding additional nodes. The final grid is shown in Figure 2.3. As this is a depth averaged model, only one vertical layer was used.

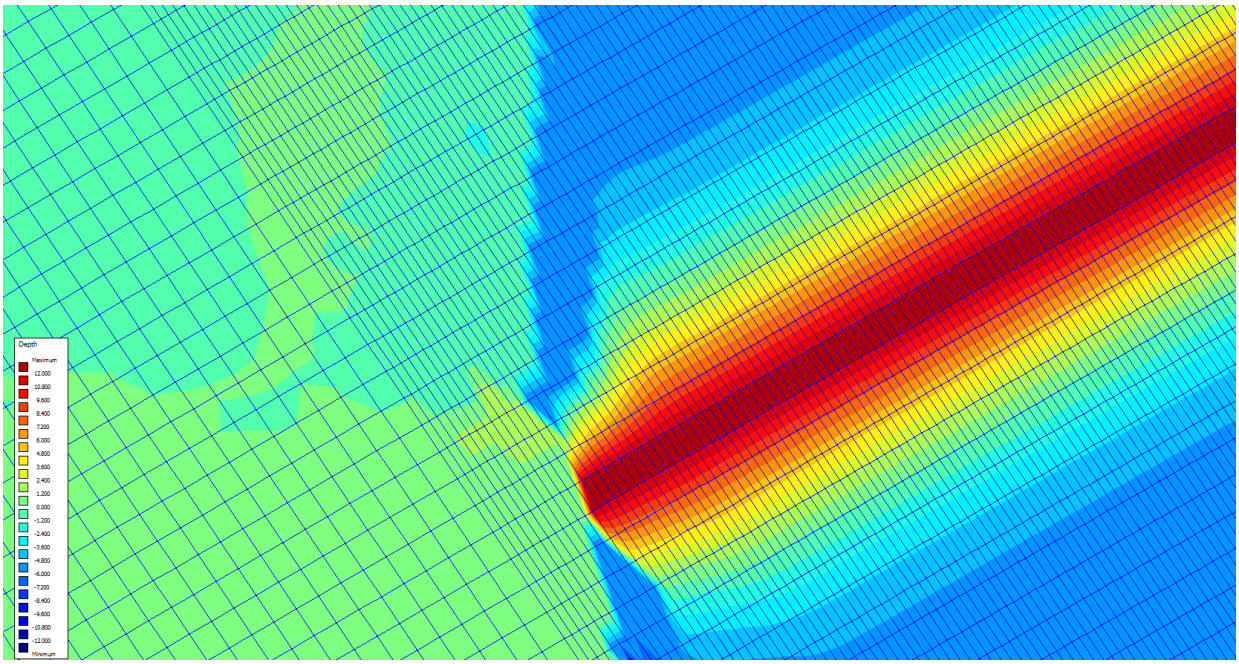

Figure 2.2: The final grid around the sediment diversion with a fine mesh around the mouth to properly account for bathymetric changes.

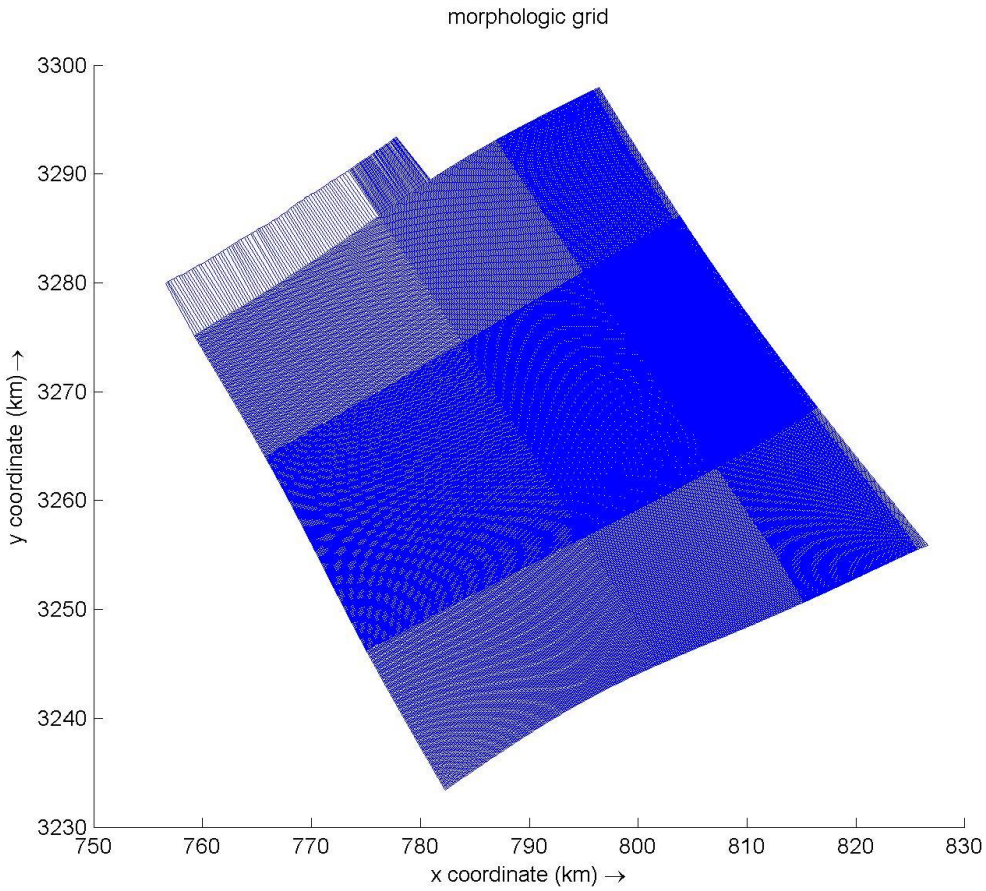

Figure 2.3: The final grid map of the entire Barataria Basin including the extended top row of cells to capture the storage of Lake Salvador.

2.4 Bathymetry

The bathymetry and topography of the basin were taken from the NOAA digital elevation data and supplemented with data collected by CPRA. Dr. Ioannis Georgiou produced the original bathymetry during the initial development of the model. To simplify the topography, the area from the river to the back levee was raised to the height of the levee system to take it out of the hydrodynamic calculations. The diversion was drawn at RM 60.7 following the angle of the grid which is near Myrtle Grove on the Mississippi River. The diversion was assumed to be 12 m deep and 100 m wide which gives a maximum velocity of 1.8 m/s and prevents in-channel deposition. The mouth of the diversion was constructed of a gradual ramp of erodible materials rising from the depth of the diversion to the depth of the receiving basin in 100 m. This allowed the diversion to scour its own path. The bottom of the diversion channel itself was set so no erosion could occur, but sediment could still be deposited and eroded on top of this non-erodible layer. Thin dams were placed on either side of the diversion until it reached the receiving basin to prevent flow moving laterally and erosion of the channel sides from occurring.

Monitoring stations were chosen to get a good coverage of the domain. A total of 21 monitoring stations were set up to track the hydrodynamic and morphologic changes across the grid. Bayou

Perot, Barataria WW, Little Lake Cutoff, Little Lake Dosgris, Hackberry Bay, and Barataria Bay were used as calibration points because the USGS has physical monitoring stations here. A map of the bathymetry and monitoring stations is shown in Figure 2.4.

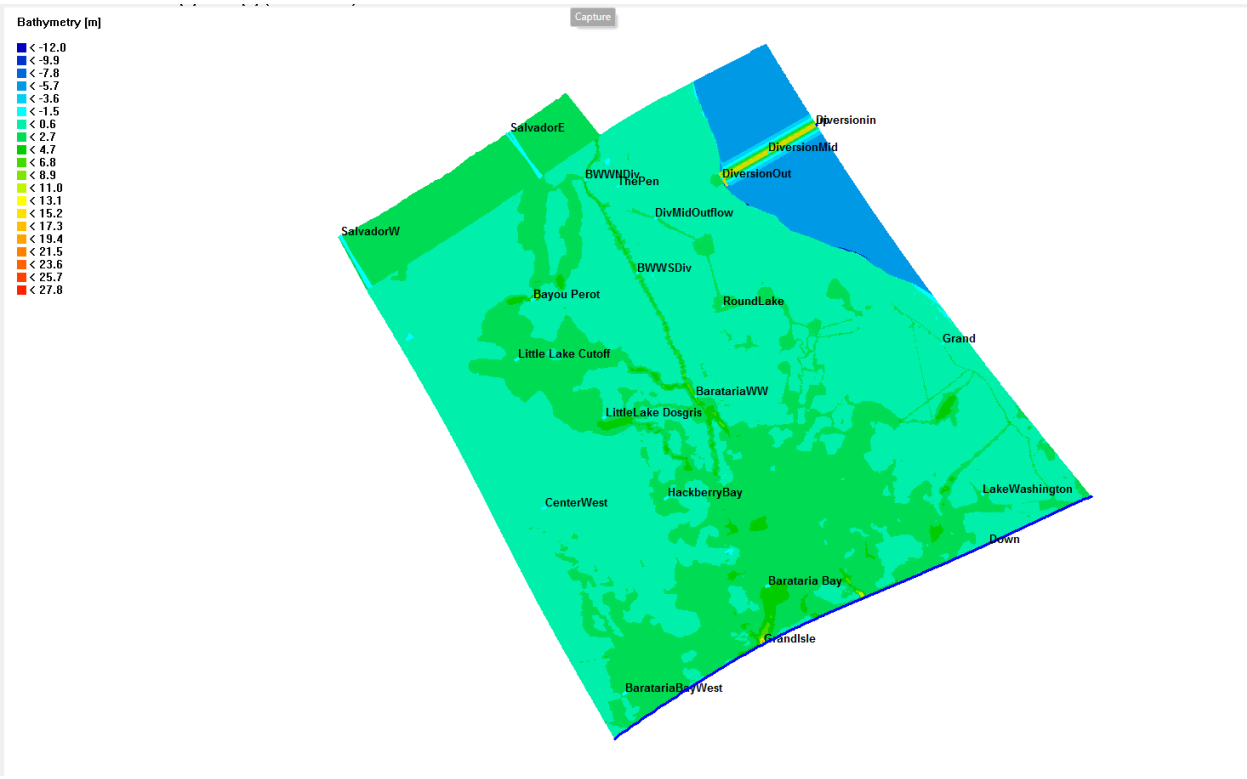

Figure 2.4: Bathymetry and monitoring station of the study domain including the storage in Lake Salvador.

2.5 Time Frame

Two different time frames were used to simulate a year with normal Mississippi River discharge and a year with high Mississippi River discharge. The year 2017 was chosen for the normal discharge year as the peak flow of the river measured at Belle Chasse was 32,000 m^3/s and the Bonnet Carré spillway was not opened. The year 2018 was chosen as a higher discharge year because the peak discharge reached 37,000 m^3/s and the Bonnet Carré Spillway was open for 22 days. These recent years were chosen because they are representative of these two flow regimes (Figure 2.5) and because these data are available at the Belle Chasse USGS Station.

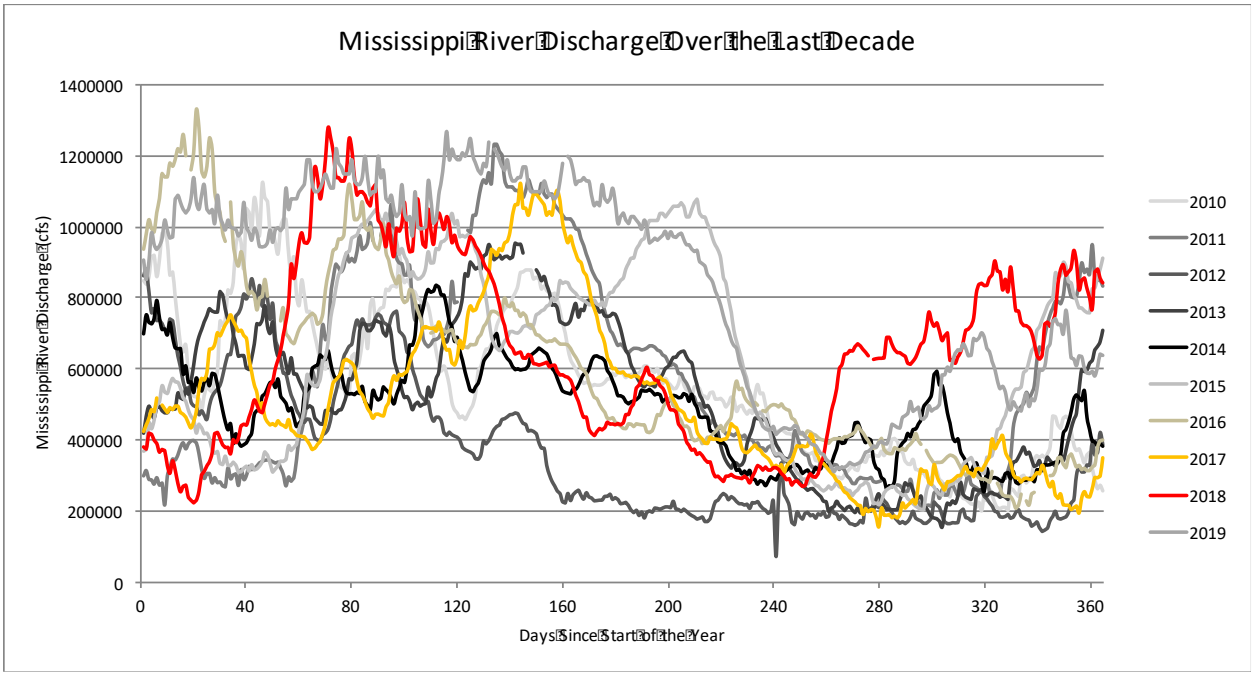

Figure 2.5: Mississippi River discharge from 2010-2019 with the selected high and normal flow year (High flow: 2018 in red. Normal Flow: 2017 in yellow)

The Normal Flow model was run using data from April 1, 2017 through July 9, 2017. The diversion was simulated to be open 79 days with it operating at peak flow for 20 days. The High Flow model was run using data from February 1, 2018 to June 30, 2018. The diversion was open 107 days. It was at peak discharge for 53 days. The time step of both the models is one minute. Results were stored hourly in history files and twice a day in map files.

2.6 Boundary Conditions

The model is driven by the Mississippi River discharge through the sediment diversion, tides at the Gulf of Mexico, wind over the domain, and Gulf salinity. Two boundary conditions were set up for the model. A Gulf of Mexico boundary condition, labeled as 'Down', was applied to the all the southernmost grid cells as a stage dependent condition. The diversion operated as its own discharge boundary. This is applied to cell (817, 561). Boundary condition data are obtained from several different sources (described in Section 2.6.1) and corroborated using other local data points.

2.6.1 River and Diversion Discharge

The Mississippi River discharge was taken from the USGS observations at Belle Chasse, LA (Station 07374525). Between the Belle Chasse station and the proposed Mid-Barataria Sediment diversion the Mississippi River loses flow through the Caernarvon Diversion on the east bank of the river at RM 82. The flow rate of this diversion is measured by USGS (USGS 295124089542100 Caernarvon Outfall Channel at Caernarvon, LA) and can reach a max discharge of 225 m^3/s. Since this volume of water is minimal compared to the Mississippi River discharge the effects are negligible on the total flow of the river and therefore not modeled.

No other diversions were modeled in this study. The largest diversion into the Barataria Basin is the Davis Pond diversion that is designed to add fresh water north of this study area. During calibration it was determined that the Davis Pond was not needed to model the hydrodynamics in the area. It did have a slight effect on the salinity in the area leading to a slight over prediction of salinities in the middle of the basin.

While some studies, such as Brown et al. (2019), only studied the effect of the Mid-Barataria Sediment Diversion operating at maximum capacity, this study uses a ramping up of the diversion from a minimum flow of 500 m^3/s when the Mississippi River discharge reaches 17,000 m^3/s to a maximum flow of 2125 m^3/s when the Mississippi River discharge is over 30,000 m^3/s. The diversion is opened when the river reaches 17,000 m^3/s because studies of rating curves at Belle Chasse show sand suspension at 12,000 m^3/s in the lowermost Mississippi River was negligible (Allison et al., 2013). USGS sediment records show that bedload movement of sand starts at approximately 8,000 m^3/s. However, significant resuspension of bed load material takes place at about 19,000 m^3/s as shown by iso-kinetic and backscatter studies on the Myrtle Grove bar (Ramirez and Allison, 2013). All diversion operations tested in this study begin at 500 m^3/s and ramp linearly to their respective max flow rates over the same number of days. This pattern with the river discharge is shown in Figure 2.6 and Figure 2.7 for the normal river flow and high river flow scenarios respectively.

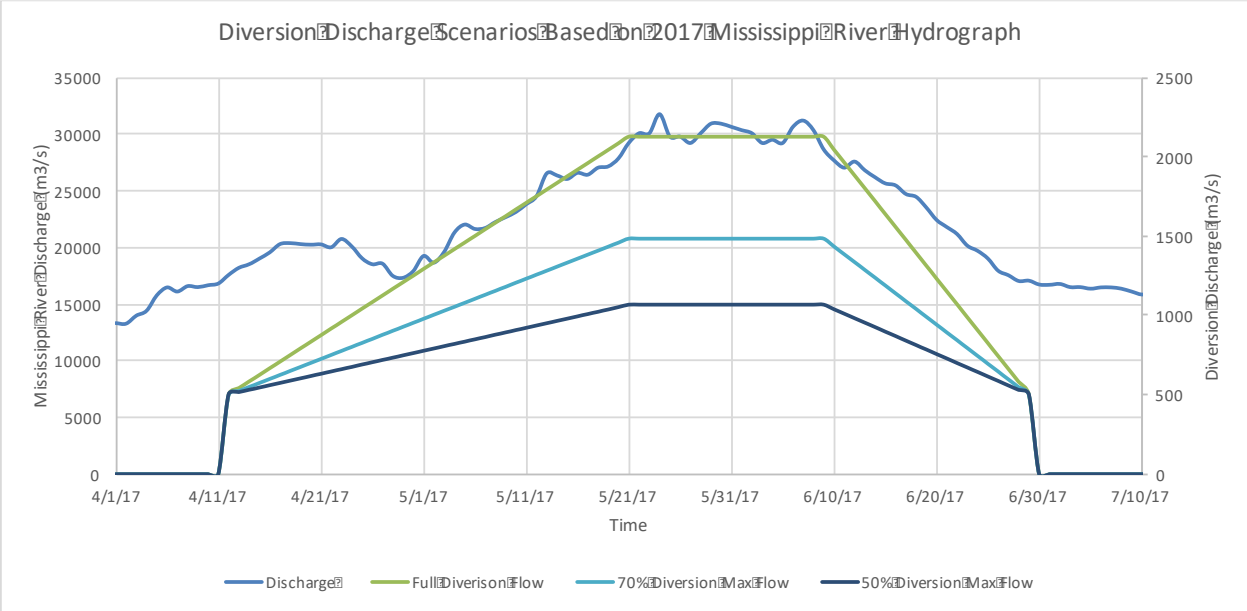

Figure 2.6: Normal river flow year using the 2017 hydrograph to determine discharge.

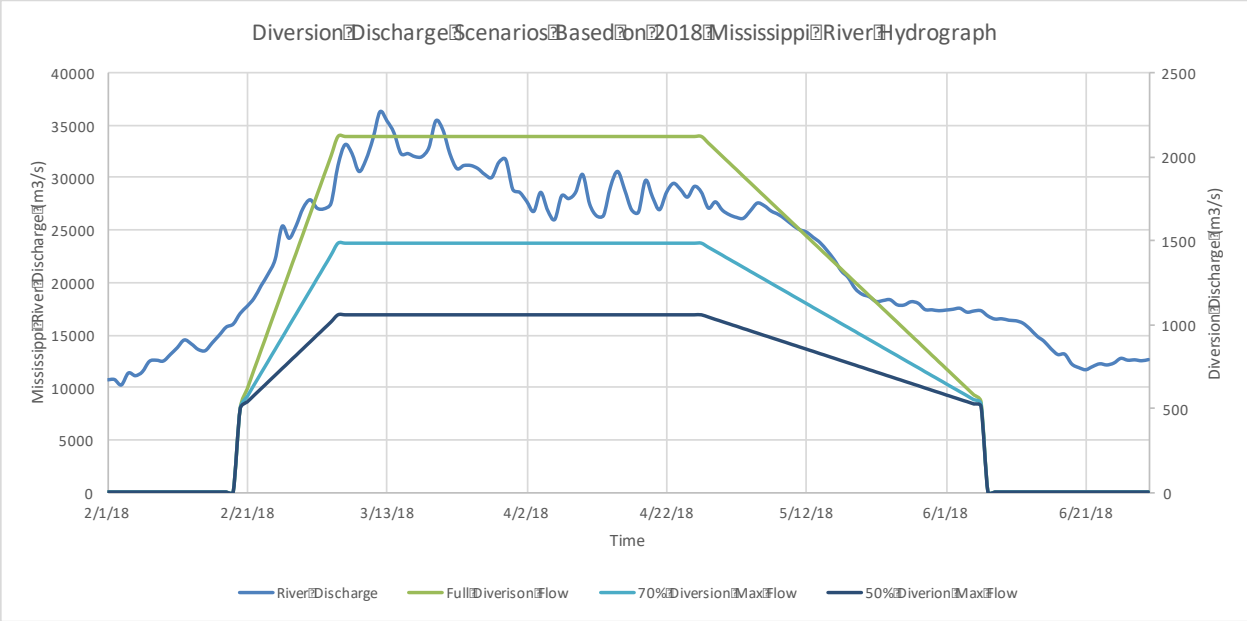

Figure 2.7: High river flow year using the 2018 hydrograph to determine discharge.

2.6.2 Tidal Flux

Brown et al. (2019) tried to use a combination of several tidal gauges and tidal harmonics to predict local tides. They found that the inherent uncertainty in the process did not guarantee a more representative tidal boundary and it created localized currents at the boundary. For this study only one tidal location is used for the Gulf of Mexico boundary condition. The data are from water levels measured at Grand Isle (USGS Station 073802516) and checked using the station at Caminada Pass northwest of Grand Isle (USGS Station 07380249). The tidal boundary for the normal and high flow years are shown in Figure 2.8 and Figure 2.9.

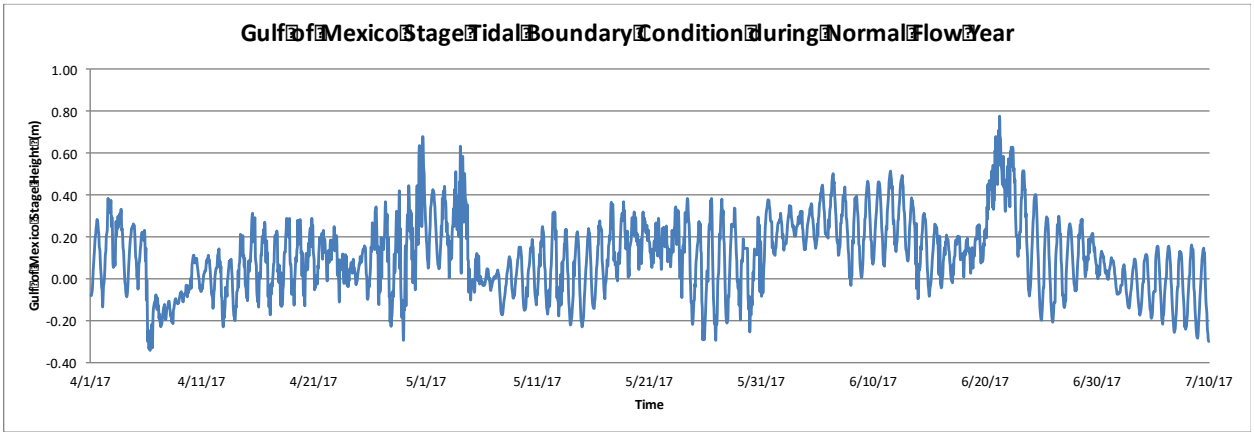

Figure 2.8: Stage level of the Gulf of Mexico during the normal river flow year as measure by USGS Station 073802516 at Grand Isle which was applied as the boundary condition in the model.

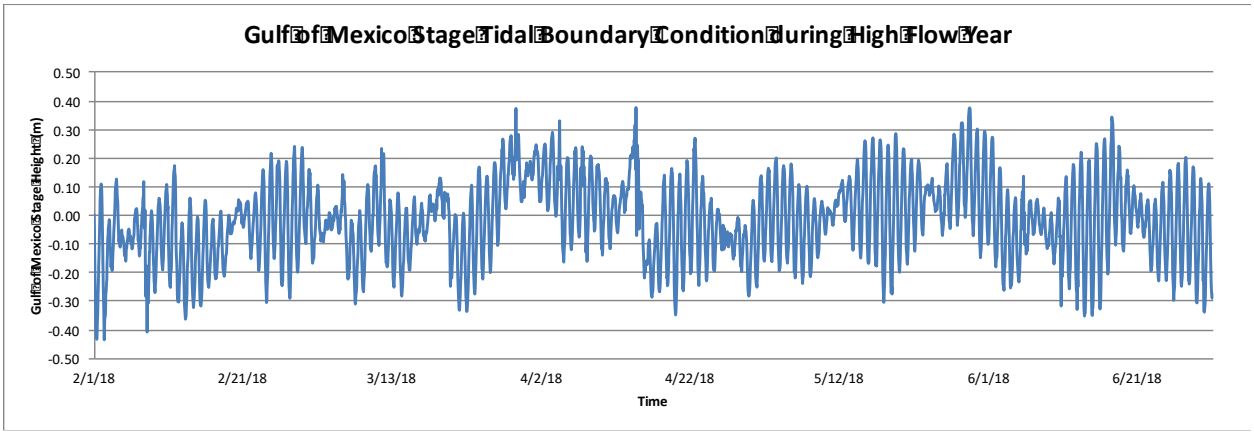

Figure 2.9: Stage level of the Gulf of Mexico during the high river flow year as measure by USGS Station 073802516 at Grand Isle which was applied as the boundary condition in the model.

2.6.3 Salinity

Salinity data were obtained from observations at Grand Isle (USGS Station 073802516) and checked using the station at Caminada Pass northwest of Grand Isle (USGS Station 07380249). During 2017, there were data missing from both of these locations so a third location within Barataria Bay was used (USGS Station 291929089562600) and the data were scaled based on previous observational differences between the stations. The complete salinity dataset is shown in Figure 2.10 and Figure 2.11 for normal and high river flow years respectively. Since Grand Isle station is in the center of the domain on the southern boundary and there are relatively small changes in salinity laterally along the boundary compared with perpendicular to it, the salinity was assumed to be constant across the Gulf of Mexico boundary. The water in the diversion was assumed to be completely fresh or a salinity of 0 ppt.

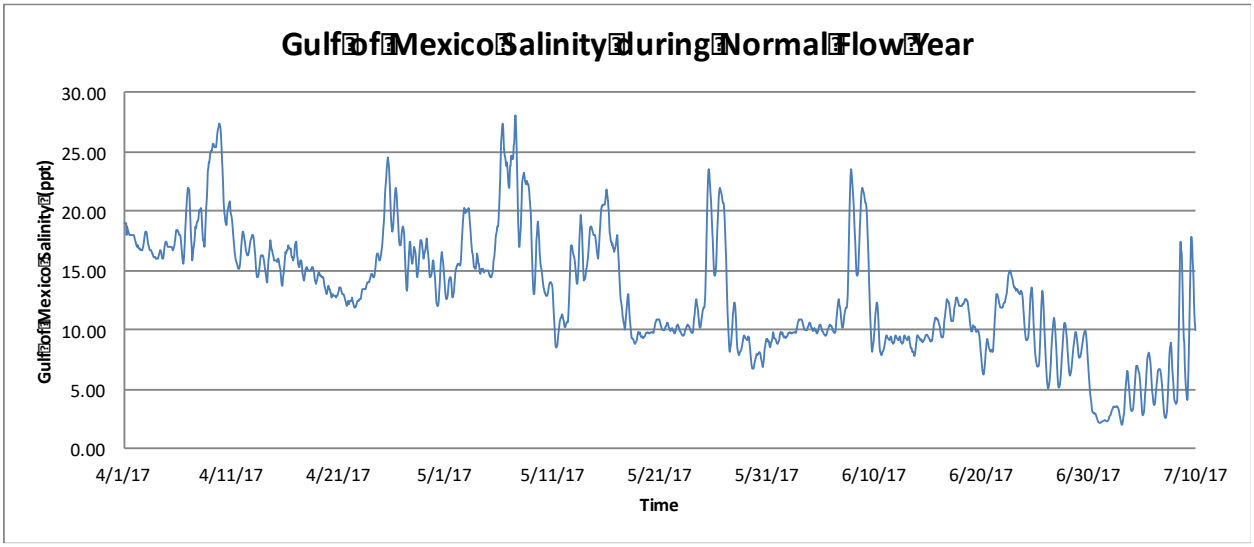

Figure 2.10: Salinity boundary condition for the Gulf of Mexico near the Barrier Islands during the normal river flow simulation.

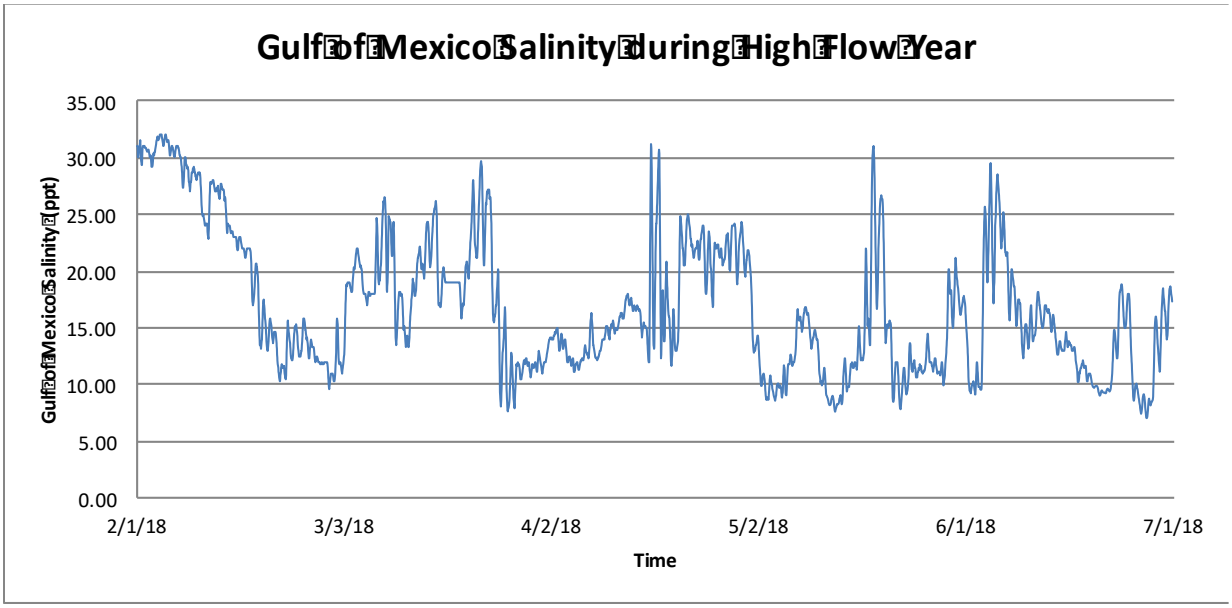

Figure 2.11: Salinity boundary condition for the Gulf of Mexico near the Barrier Islands during the normal river flow simulation.

2.6.4 Sediment

The model was designed for one class of non-cohesive sediments and two classes of cohesive sediments. A dynamic sediment rating curve produced by McCorquodale et al. (2017) was utilized to produce concentrations in mg/L. Equation 2.1 calculates the sand concentration in the river based on the discharge at Tarbert Landing. This equation uses a variable based on the rising and falling limbs as well as past history of the discharges in the river shown in Equations 2.2 and 2.3.

$$[2.1] \quad C_{sand} = \begin{Bmatrix} C_{sand\ High} for\ \frac{dQ}{dt} positive \\ C_{sand\ Low} for\ \frac{dQ}{dt} negative \end{Bmatrix} \left\{ \frac{3.5}{1+\frac{\langle Q \rangle_{12\ mo}}{\langle Q \rangle_{56\ yr}}} \right\} \left\{ \frac{3.5}{1+\frac{\langle Q \rangle_{3\ mo}}{\langle Q \rangle_{56\ yr}}} \right\}^{\frac{3}{4}}$$

$$[2.2] \quad C_{sand\ high} = 1.7327 * 10^{-4} Q_{cfs} - 5.580 * 10^{-11} Q_{cfs}^2 - 50.$$

$$[2.3] \quad C_{sand\ low} = 15.48667 * 10^{-5} Q_{cfs} - 6.48148 * 10^{-11} Q_{cfs}^2 + 13.$$

Where,
The sign of dQ/dt is based on a 6 day average;
$\langle Q \rangle_{12\ mo}$= preceding 12 month mean daily flow;
$\langle Q \rangle_{3\ mo}$= preceding 3 month mean daily flow;
$\langle Q \rangle_{56\ yr}$= preceding 56 year mean daily flow;
Q_{cfs}= present time daily flow.

Fines were calculated using a similar strategy shown in Equations 2.4 through 2.6.

$$[2.4]\quad C_{fines} = \begin{Bmatrix} C_{fines\ High}\ for \frac{dQ}{dt} positive \\ C_{fines\ Low} for \frac{dQ}{dt} negative \end{Bmatrix} \left\{ \frac{\begin{bmatrix} 1.8\ for \frac{dQ}{dt} positive \\ 2.5\ for \frac{dQ}{dt} negative \end{bmatrix}}{1+\frac{\langle Q \rangle_{12\ mo}}{\langle Q \rangle_{56\ yr}}} \right\} \left\{ \frac{2.5}{1+\frac{\langle Q \rangle_{3\ mo}}{\langle Q \rangle_{56\ yr}}} \right\}^{\frac{1+sign(\frac{dQ}{dt})}{2}}$$

$$[2.5]\quad C_{fines\ high} = 8.2963 * 10^{-4} Q_{cfs} - 7.3343 * 10^{-10} Q_{cfs}^2 + 1.2673 * 10^{-16} Q_{cfs}^3 - 68.7$$

$$[2.6]\quad C_{fines\ low} = 5.18667 * 10^{-4} Q_{cfs} - 6.40537 * 10^{-9} Q_{cfs}^2 + 1.9032 * 10^{-16} Q_{cfs}^3 - 40.3$$

Where,
The sign of dQ/dt is based on a 6 day average;
$\langle Q \rangle_{12\ mo}$= preceding 12 month mean daily flow;
$\langle Q \rangle_{3\ mo}$= preceding 3 month mean daily flow;
$\langle Q \rangle_{56\ yr}$= preceding 56 year mean daily flow;
Q_{cfs}= present time daily flow.

It is assumed that 70% of the fines are silt and 30% are clay. The results of these equations are shown in Figure 2.12 and 2.13 for normal and high river flow years respectively along with the discharge associated with these concentrations.

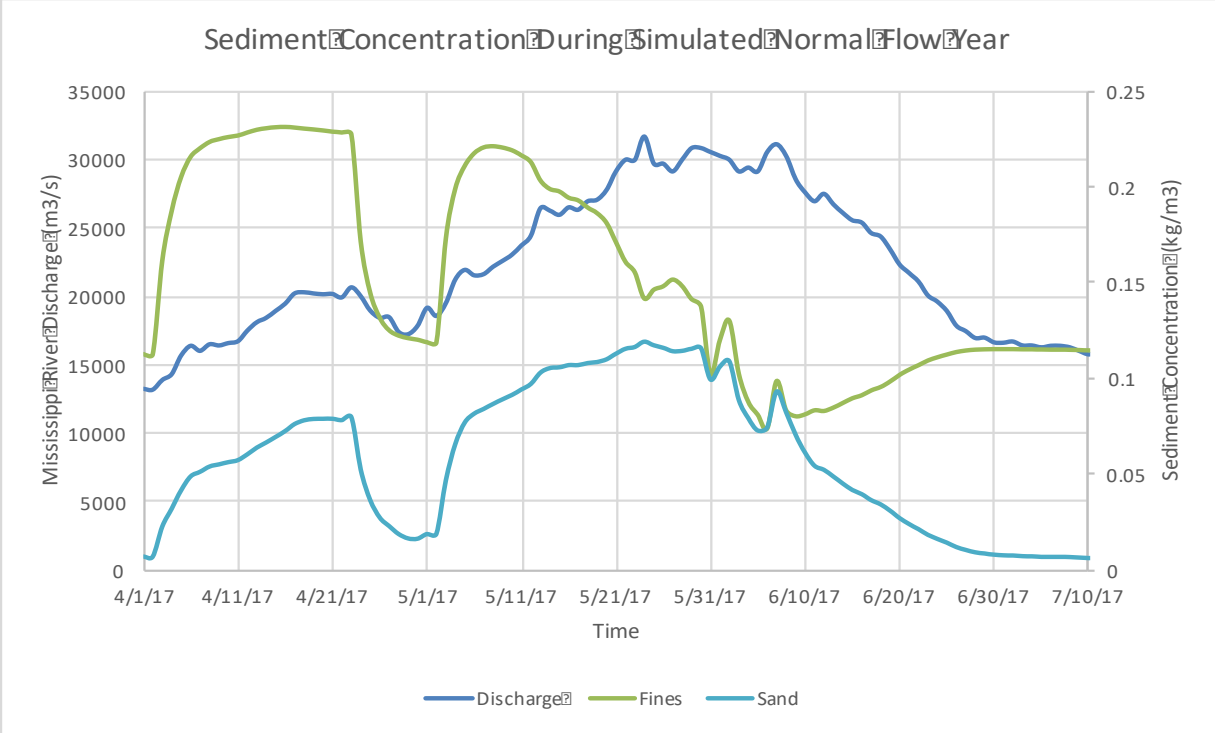

Figure 2.12: Sediment concentrations in the diversion produced by dynamic sediment rating curves for the normal river flow year.

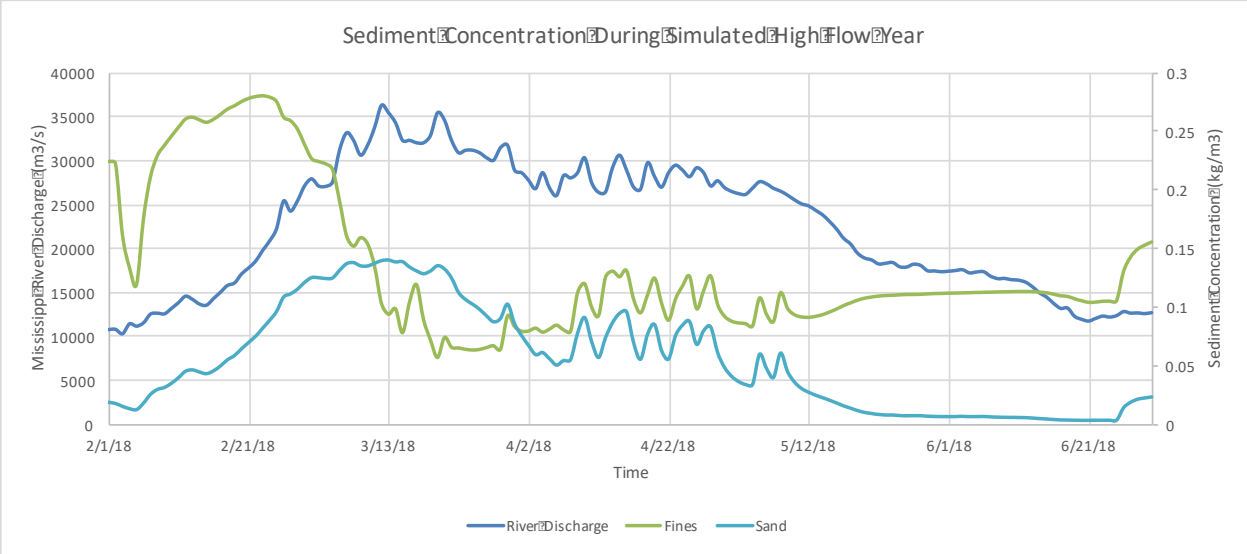

Figure 2.13: Sediment concentrations in the diversion produced by dynamic sediment rating curves for the normal river flow year.

This load was imposed at the diversion boundary. It was assumed that the concentration of sediment coming in from the Gulf of Mexico was negligible.

2.7 Wind Forcing

Wind data were obtained from three stations around Grand Isle since this is the area of the model where the effect of the wind is largest. The stations were labelled by priority. Any data gaps were filled by the next station on the list. Table 2.1 gives the wind station information. Figure 2.14 and Figure 2.15 give the final wind data that were applied uniformly across the domain during the normal and high flow year respectively. Air density was assumed to be 1 kg/m^3 and the temperature 15 C during the entire run. Barometric pressure gradient over the domain were neglected.

Location ID	Description
USGS 073802516	Barataria Pass at Grand Isle, LA
USGS 07380249	Caminada Pass NW of Grand Isle, LA
USGS 291929089562600	Barataria Bay near Grand Terre Island, LA

Table 2.1: Wind Observation Stations Used in Boundary Conditions

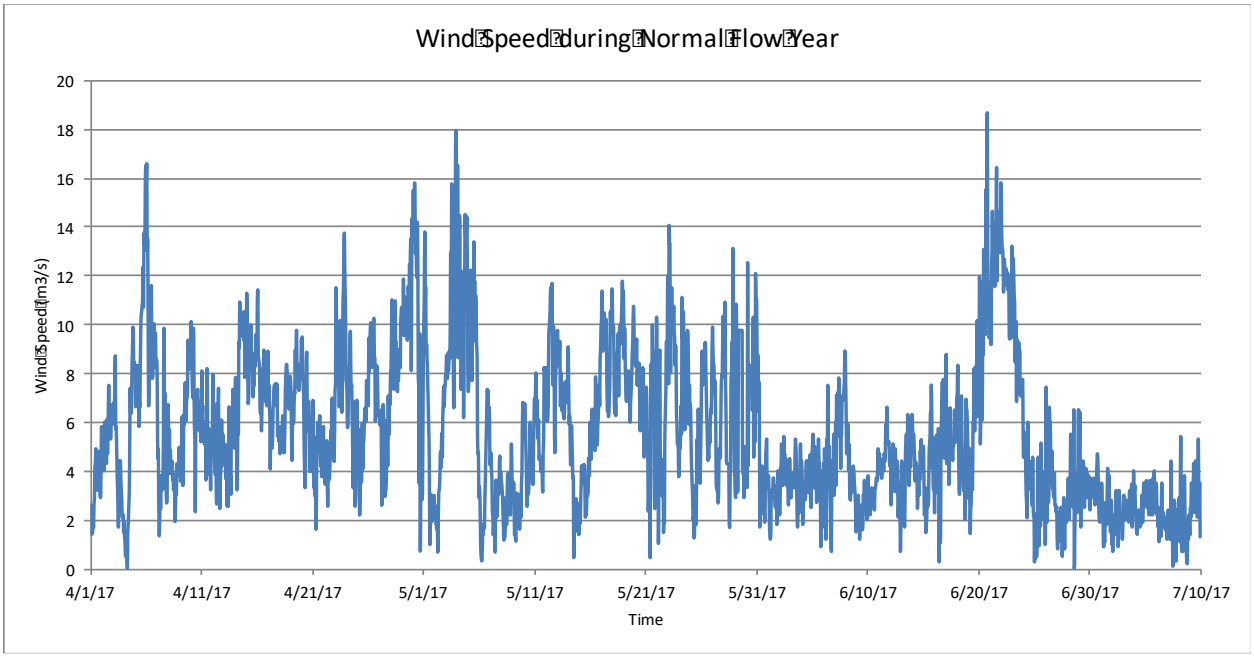

Figure 2.14: Wind speed as observed at Grand Isle during the spring of 2017 which will be used as the wind data for the normal flow year.

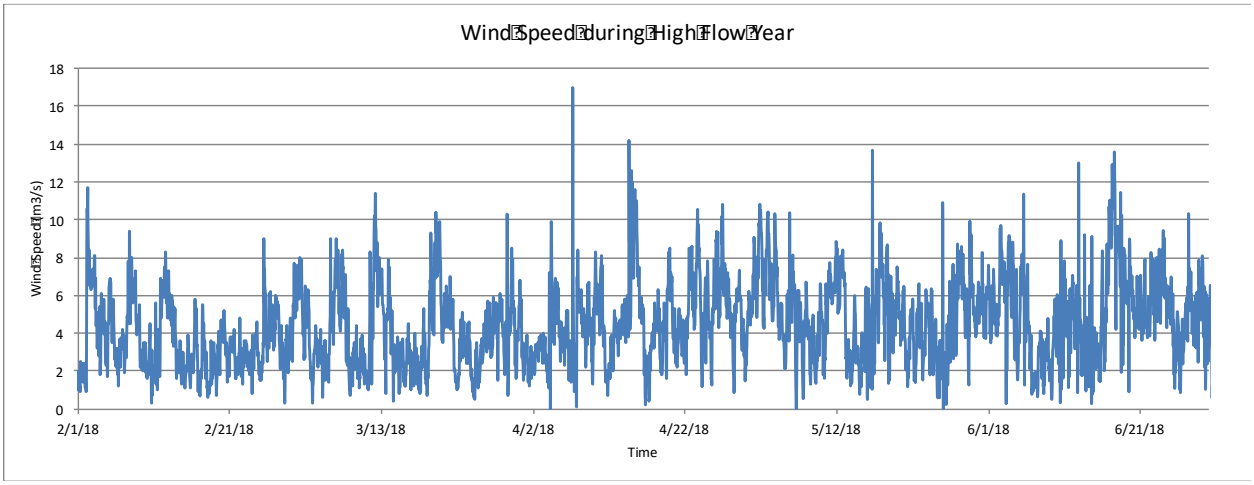

Figure 2.15: Wind speed as observed at Grand Isle during 2018 which will be used as the wind data for the normal flow year.

2.8 Initial Conditions

Initial sediment concentrations within the domain were assumed to be zero. The initial water level was set to sea level across the entire grid. Salinity within the basin was analyzed for the last decade to determine average salinity levels in the basin during the model run. Salinity levels at the start of February in 2018 was used as the initial condition for the 2018 calibration run and were determined to be close to the average values for the last decade. These values, shown in the Lake Pontchartrain Basin Foundation Hydrocoast maps in Figure 2.16, were then used for all model runs.

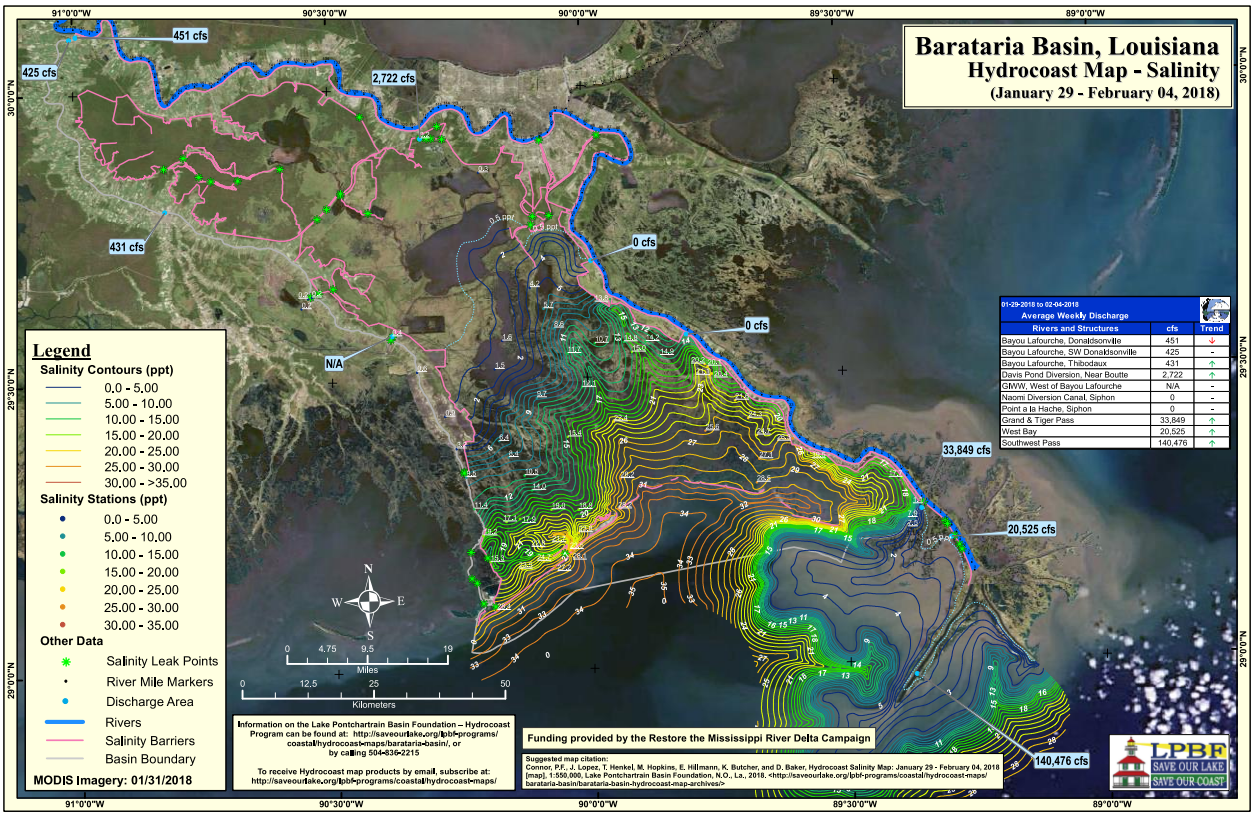

Figure 2.16: Hydrocoast from Lake Pontchartrain Basin Foundation used as the initial salinity condition for the model (LPBF, 2018).

2.9 Morphology

Five layers of bed sediment were used to create an erodible bed. Space varying thickness was used to determine depth of erosion availability. The thickness of the layers in the bed of the channels was set to 2 m while the marshland was set to 1 m. The sediment concentration of each layer is shown in Table 2.2. Roughness of the bed is also spatially varying. Manning's n of 0.023, 0.033, and 0.098 are used for the bed of the channels, the edge of the marshland, and the central marsh respectively. Marsh channels were assumed to be anything with an initial depth of 0.25 m; Marsh centers were defined as any area over 0.5 m above sea level and the marsh edge is between these values. However, before any morphologic change could occur a spin up interval of 1440 minutes was applied.

Sediment Mass Fraction by Layer					
Layer	1	2	3	4	5
Clay	0.25	0.22	0.22	0.2	0.2
Silt	0.7	0.68	0.68	0.6	0.6
Sand	0.05	0.1	0.1	0.2	0.2

Table 2.2: Sediment mass fraction by layer

Specific density of the fines was assumed to be 2650 kg/m^3 and the dry bed density 500 kg/m^3. The critical bed shear stress was assumed to be 0.1 Pa (van Ledden, 2003; Pandoe and Edge,

2008; Deltares, 2013; Ghose Hajra et al., 2014). Sand was assumed to have a dry bed density of 1600 kg/m^3 and a D50 of 183.34 mm. Settling velocity of each sediment class is laid out in Table 2.3.

Sediment Type	Settling velocity
Clay	0.00275 mm/s unflocculated (Mikes and Manning, 2010; Reins, 2018)
Silt	0.71 mm/s (Maggi, 2013; Reins, 2018)
Sand	Use Van Rijn 84 equations to predict settling with a reference height of 1 and a threshold sediment thickness of 0.05m

Table 2.3: Settling velocity parameters based on sediment type

2.10 Changing Conditions

Day et al. (2012) and Blankespoor et al. (2012) find that coastal restoration and protection projects should consider the impacts of relative sea level rise when predicting benefits. Since, this model is only looking at the early development of the distributary channels sea level rise was not simulated. Likewise, no large storms were modeled in the selected scenarios.

Chapter 3: Calibration

3.1 Calibration Overview

The calibration was run using water depth and salinity data at multiple locations throughout the study area (Table 3.1) and simulated during two years with varying river discharge. Since the model is looking at small time scales in channel development, the model was calibrated over a small time scale. One month from 2017, representing a normal river discharge year, and one month from 2018, representing a high river discharge year, were used to calibrate the model.

USGS Station Number	Latitude	Longitude	Site Description
07380330	29.56577778	-90.16555556	Bayou Perot at Point Legard near Cutoff, LA
07380335	29.51750000	-90.18138889	Little Lake near Cutoff, LA
292800090060000	29.46666667	-90.10000000	Little Lake near Bay Dosgris east of Galliano, LA
292859090004000	29.48305556	-90.01111111	Barataria Waterway south of Lafitte, LA
07380251	29.42250000	-89.95055556	Barataria Bay north of Grand Isle, LA
073802512	29.39833333	-90.04111111	Hackberry Bay northwest of Grand Isle, LA

Table 3.1: Geographic location of USGS stations used during the calibration of the model

For this calibration, statistical measures established by Meselhe and Rodrigue (2013) were used. A Normalized Root Mean Square Error, the Pearson Product-Moment Correlation Coefficient, and the Percent Bias were all calculated for each station and assed based on the criteria established in the same paper. These statistics were computed using hourly averaged data for the modeled and field data. To produce useful statistics, the vertical datum was shifted by one meter to ensure there were no negative values. The model's roughness coefficient (at bed level, marsh edge, and marsh center), horizontal eddy viscosity and diffusivity, and initial conditions were adjusted until the statistical analysis proved the model was operating within an acceptable range. A minimum eddy viscosity of $1 m^2/sec$ is enforced on the model but the turbulence equations can yield more viscosity. This number was determined through model calibration and previous research. Originally, an eddy viscosity of 0.1 m^2/s was used since this was the value used in Brown et al. (2019) but the calibration showed this was insufficient. Horizontal diffusivity was 60 m^2/s and roughness was space varied. These parameters resulted in 83% of stations passing on water depth and 67% of stations passing on salinity. The remaining poor caparisons in modeled results could be due to gaps in field data and outliers in the observed data that skews the results.

3.2 Water Depth Calibration

Figure 3.1 through Figure 3.6, represent a sample of the calibration curves for water surface elevation around Barataria Bay. These points were displayed because they represent spatially diverse points within the system and also correspond to areas of interest during the sediment diversion simulations. The water surface elevation produced by the model closely resembles the observed data. Storm induced changes to the water surface elevation appears to be captured at each calibration point. This calibration verifies that roughness coefficient and conveyance volumes are sufficient to produce realistic results. The roughness is particularly important because it will determine the spatial extent of inundation associated with the sediment diversion. It also confirms that the assumption of spatially static wind and uniform tidal influence along the boundary.

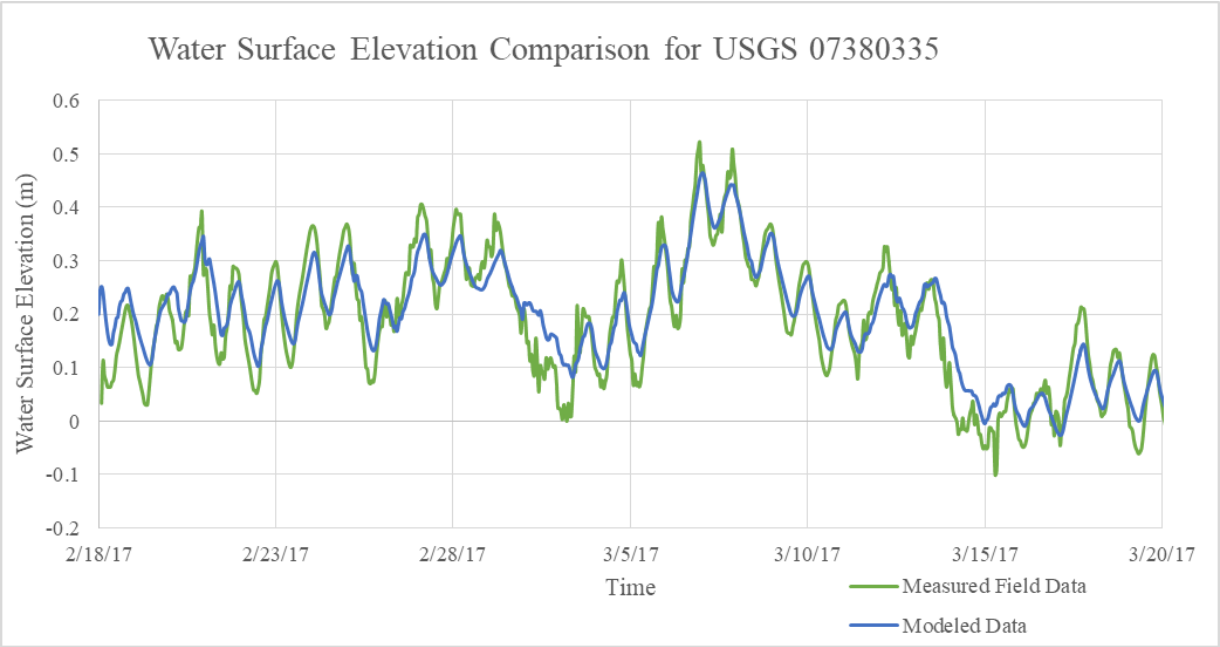

Figure 3.1: Modeled and field surface elevation data at Little Lake Near Cutoff, LA during the normal river flow model calibration.

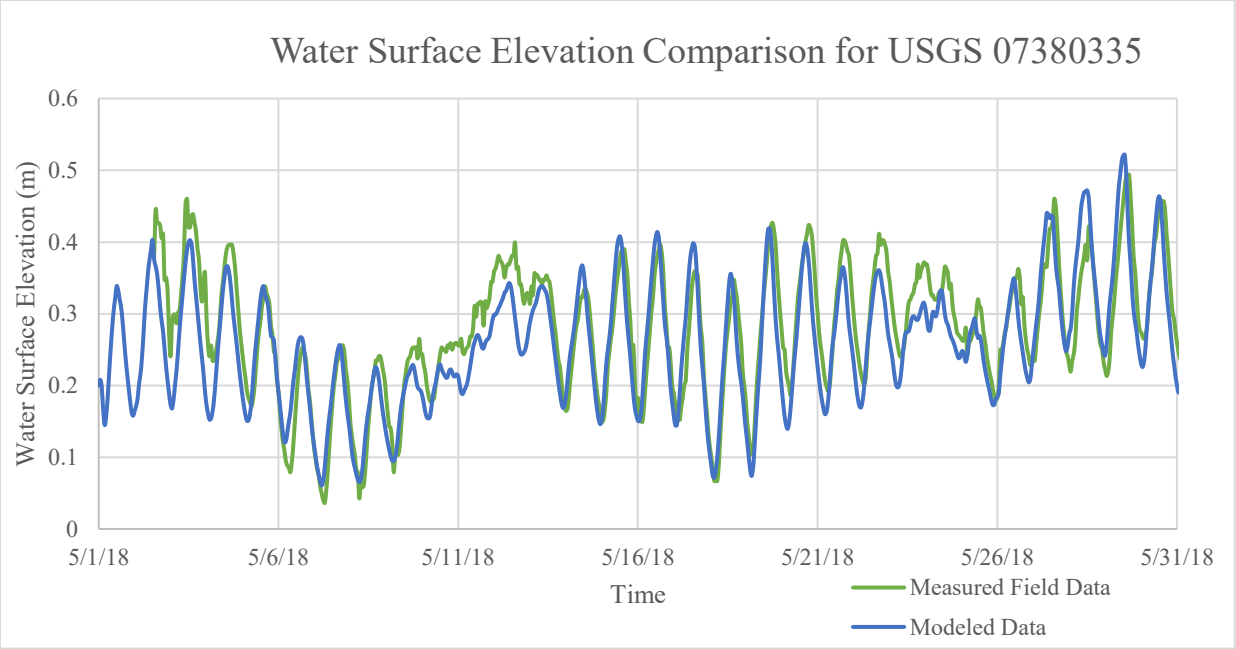

Figure 3.2: Modeled and field surface elevation data at Little Lake Near Cutoff, LA during the high river flow model calibration.

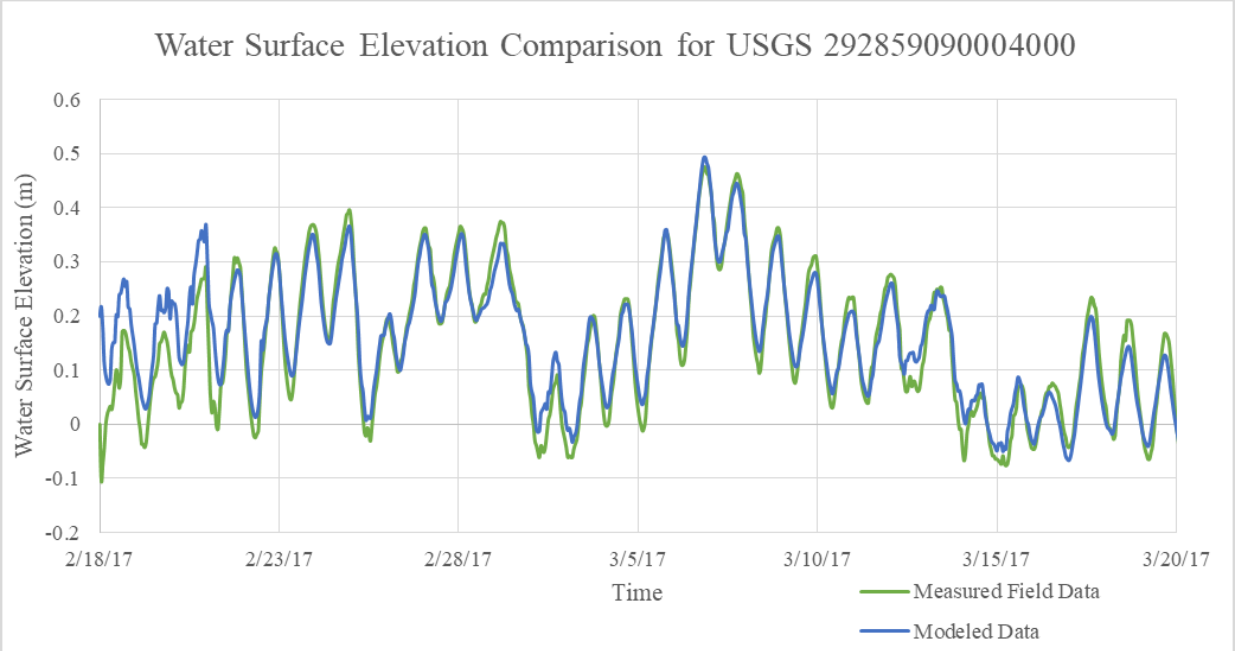

Figure 3.3: Modeled and field surface elevation data at Barataria Waterway South of Lafitte, LA during the normal river flow model calibration.

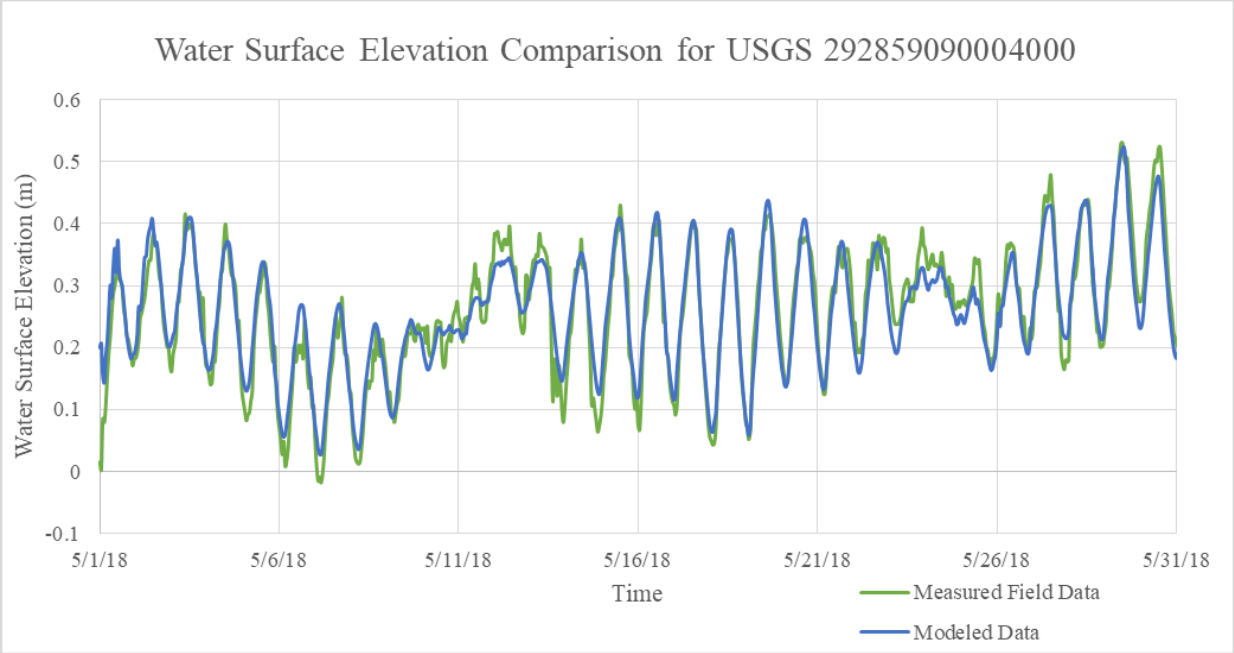

Figure 3.4: Modeled and field surface elevation data at Barataria Waterway South of Lafitte, LA during the high river flow model calibration.

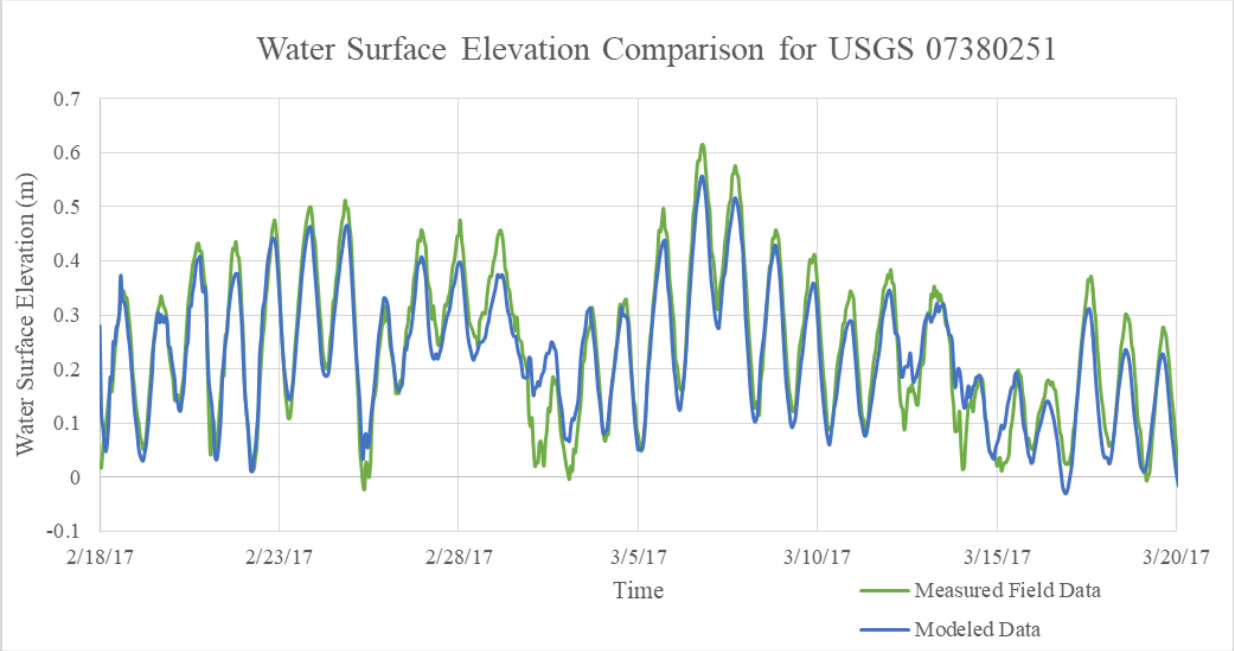

Figure 3.5: Modeled and field surface elevation data at Barataria Bay North of Grand Isle, LA during the normal river flow model calibration.

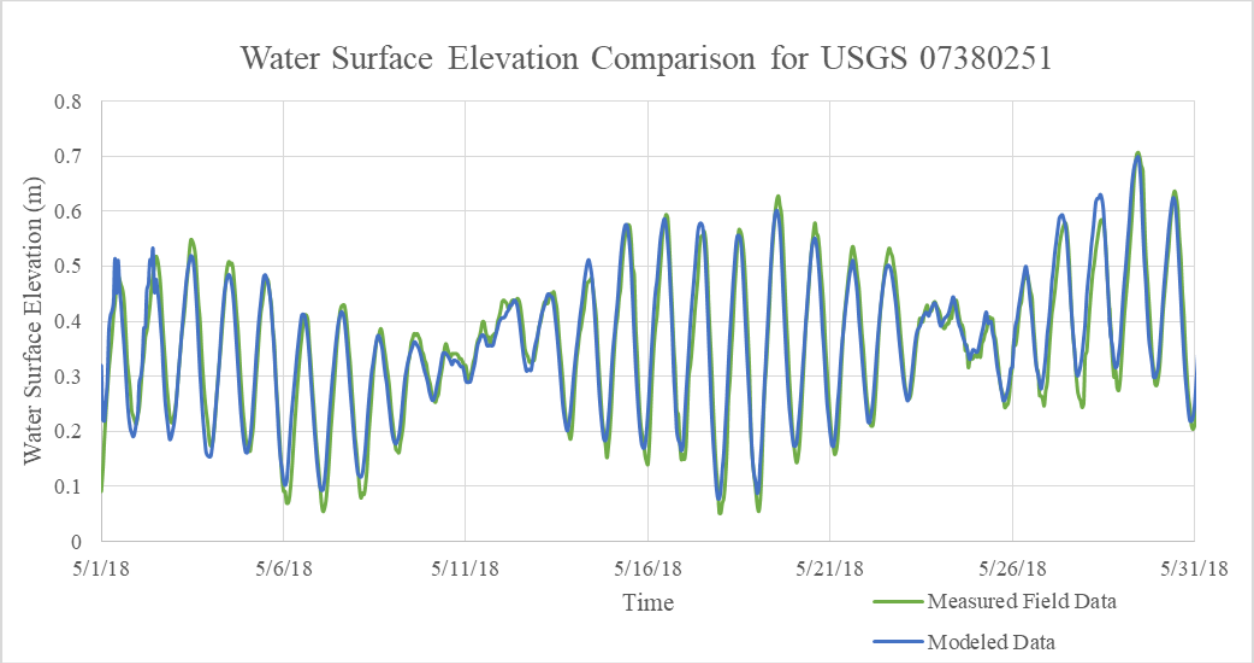

Figure 3.6: Modeled and field surface elevation data at Barataria Bay North of Grand Isle, LA during the normal river flow model calibration

Water level during the high flow matches the observations better than the low flow year, however, both seem to represent the observed data quite well. Open areas show a very strong calibration but smaller waterways such as Hackberry Bay and Little Lake near Bay Dosgris show a slight damping of amplitude. This is apparent in both high and low flow years and could be due to the resolution of the model not capturing the full volume of smaller canals.

3.3 Salinity Calibration

Salinity is much harder to model accurately in part because salinity transport is a three dimensional phenomenon. The mixing is determined by roughness and geometry which are already validated using hydrodynamic variables. The calibration of salinity involve adjustment of the dispersivity. Any large discrepancies in the salinity models may indicate errors with the hydrodynamic model that were not detected during that calibration. Figures 3.7 through 3.12 show modeled and field observed hourly salinity data at various locations within the domain. Some field observations were not available during the timeframe chosen to calibrate the model.

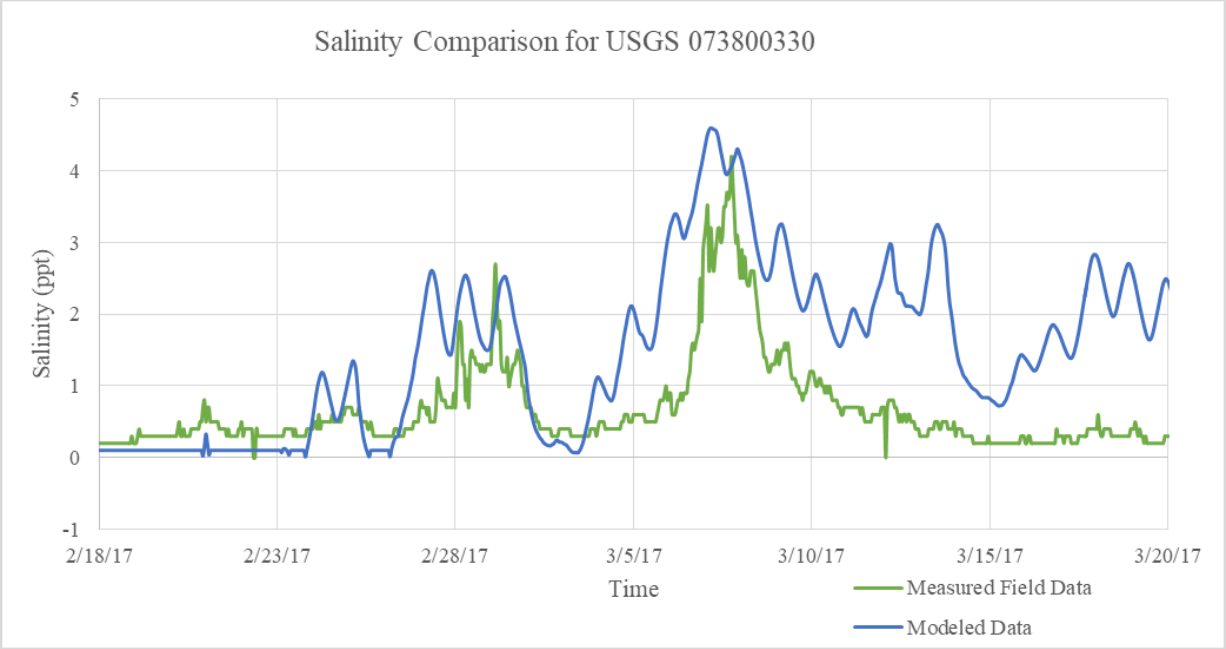

Figure 3.7: Modeled and field measures of salinity in Bayou Perot at Point Legard near Cutoff, LA during the normal river flow model calibration.

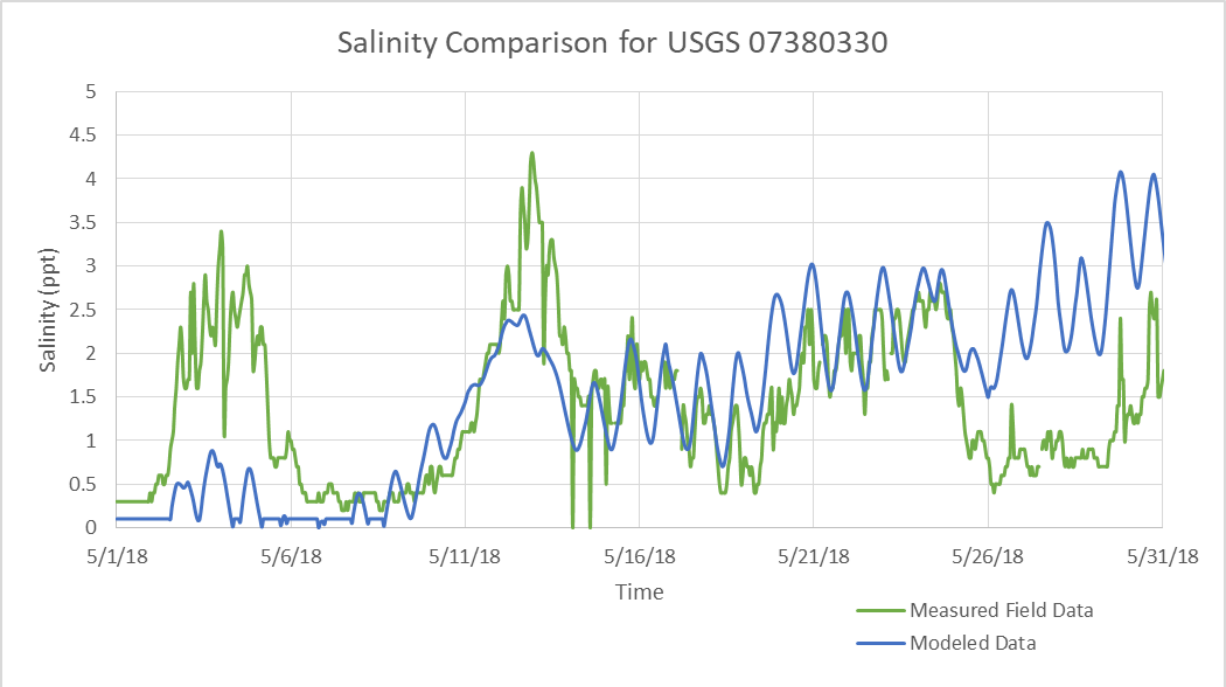

Figure 3.8 Modeled and field measures of salinity in Bayou Perot at Point Legard near Cutoff, LA during the high river flow model calibration.

Figure 3.9: Modeled and field measures of salinity at Barataria Waterway South of Lafitte, LA during the normal river flow model calibration.

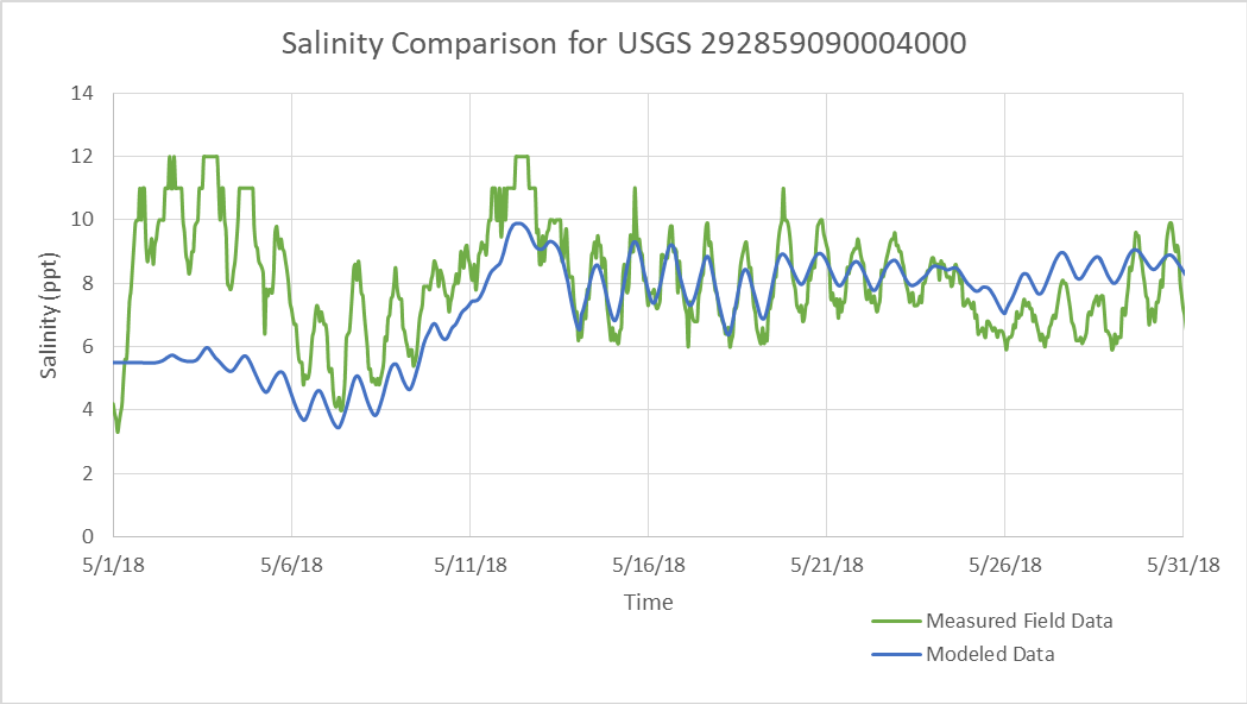

Figure 3.10: Modeled and field measures of salinity at Barataria Waterway South of Lafitte, LA during the high river flow model calibration.

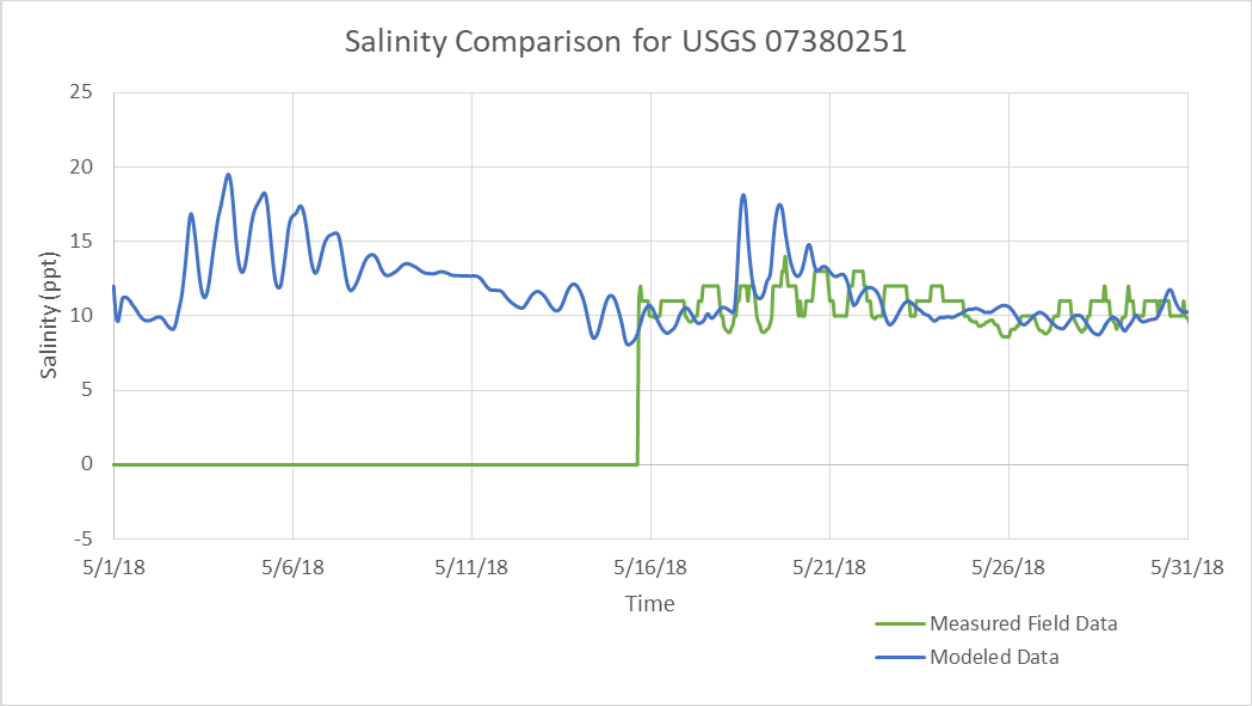

Figure 3.11: Modeled and field measures of salinity at Barataria Bay North of Grand Isle, LA during the normal river flow model calibration.

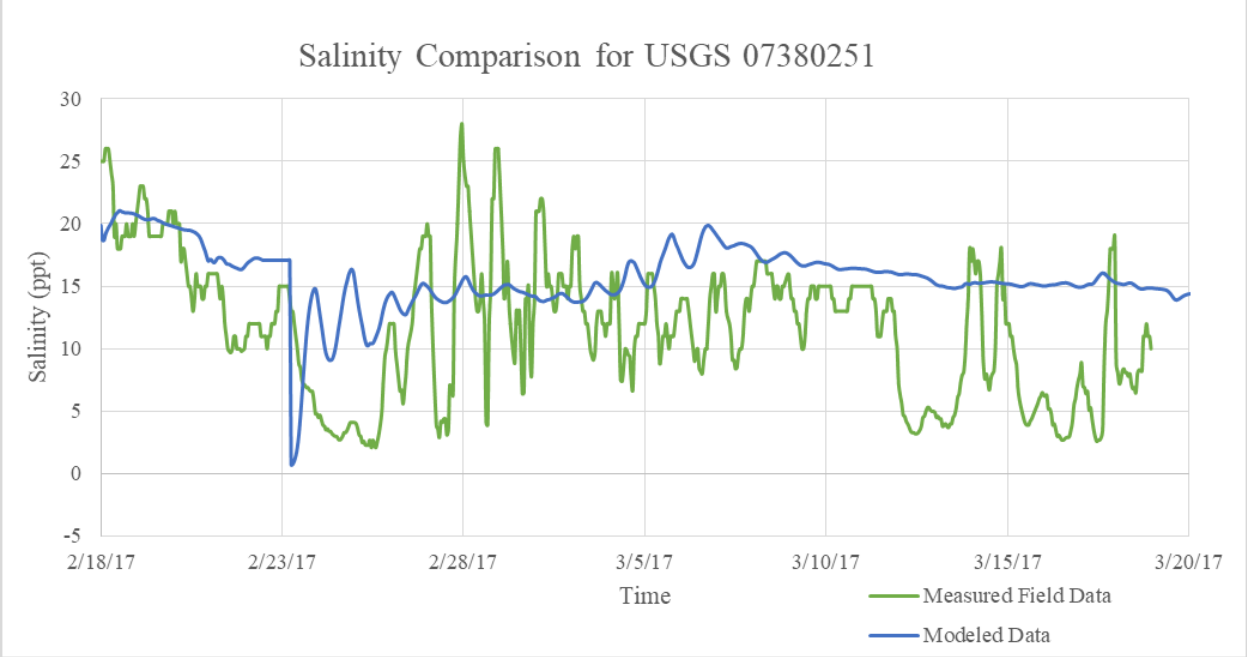

Figure 3.12: Modeled and field measures of salinity at Barataria Bay North of Grand Isle, LA during the high river flow model calibration.

The model starts to track salinity data after about 7 days of real time simulation. After this time, the model does a fairly good job at predicting salinity levels. During storms the salinity response is dampened in larger bodies of water and is highly variable in smaller systems. Part of this could

be due to the fact that there are 3D features in the salinity circulation that are not represented in this depth averaged model.

3.4 Calibration Equations

3.4.1 Root Mean Square Error

The RMSE measures the variation of the modeled data to observed data (Legates and McCabe, 1999). This is estimated by taking the square root of the average of differences between modeled and observed data. It is calculated using Equation 3.1.

[3.1] $$RMSE = \sqrt{\frac{\sum_{i=1}^{n}(M_i - O_i)^2}{n}} * \frac{n}{\sum_{i=1}^{n}(O_i)^2}$$

Where,
M=Modeled Value
O=Observed Value
n=number of observations

Small RMSE percentages mean a better fit of the data. For the RMSE analysis water depth is used instead of stage because stage is in reference to an arbitrary datum. However, the graphs of the results are shown in stage. For two dimensional models, the desired target for water depth is less than 0.15 for all stations. Acceptable range is less than 0.15 for 80% of stations. All of modeled stations achieved the values of less than 0.15.

Modeled salinity values are commonly out of phase with the observed values. To counteract this, daily mean salinities were compared instead of hourly data (Meselhe, 2013). Over 80% of stations had RMSE values below 0.5 during the high flow year and 67% of stations surpassed this threshold during a normal flow year meaning that salinity falls within the acceptable range. Results of both the water depth and salinity RMSE calculations are shown in Table 3.2.

RMSE Analysis				
Station	2018 Water Depth (m)	2017 Water Depth (m)	2018 Salinity (ppt)	2017 Salinity (ppt)
USGS 292800090060000	0.136	0.138	0.368	0.365
USGS 7380335	0.141	0.107	0.543	0.139
USGS 073802512	0.126	0.132	0.230	0.258
USGS 292859090004000	0.105	0.100	0.253	0.345
USGS 07380330	0.054	0.066	0.684	0.572
USGS 07380251	0.045	0.049	0.256	0.627
Number of Passing Stations	5	5	4	4

Table 3.2: Results of RMSE analysis at the calibration points for 2018, representing a high flow year, and 2017, representing a normal flow year, along with the number of passing stations.

3.4.2 Pearson Product-Moment Correlation Coefficient

The Pearson product-moment correlation coefficient, r, determines the phasing between the modeled and observed values (Legates and McCabe, 1999) by accounting for how well the peaks and troughs of the curve line up. This is calculated using Equation 3.2:

[3.2] $$r = \frac{\sum_{i=1}^{n}(M_i-\bar{M})(O_i-\bar{O})}{\sqrt{\sum_{i=1}^{n}(M_i-\bar{M})^2}\sqrt{\sum_{i=1}^{n}(O_i-\bar{O})^2}}$$

Where,
M=Modeled Value
$\bar{M}$ = Mean of modeled values
O=Observed Value
$\bar{O}$ = Mean of observed values
n=number of observations

The results of this calculation can be -1 to +1, where a value of +1 means the crests and troughs are perfectly in alignment. This measure is not as reliable in this model calibration since the sample size is small and data are scarce for salinity. Water depth achieved greater than 0.9 for over 80% of the stations during the 2018 calibration and 100% of the stations during the 2017 calibration meaning the data falls in the acceptable range as shown in Table 3.4.2.1. USGS Station 7380335 experienced a slight phase shift causing this to fail the test. The salinity values are greater than 0.5 for 50% of the stations for both years meaning that the salinity is acceptable (Meselhe, 2013). However, all of the low predictions of salinity come from records with incomplete field data.

Pearson Product-Moment Correlation Coefficient Analysis				
Station	2018 Water Depth, r (r^2)	2017 Water Depth, r (r^2)	2018 Salinity, r (r^2)	2017 Salinity, r (r^2)
USGS 292800090060000	0.903 (0.82)	0.914 (0.84)	0.175 (0.03)	0.858 (0.74)
USGS 7380335	0.708 (0.5)	0.931 (0.87)	0.592 (0.35)	0.596 (0.36)
USGS 073802512	0.918 (0.84)	0.995 (0.99)	0.139 (0.02)	0.119 (0.01)
USGS 292859090004000	0.953 (0.91)	0.946 (0.89)	0.508 (0.26)	0.747 (0.56)
USGS 07380330	0.965 (0.93)	0.903 (0.82)	0.561 (0.31)	0.62 (0.38)
USGS 07380251	0.947 (0.9)	0.944 (0.89)	0.671 (0.45)	0.263 (0.07)
Number of Passing Stations	5	6	4	4

Table 3.3: Results of Pearson Product-Moment Correlation Coefficient analysis at the calibration points for 2018, representing a high flow year, and 2017, representing a normal flow year, along with the number of passing stations.

3.4.3 Bias

Bias occurs when a model is constantly over or under predicting quantities which is calculated using Equation 3.3. Bias can usually be corrected or taken into account for analysis

[3.3] $$Bias = \frac{\bar{M}-\bar{O}}{\bar{O}}$$

Where,
$\bar{M}$ = Mean of modeled values
$\bar{O}$ = Mean of observed values

Bias can be returned as positive or negative. Desired values are within 10 for water depth and within 20 for salinities. Both of these metrics were achieved for each flow regime as shown in Table 3.4.

Bias Analysis				
Station	2018 Water Depth	2017 Water Depth	2018 Salinity	2017 Salinity
USGS 292800090060000	0.053	0.117	0.200	0.483
USGS 7380335	0.097	0.094	0.382	2.399
USGS 073802512	0.063	0.105	0.142	0.395
USGS 292859090004000	0.000	0.091	0.090	0.756
USGS 07380330	0.011	0.041	0.058	0.289
USGS 07380251	0.018	0.015	0.135	0.653
Number of Passing Stations	6	6	6	6

Table 3.4: Results of bias analysis at the calibration points for 2018, representing a high flow year, and 2017, representing a normal flow year, along with the number of passing stations.

3.4.4 Critical Model Outputs

The stage and salinity can be calibrated directly on this model. Unfortunately, since no other diversions were modeled, sediment cannot be directly calibrated. Instead the values of settling velocity, sediment formulation coefficients, sediment substrate parameters, and morphological parameters were all determined using previous research.

Chapter 4: Results

4.1 Introduction

The stage level, erosion, velocity, and sediment transport of the model runs were processed to show the variation from the No Diversion scenario. The various diversion scenarios are compared to each other under each Mississippi River flow year shown in Figure 4.1 and 4.2 and described in Section 2.6.

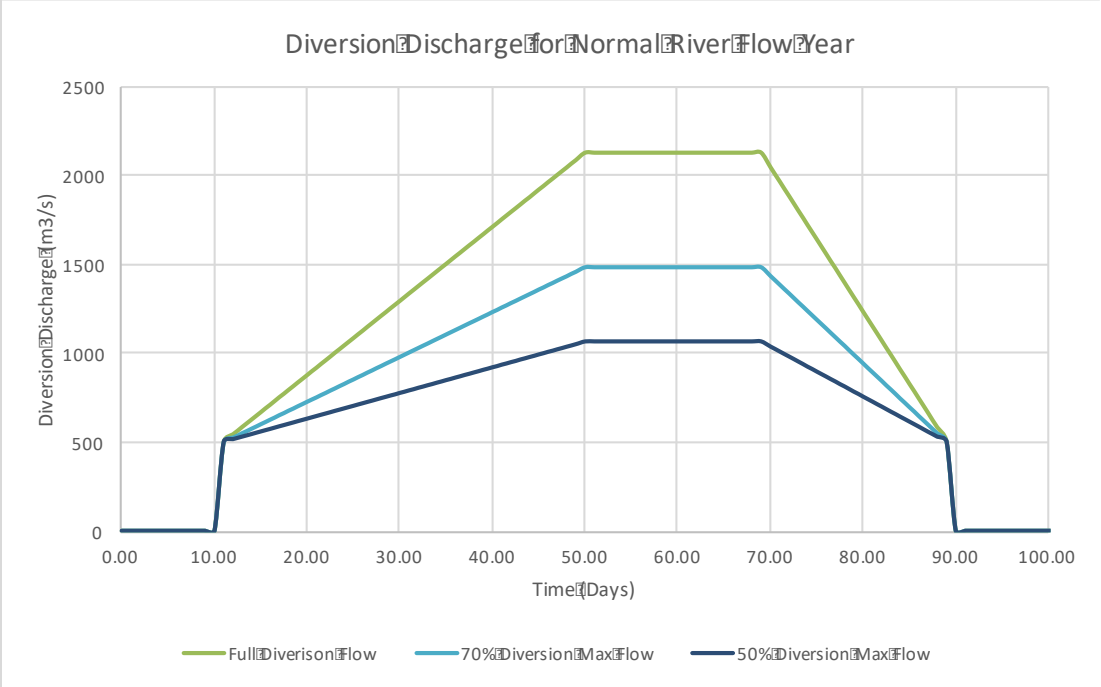

Figure 4.1: The operation scenarios for the Mid-Barataria Sediment Diversion during the Normal River Flow Year

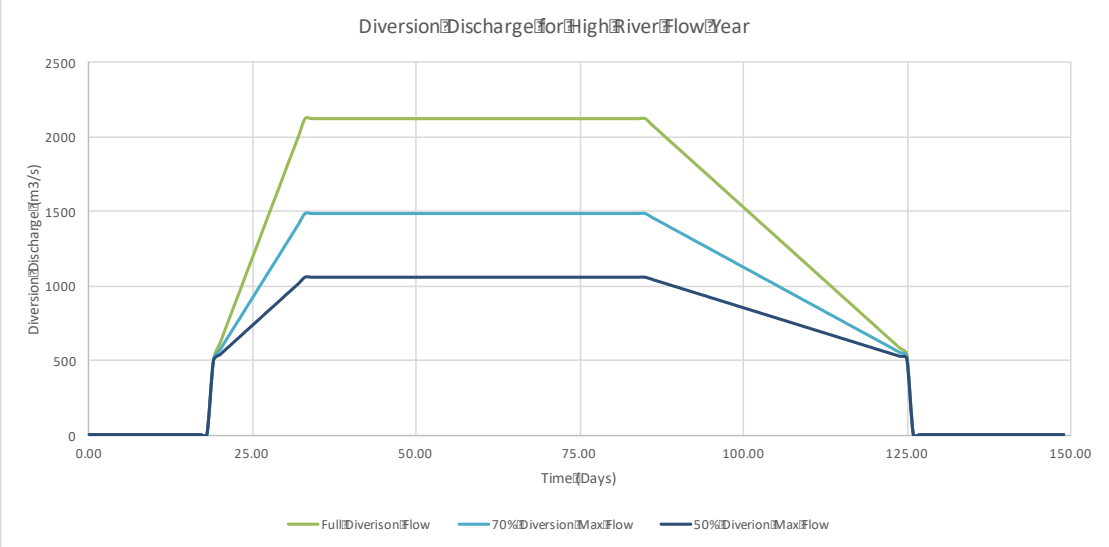

Figure 4.2: The operation scenarios for the Mid-Barataria Sediment Diversion during the High River Flow Year

Monitoring stations over the model domain was analyzed and three district distributary channels develop from the diversion shown in Figure 4.3, so only information from monitoring stations within these paths were shown. The paths are as flows: The Northern Path flows from the diversion south west to Bayou DuPont and then north west through Bayou DuPont to The Pen, over into North Barataria Waterway then travels through Bayou Rigolettes/Perot into Barataria Bay through Little Lake. The Southern Path flows south and then west through the broken marshland into Bayou DuPont, then south into Round Lake east into Lake Laurier and into Wilkinson Bayou. The Mid-Barataria Waterway Path comes from a collection of flow through the broken marsh system east through the open water of Bayou DuPont and into Mid-Barataria Waterway. From there it flows south through the waterway into the bay. All of these locations are shown in Figure 4.4 along with the observations points in the model.

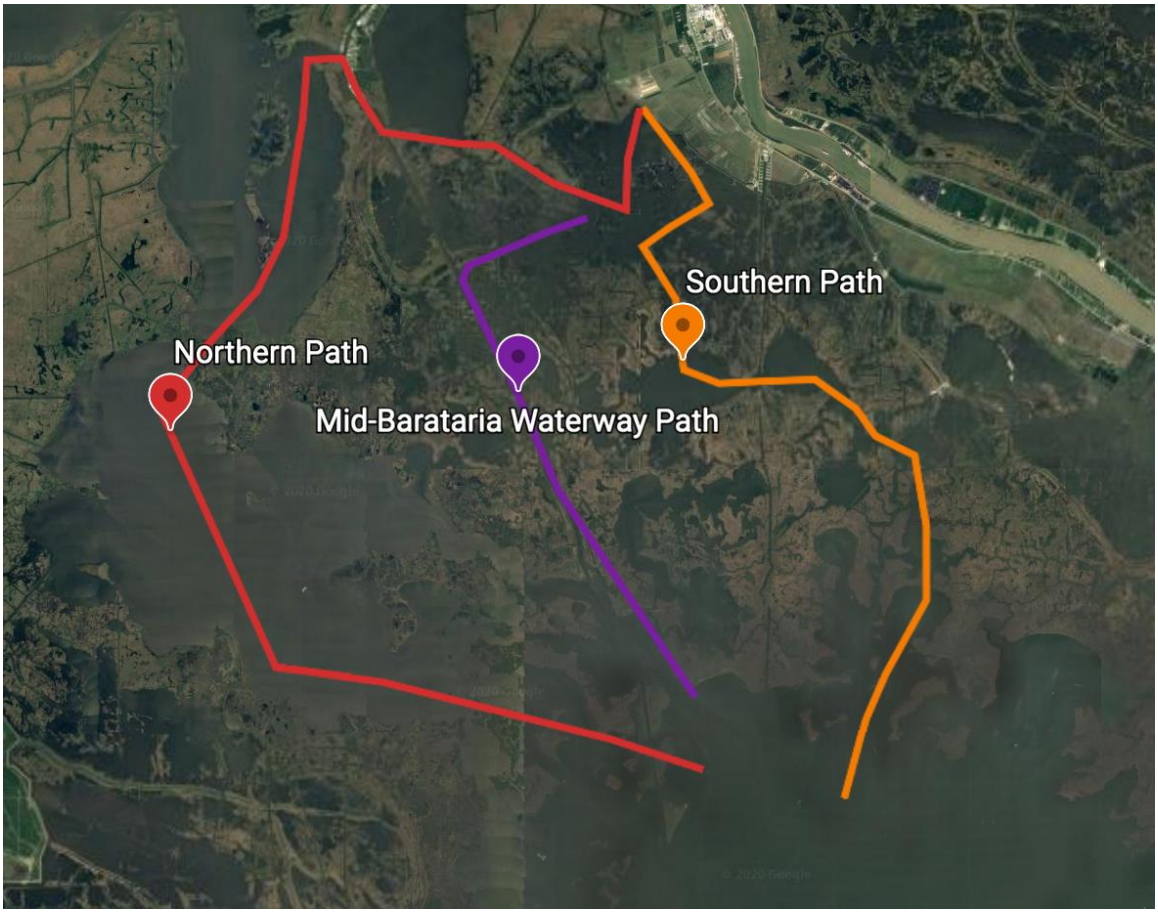

Figure 4.3: Three major distributary channels established by the Mid-Barataria Sediment Diversion.

Figure 4.4: Locations described in this chapter are in blue and monitoring stations with data displayed in this chapter are in red.

4.2 Water Level

The Mid-Barataria Sediment Diversion will introduce a large quantity of Mississippi River water into the receiving basin. Where this water will flow depends on how the water interacts with the distributary channels already present in the receiving basin. Monitoring stations placed in the model domain captured this rise in water level. All monitoring stations and location references are shown in Figure 4.1. Water level data are displayed using a 48-hour moving average filter to remove all tidal signals still present in the difference files.

The station closest to the diversion is Bayou DuPont just over 3 km away. Even with the gradual opening of the diversion, the water levels rise over half a meter within the first week of the diversion opening. Figure 4.5 shows the difference in water level between each operational scenario of the diversion and the reference No Diversion datum at Bayou DuPont. The first ten days the diversion is not open and water levels are nearly constant with the No Diversion water levels. Once the diversion is opened and flow begins to increase, water levels increase based upon operational scenario of the diversion. This is the same for the high and normal flow years. The operation of the diversion can change water levels at this point greatly. Operating the diversion at maximum flow during a high flow year can cause up to 1 m in water level rise above the No Diversion water levels but operating the diversion at 50% maximum flow during a normal flow year only causes an increase in water levels of 0.6 m above the No Diversion case. During the normal flow year, the maximum water level at this point is reached before the diversion reaches its full capacity at Day 50. Then there is a significant decrease in water levels between Day 60 and Day 70 while the diversion was still operating at capacity. During the high flow year, the water level peaks at this location at Day 35 when the diversion reaches its peak discharge but the water level soon begins to decrease at this station while the diversion is still operating at its capacity (Figure 4.6).

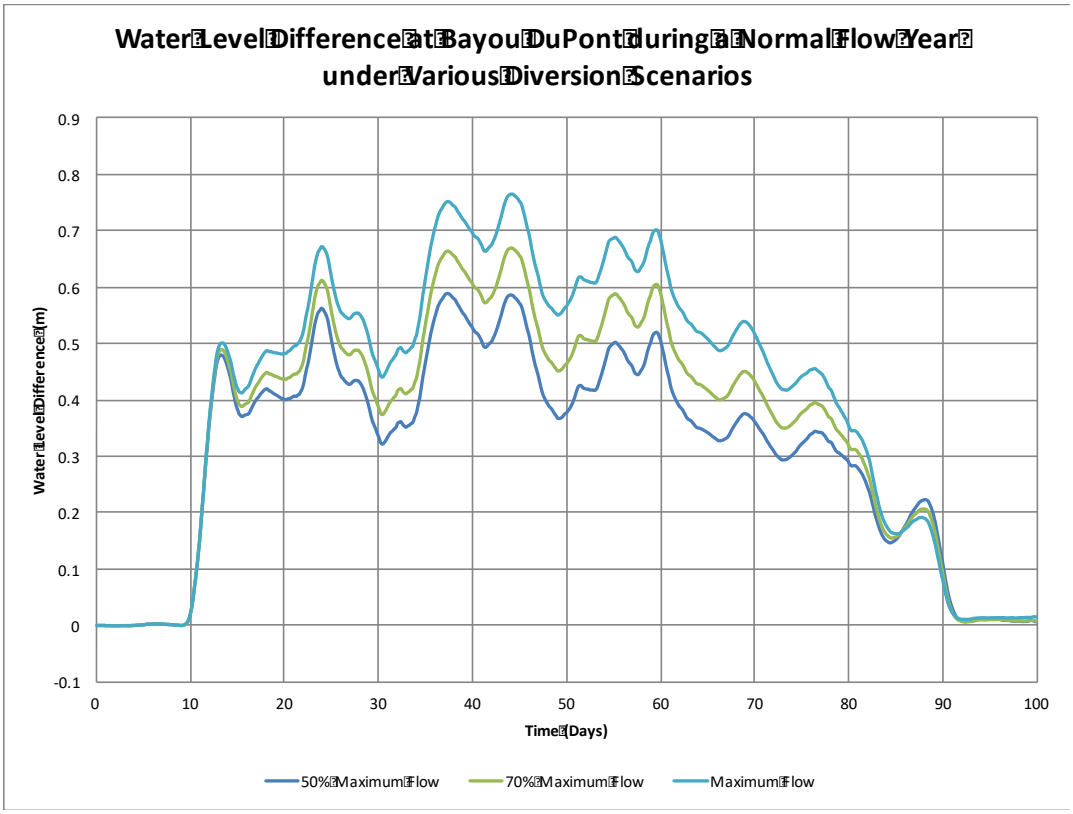

Figure 4.5: The difference in water levels at Bayou DuPont during a normal Mississippi River discharge year as compared to the No Diversion scenario with a 48-hour centered moving average filter applied to remove tidal differences.

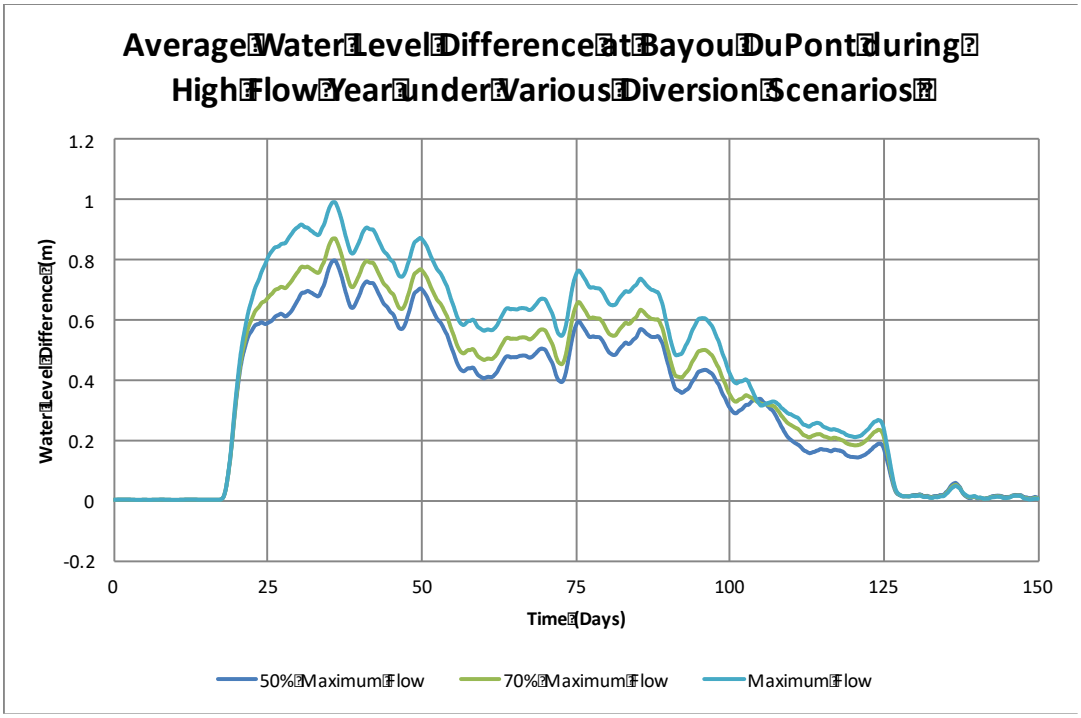

Figure 4.6: The difference in water levels at Bayou DuPont during a high Mississippi River discharge year as compared to the No Diversion scenario with a rolling 48-hour average filter applied to remove tidal differences.

Approximately 11 km south of the diversion is Round Lake. This significant lake is the first lake that flow from the diversion will reach. This location shows similar water level elevations as Bayou DuPont (Figure 4.7). Its initial rise in water level is over the same amount of time during both river flow scenarios (Figure 4.8). After the initial rise, flood levels remain similar between Bayou DuPont and Round Lake. When the diversion closes it takes water levels at each location less than a day to return to the no diversion scenario.

In Barataria Waterway, water levels increase as the flow out of the diversion increases, peaking when the diversion reaches its maximum capacity before dropping back to almost zero after closure of the diversion. In the northern and central parts of Barataria Waterway the flow is dominated by the diversion which increases water levels 0.4 m when the diversion is operating at maximum capacity and 0.2 m when it is at 50% capacity during a normal flow year (Figure 4.9 and 4.10). The high flow conditions increase water levels to 0.4 m when the division is at capacity and 0.2 m at 50% capacity as compared to No Diversion scenario (Figure 4.11 and 4.12).

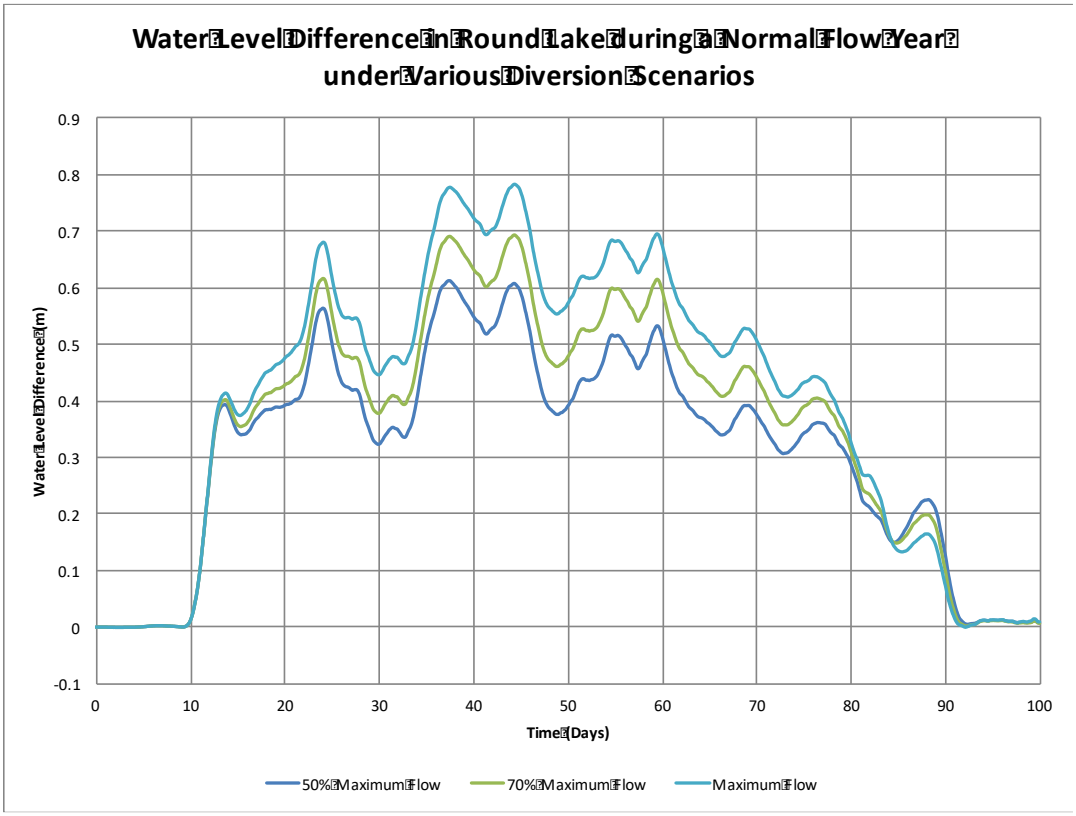

Figure 4.7: The difference in water levels at Round Lake during a normal Mississippi River discharge year as compared to the No Diversion scenario with a rolling 48-hour average filter applied to remove tidal differences.

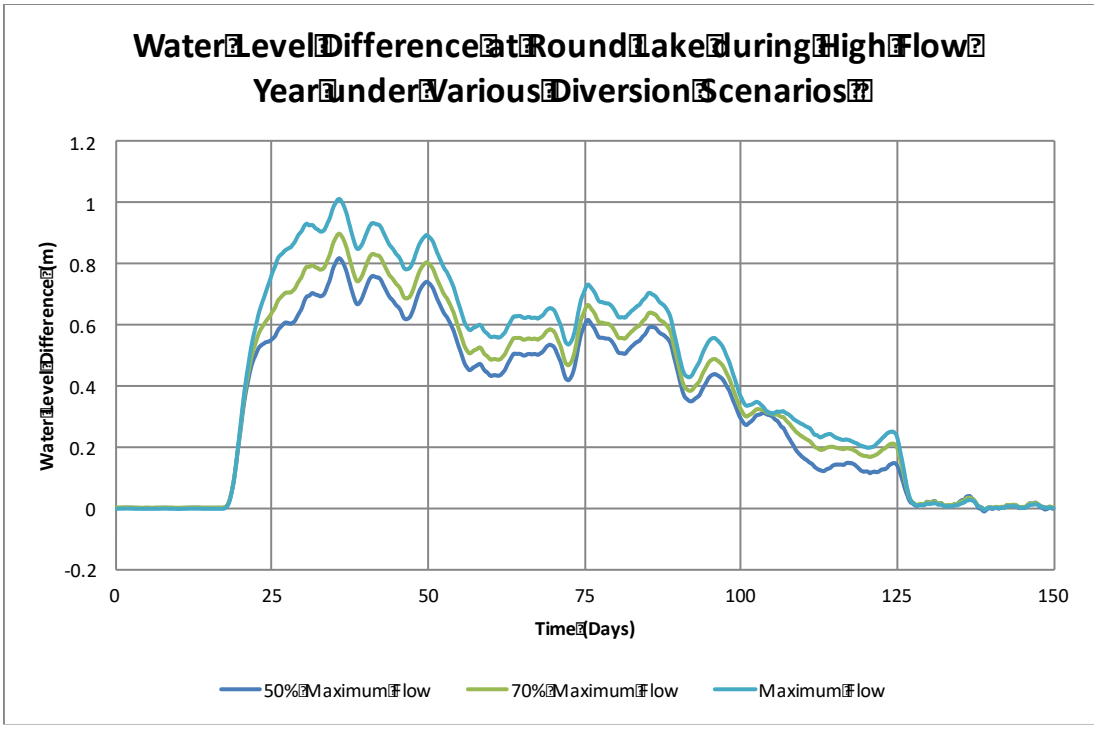

Figure 4.8: The difference in water levels at Round Lake during a high Mississippi River discharge year as compared to the No Diversion scenario with a rolling 48-hour average filter applied to remove tidal differences.

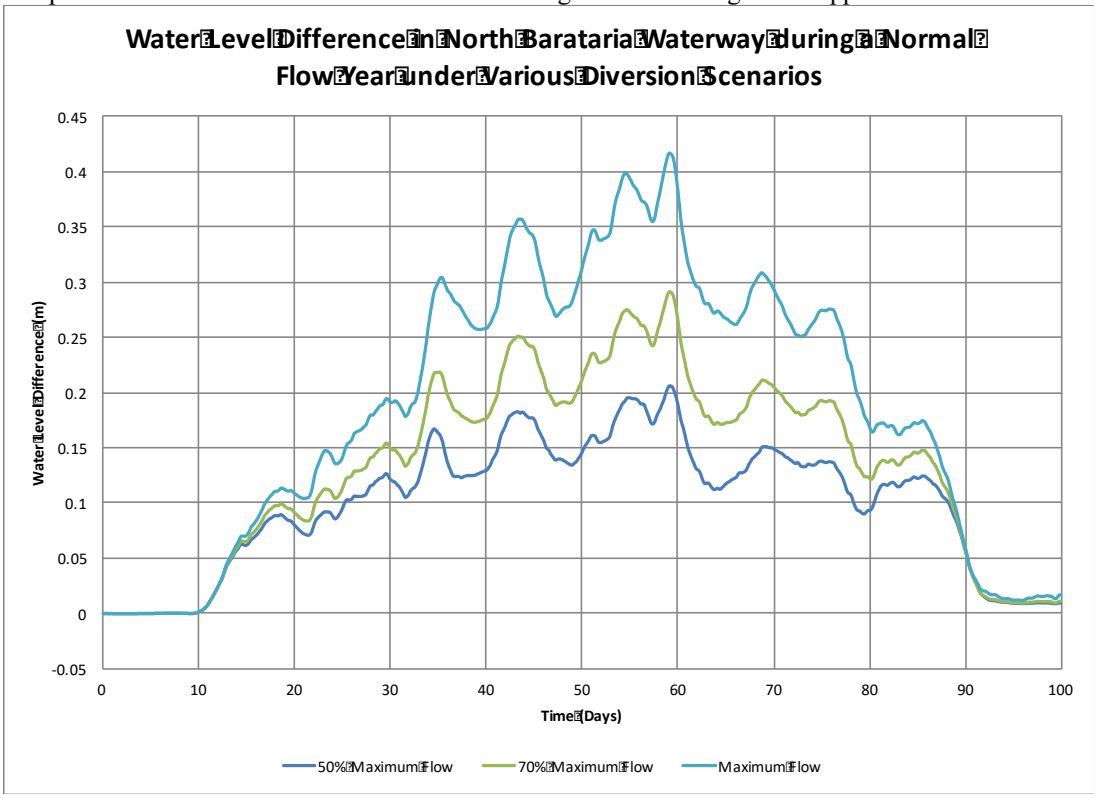

Figure 4.9: The difference in water levels in North Barataria Waterway during a normal Mississippi River discharge year as compared to the No Diversion scenario with a rolling 48-hour average filter applied to remove tidal differences.

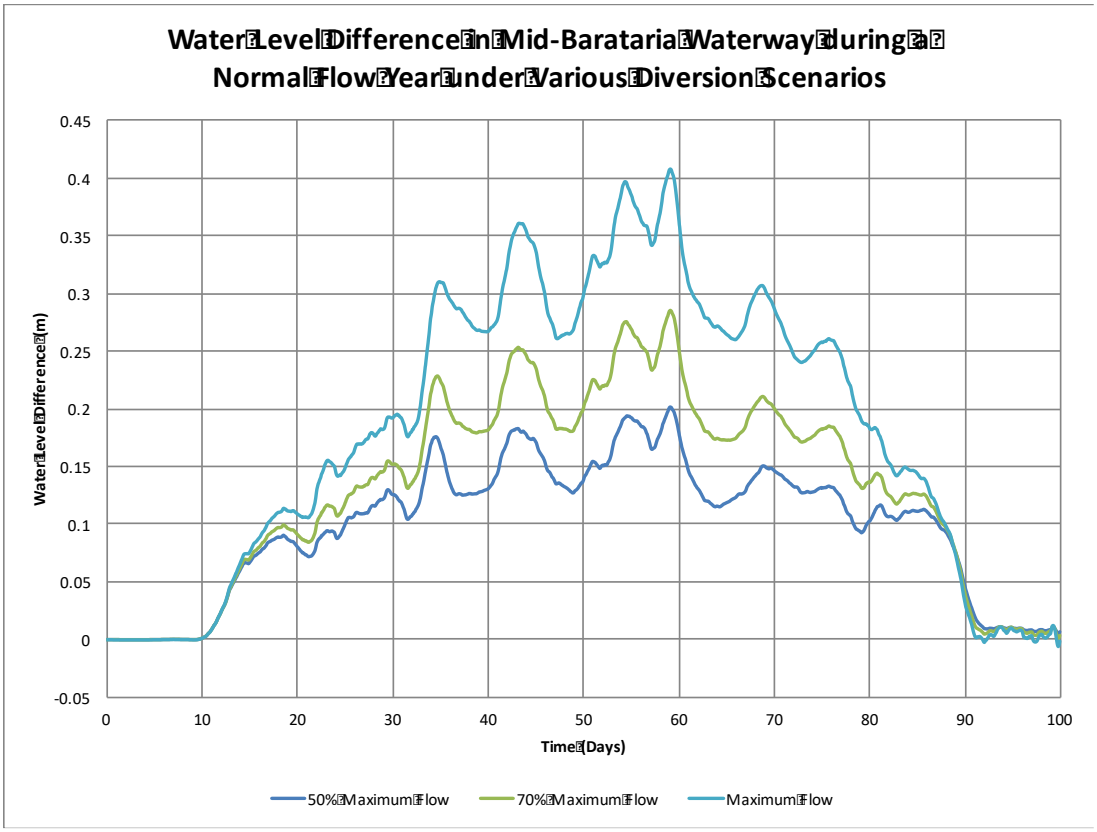

Figure 4.10: Mid-Barataria Waterway water level difference during a normal Mississippi River discharge year as compared to the No Diversion scenario with a rolling 48-hour average filter applied to remove tidal differences.

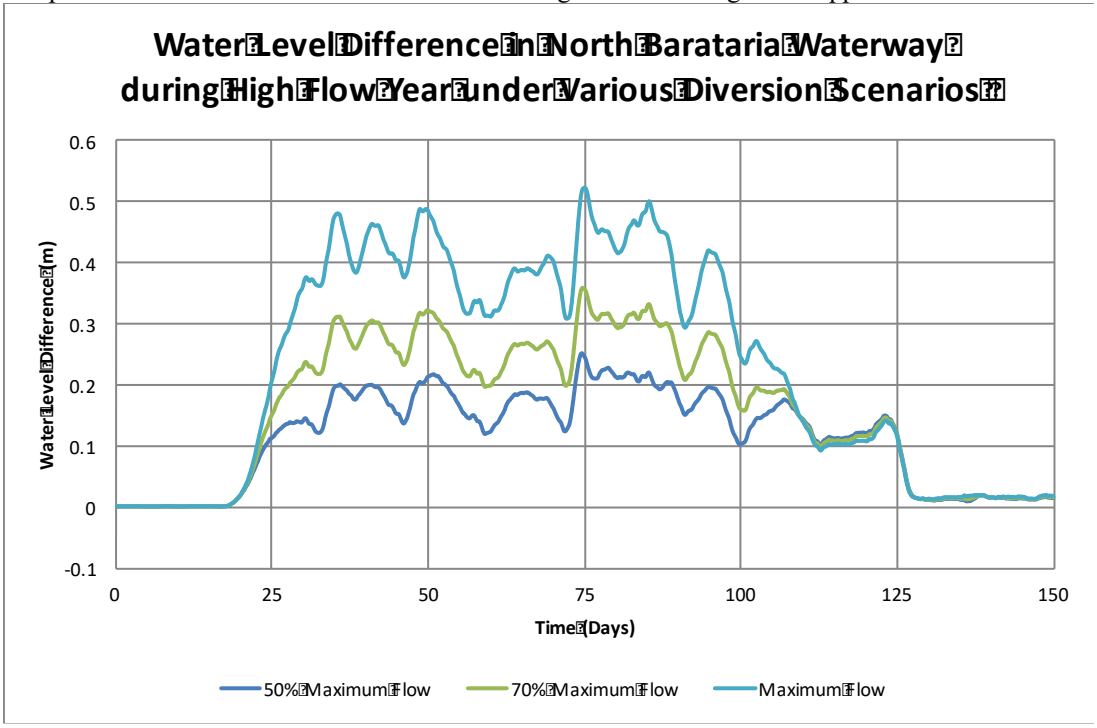

Figure 4.11: North Barataria Waterway water level difference during a high Mississippi River discharge year as compared to the No Diversion scenario with a rolling 48-hour average filter applied to remove tidal differences.

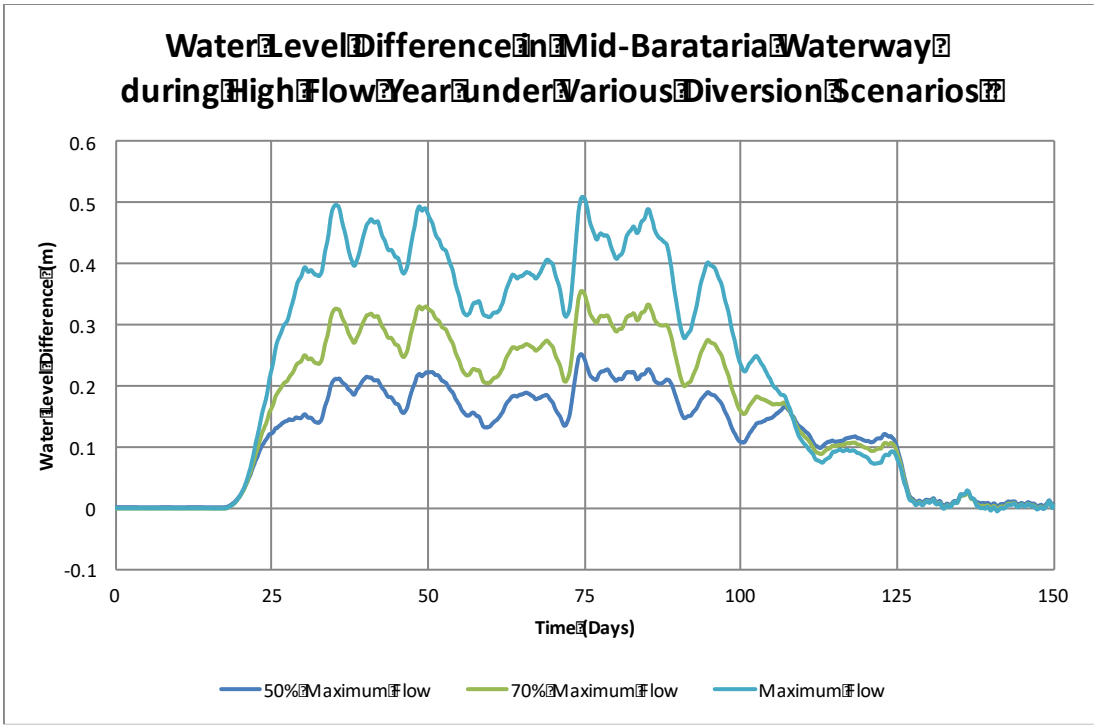

Figure 4.12: The difference in water levels in Mid-Barataria Waterway for the 50% maximum, 70% maximum, and maximum flow of the diversion during a high Mississippi River discharge year as compared to the No Diversion scenario with a rolling 48-hour average filter applied to remove tidal differences.

The southern terminus of Barataria Waterway is tide dominated, but the diversion still increases the water level here by 0.17 - 0.22 m when the diversion reaches capacity as shown in Figure 4.13 and Figure 4.14. Tides can still alter the water level by more than this amount.

Outflow from the diversion also travels north into Lake Salvador as shown in Figure 4.15 and Figure 4.16. Here the water levels can rise as high as 0.4 m during the maximum flow in the diversion, which is similar to the water levels in Barataria Waterway.

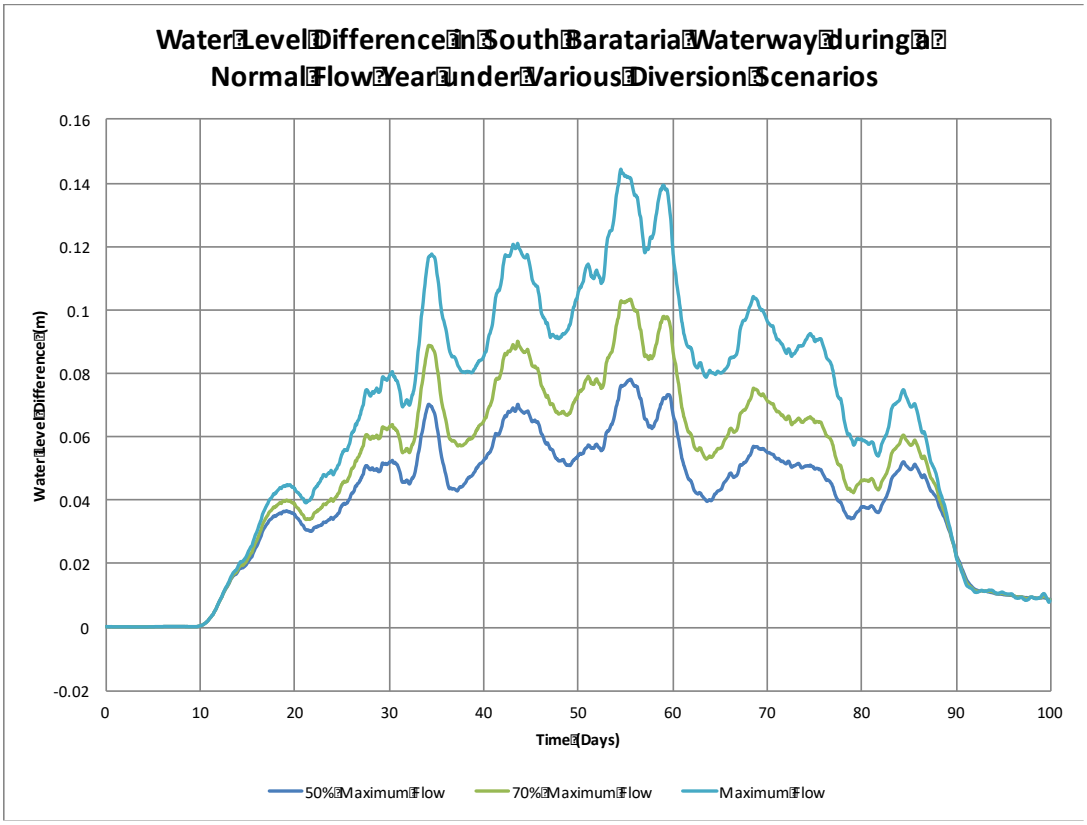

Figure 4.13: South Barataria Waterway water level difference during a normal Mississippi River discharge year as compared to the No Diversion scenario with a rolling 48-hour average filter applied to remove tidal differences.

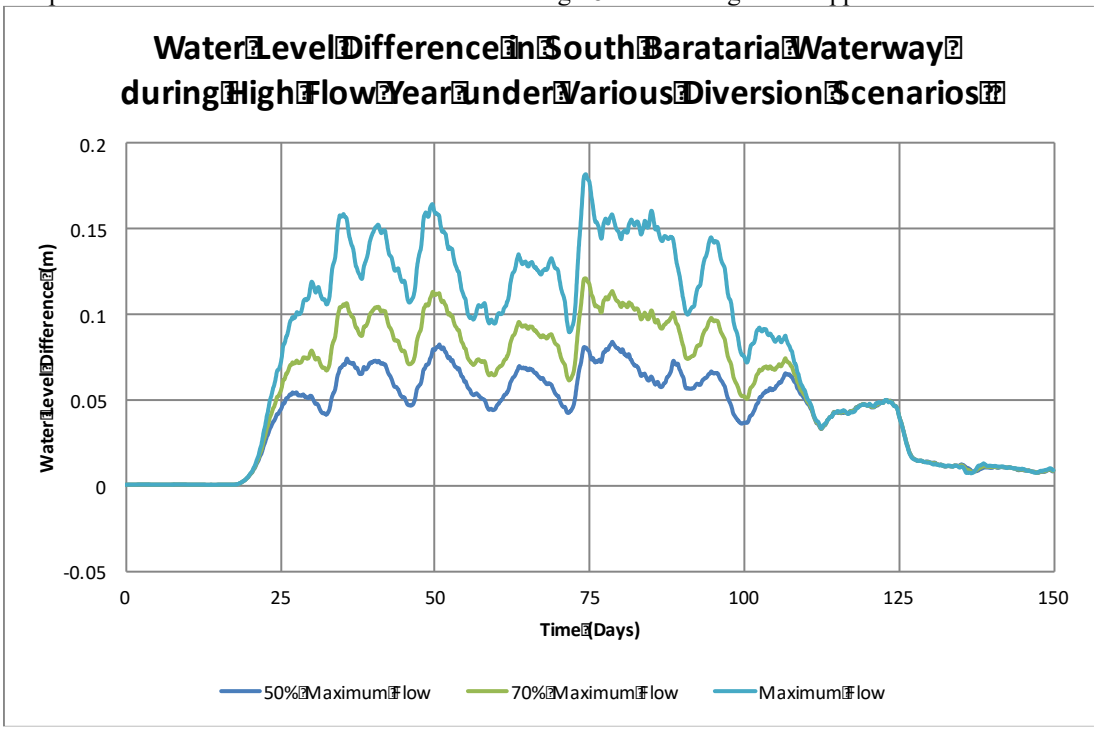

Figure 4.14: South Barataria Waterway water level difference during a normal Mississippi River discharge year as compared to the No Diversion scenario with a rolling 48-hour average filter applied to remove tidal differences.

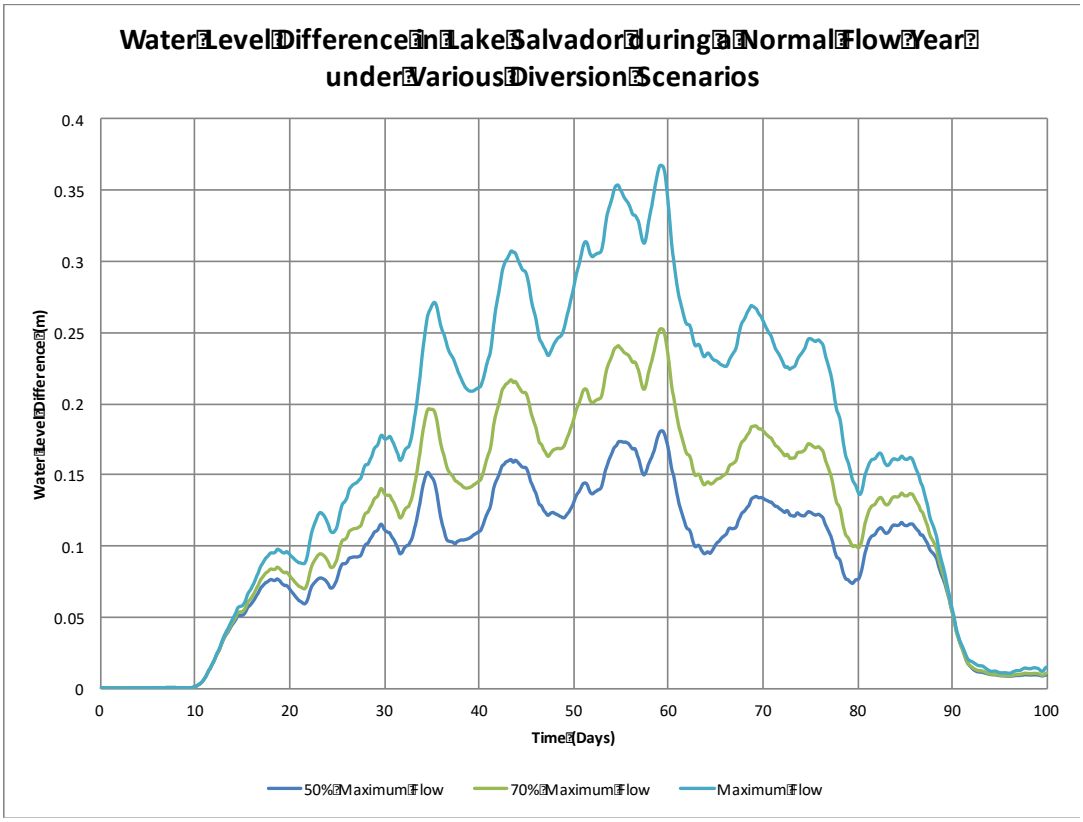

Figure 4.15: The difference in water levels in Lake Salvador during a normal Mississippi River discharge year as compared to the No Diversion scenario with a rolling 48-hour average filter applied to remove tidal differences.

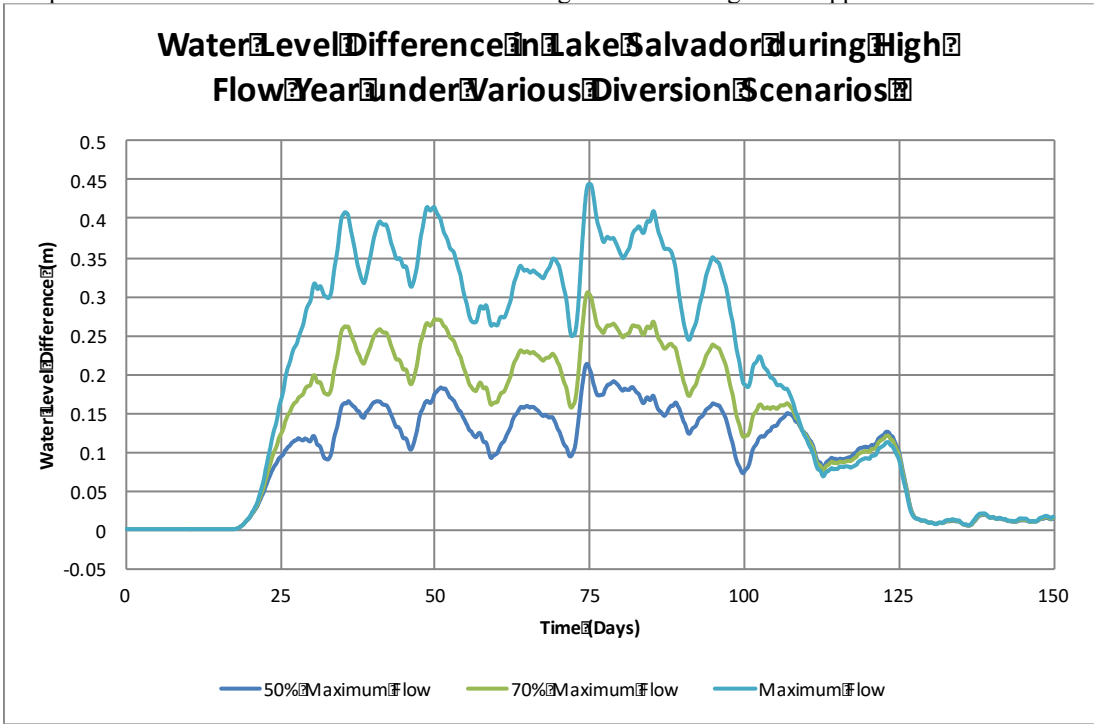

Figure 4.16: The difference in water levels in Lake Salvador during a high Mississippi River discharge year as compared to the No Diversion scenario with a rolling 48-hour average filter applied to remove tidal differences.

Grand Bayou also has a large tidal influence like the southern terminus of Barataria Waterway. However, it reaches a maximum water level much sooner and resembles the areas nearest the diversion during both normal and high flow year, shown in Figure 4.17 and Figure 4.18. During the high flow year, the water level begins to taper off around Day 60 which is 10 days before the diversion begins to reduce flow. Operating the diversion at 50% of the maximum flow will reduce flood heights in the area by 0.15 m during the operation of the diversion. Once the diversion is closed it takes less than a day for the water levels to return to normal.

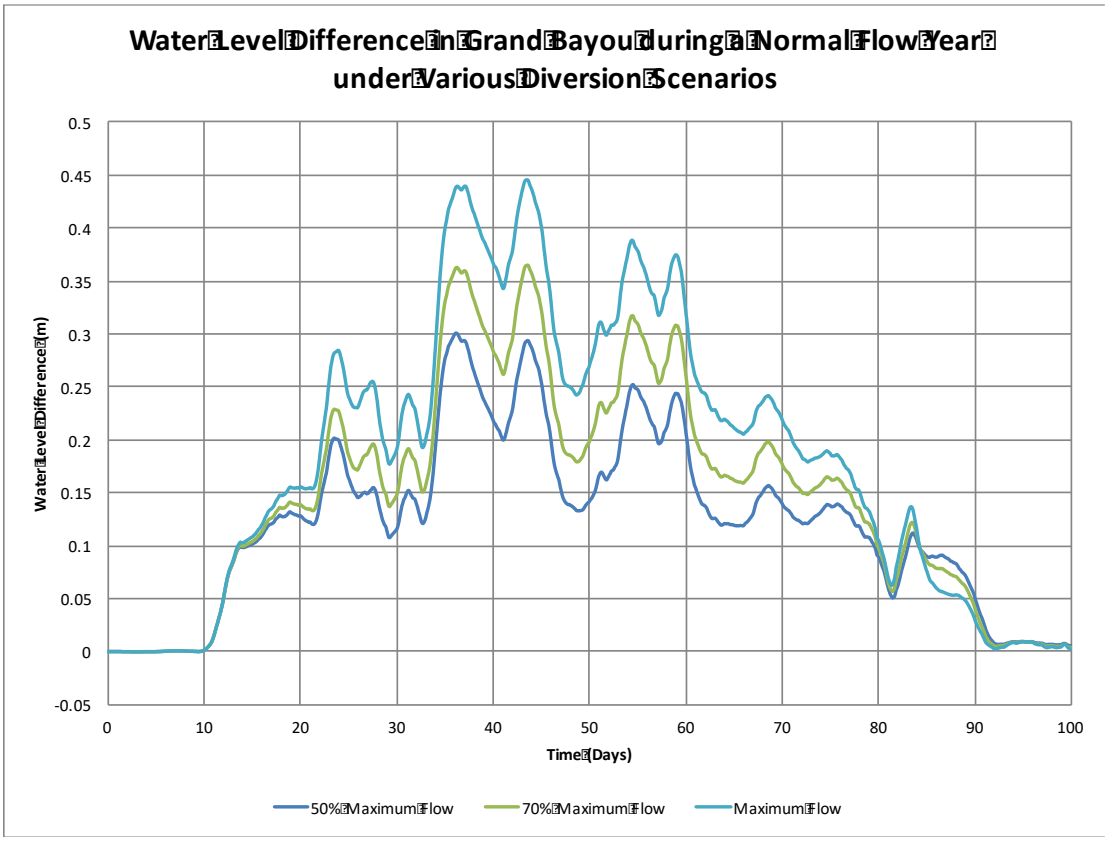

Figure 4.17: The difference in water levels in Grand Bayou for the 50% maximum, 70% maximum, and maximum flow of the diversion during a normal Mississippi River discharge year as compared to the No Diversion scenario with a rolling 48-hour average filter applied to remove tidal differences.

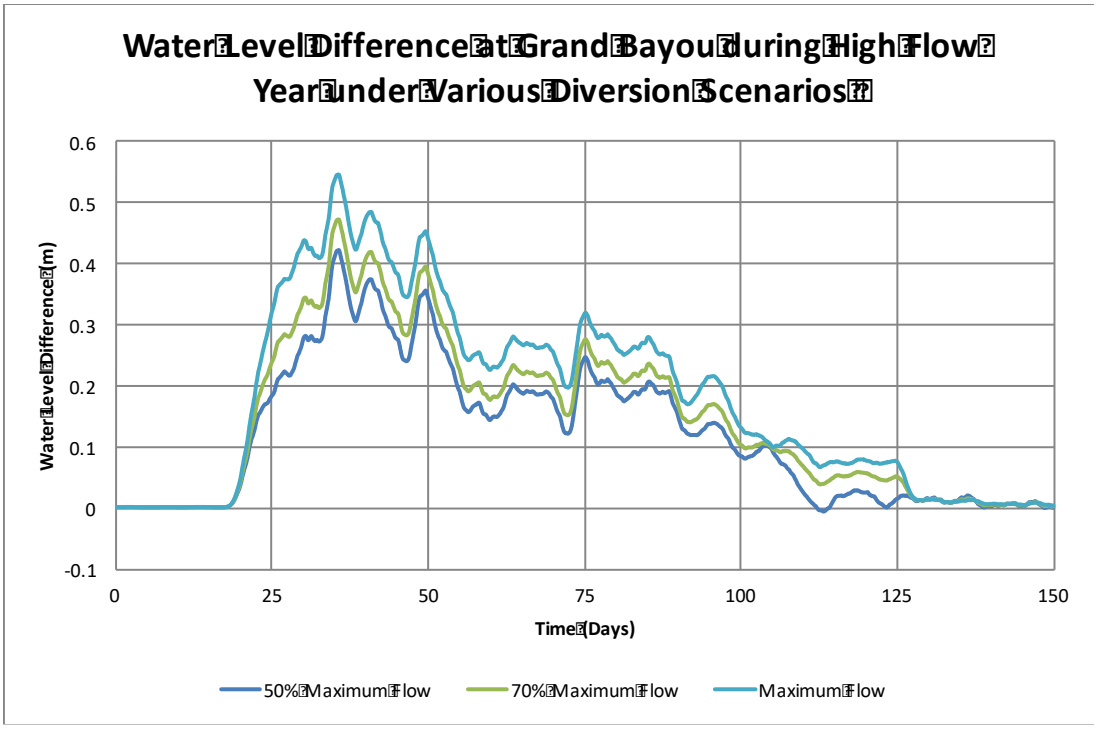

Figure 4.18: The difference in water levels in Grand Bayou for the 50% maximum, 70% maximum, and maximum flow of the diversion during a high Mississippi River discharge year as compared to the No Diversion scenario with a rolling 48-hour average filter applied to remove tidal differences.

4.3 Depth Averaged Velocity

Velocities were calculated throughout the domain. Areas of high velocity indicate potential erosion and low velocities indicate potential deposition. Selected velocities shown below are compared to the No Diversion scenario which should mostly remove the influences of tides. However, these velocities would contain the velocity change due to a changing tidal prism caused by the diversion or phase changes due to changes in the flow pathways.

As the diversion is opening, water rushes into the 'still' water receiving basin. After the flow enters the marsh, higher velocities occur south of the diversion during both normal and high flow years as shown in Figure 4.19 and Figure 4.20. Soon the diversion starts to develop three major distributary channels: a) south through Round Lake and Wilkinson Bayou, b) west through multiple small channels created by the diversion that eventually connect to Barataria Waterway, and c) north via Bayou DuPont into northern Barataria Waterway and eventually south through Bayou Rigolettes/Perot as shown in Figure 4.21 and Figure 4.22. Once these three channels develop, flow through Grand Bayou begins to drop as indicated in Figure 4.23 and Figure 4.24.

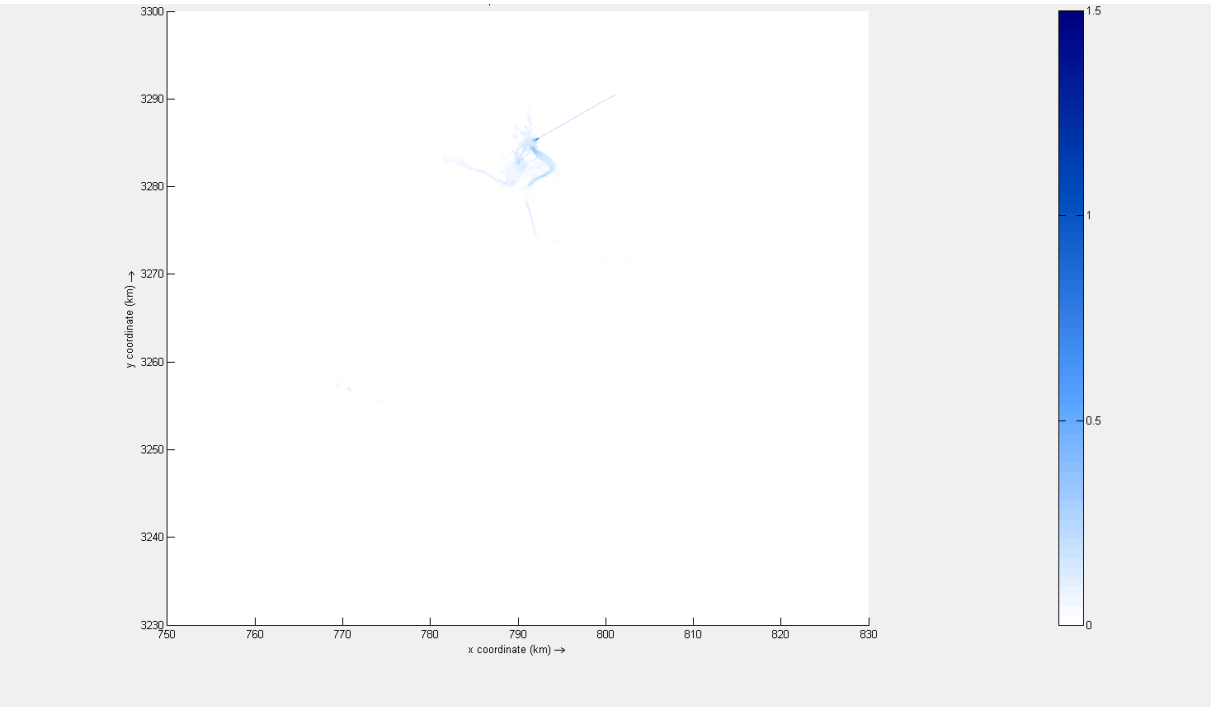

Figure 4.19: Depth averaged velocity in m/s one day after the diversion is opened (Day 11) during the normal Mississippi River discharge year over the domain based on Universal Trans-Mercator Zone 15R.

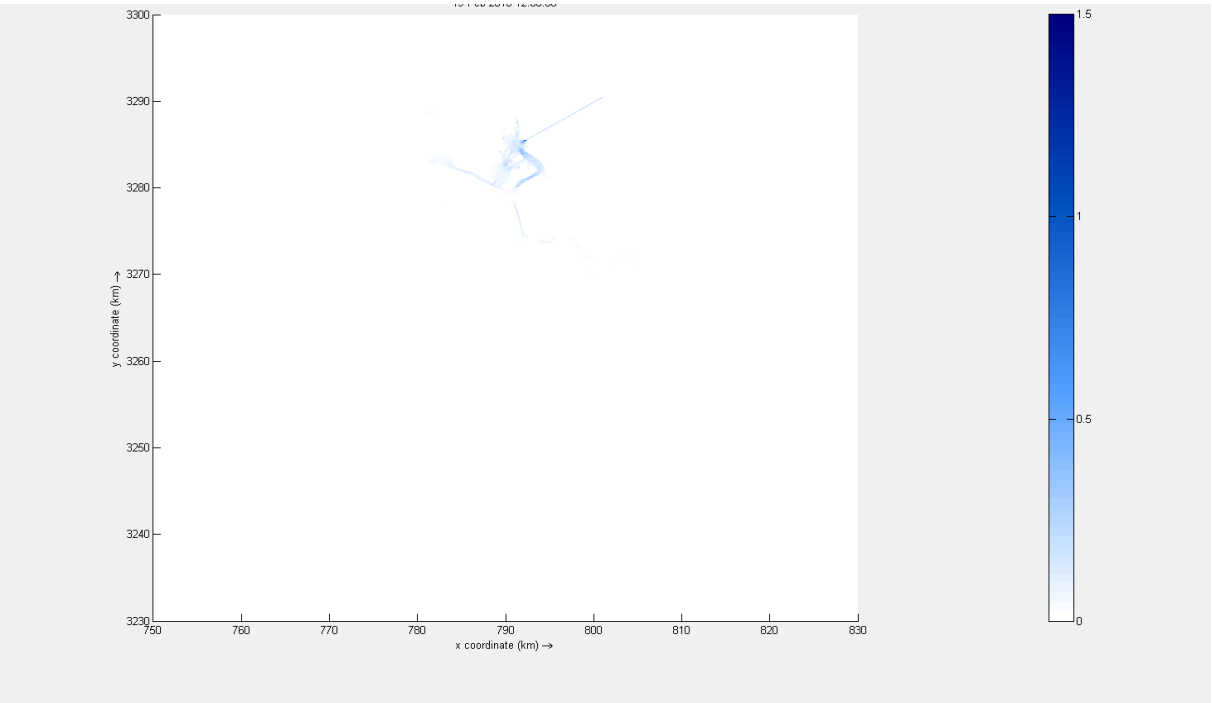

Figure 4.20: Depth averaged velocity in m/s one day after the diversion is opened (Day 19) during the high Mississippi River discharge year over the domain based on Universal Trans-Mercator Zone 15R.

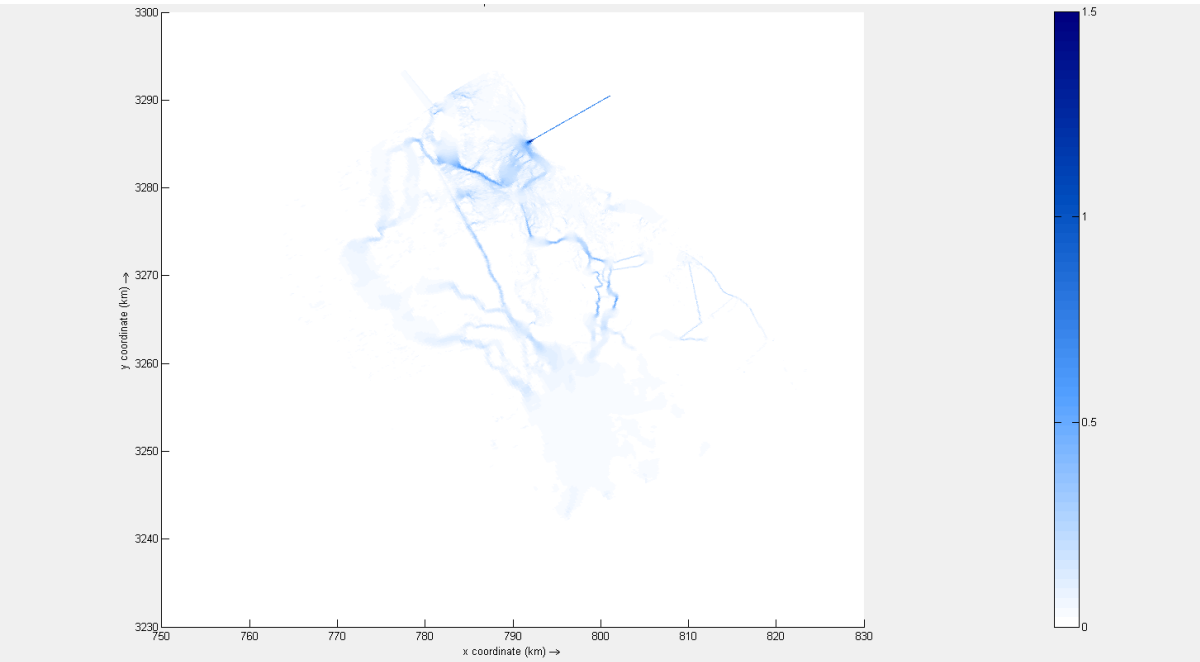

Figure 4.21: Depth averaged velocity in m/s once the diversion reaches maximum capacity on Day 50 during the normal Mississippi River discharge year over the domain based on Universal Trans-Mercator Zone 15R.

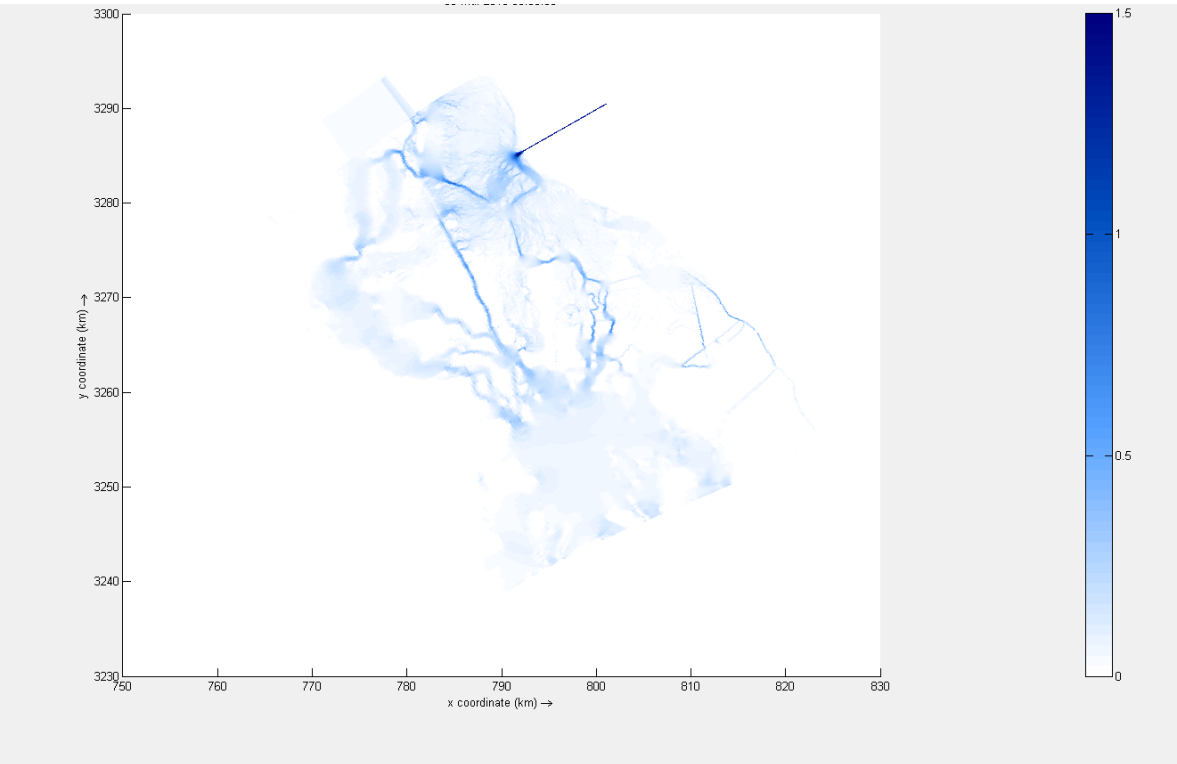

Figure 4.22: Depth averaged velocity in m/s once the diversion reaches maximum capacity on Day 36 during the high Mississippi River discharge year over the domain based on Universal Trans-Mercator Zone 15R.

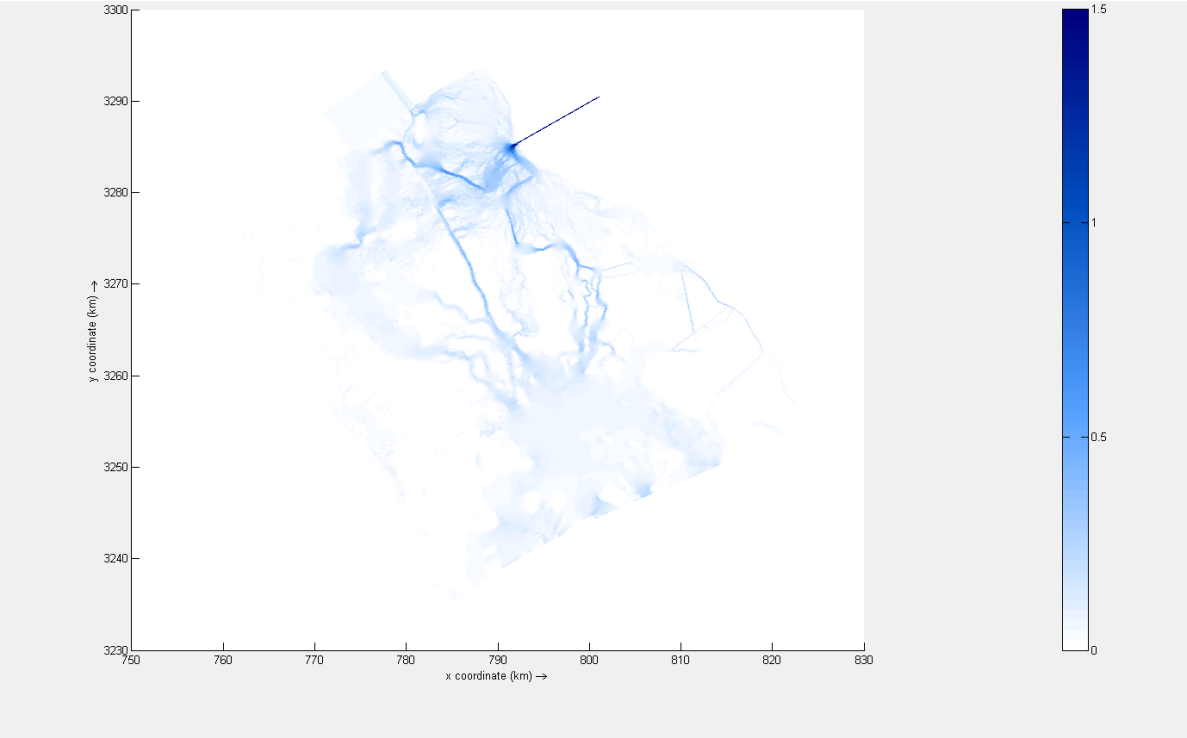

Figure 4.23: Depth averaged velocity in m/s just prior to the diversion reducing flow (Day 69) during the normal Mississippi River discharge year over the domain based on Universal Trans-Mercator Zone 15R.

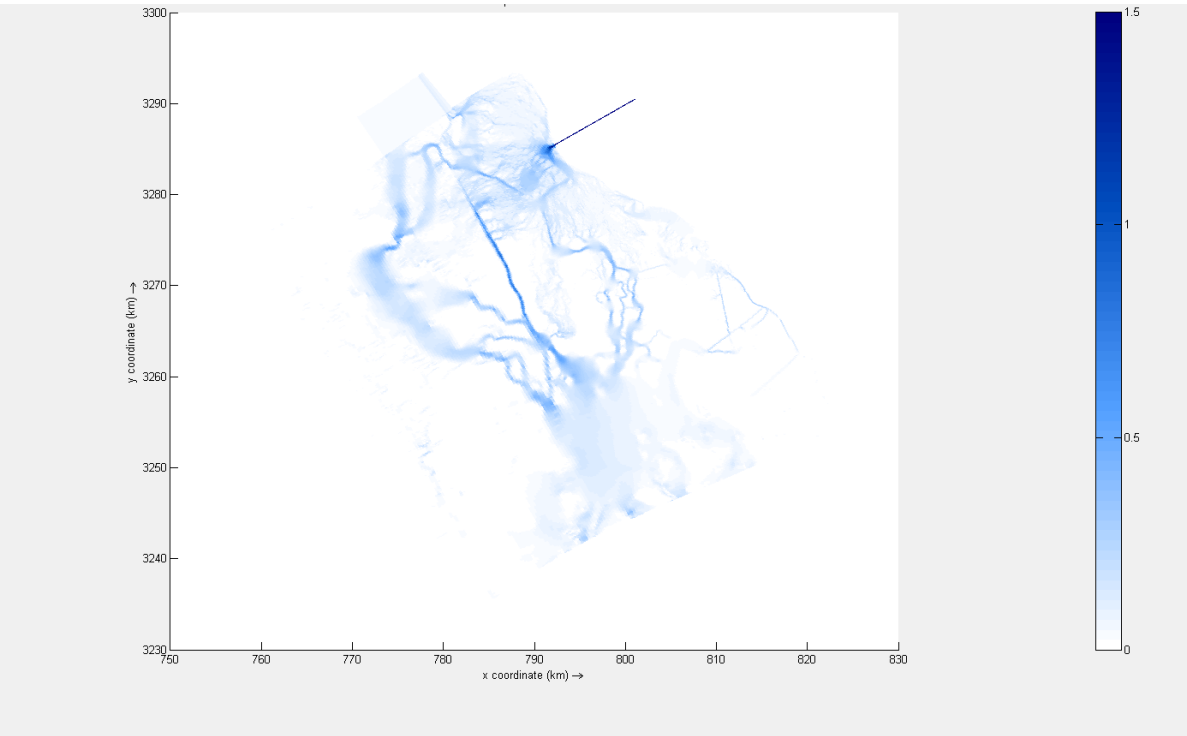

Figure 4.24: Depth averaged velocity in m/s just prior to the diversion reducing flow (Day 86) during the high Mississippi River discharge year over the domain based on Universal Trans-Mercator Zone 15R.

The Barataria Waterway carries two of the major distributary channels. Northern Barataria Waterway has an increase in velocity of about 0.17 m/s during the normal and high flow years regardless of the diversion's operation scenario. The peak of this flow happens before the diversion reaches full capacity during the normal flow year (Figure 4.25) and right as the diversion reaches capacity during a high flow year (Figure 4.26). This part of the Barataria Waterway receives flow from Bayou DuPont while the middle part of Barataria Waterway receives flow from the small distributary channels already present in the marsh but enhanced by the diversion. The velocity in the middle of Barataria Waterway follows the operation of the diversion closely peaking at Day 60 during the normal flow year and Day 80 during a high flow year. Operating the diversion at capacity increases velocity here by 0.5 m/s during normal flow years and 0.6 m/s during high flow years (Figure 4.27 and 4.28). This is similar to the southern terminus of the waterway as well (Figure 4.29 and 4.30).

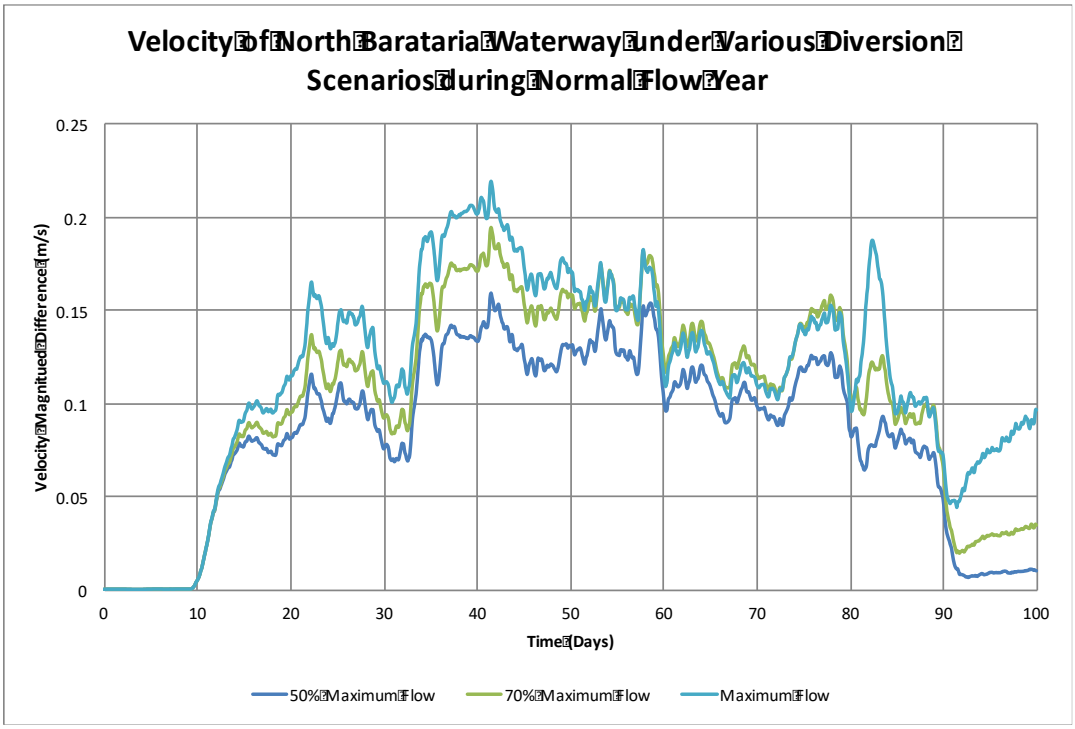

Figure 4.25: Depth averaged velocity due to different diversion operational strategies in North Barataria Waterway during a normal Mississippi River discharge year compared to the No Diversion scenario with a rolling 48-hour average filter applied to remove tidal differences.

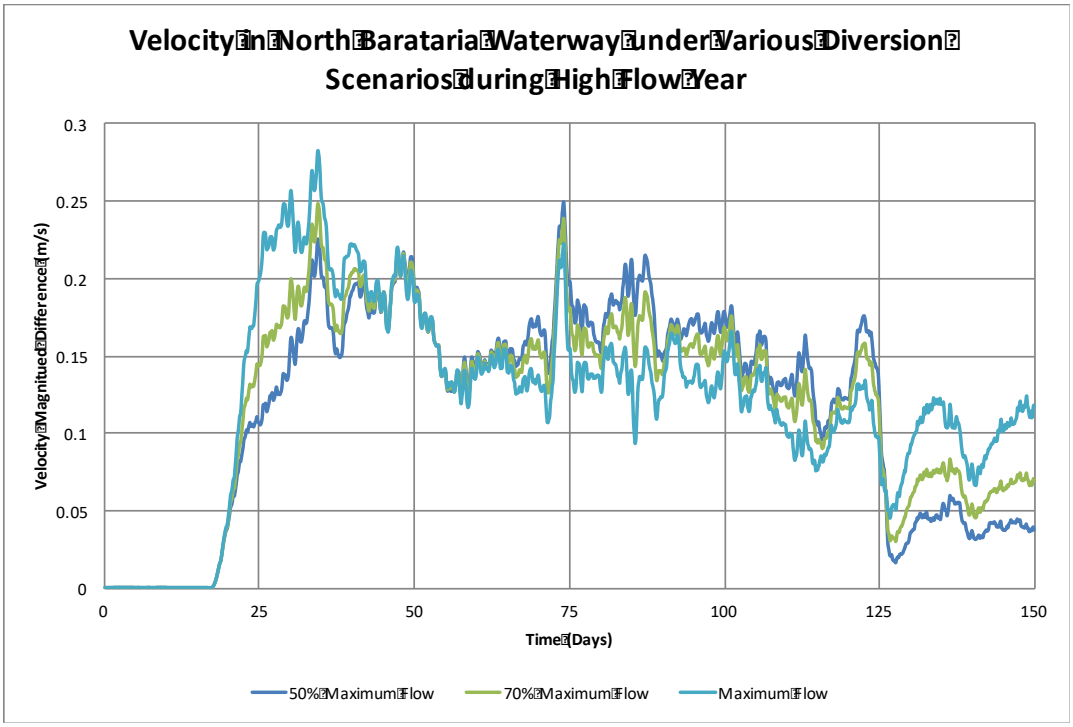

Figure 4.26: Depth averaged velocity due to different diversion operational strategies in North Barataria Waterway during a high Mississippi River discharge year compared to the No Diversion scenario with a rolling 48-hour average filter applied to remove tidal differences.

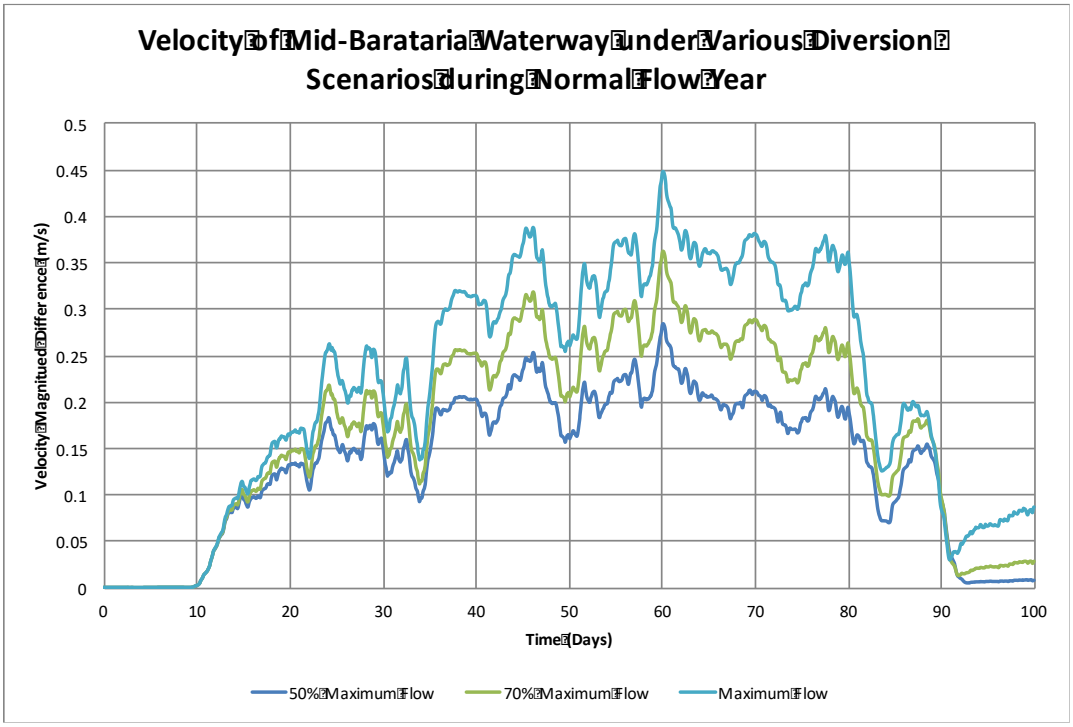

Figure 4.27: Depth averaged velocity due to different diversion operational strategies in Mid-Barataria Waterway during a normal Mississippi River discharge year compared to the No Diversion scenario with a rolling 48-hour average filter applied to remove tidal differences.

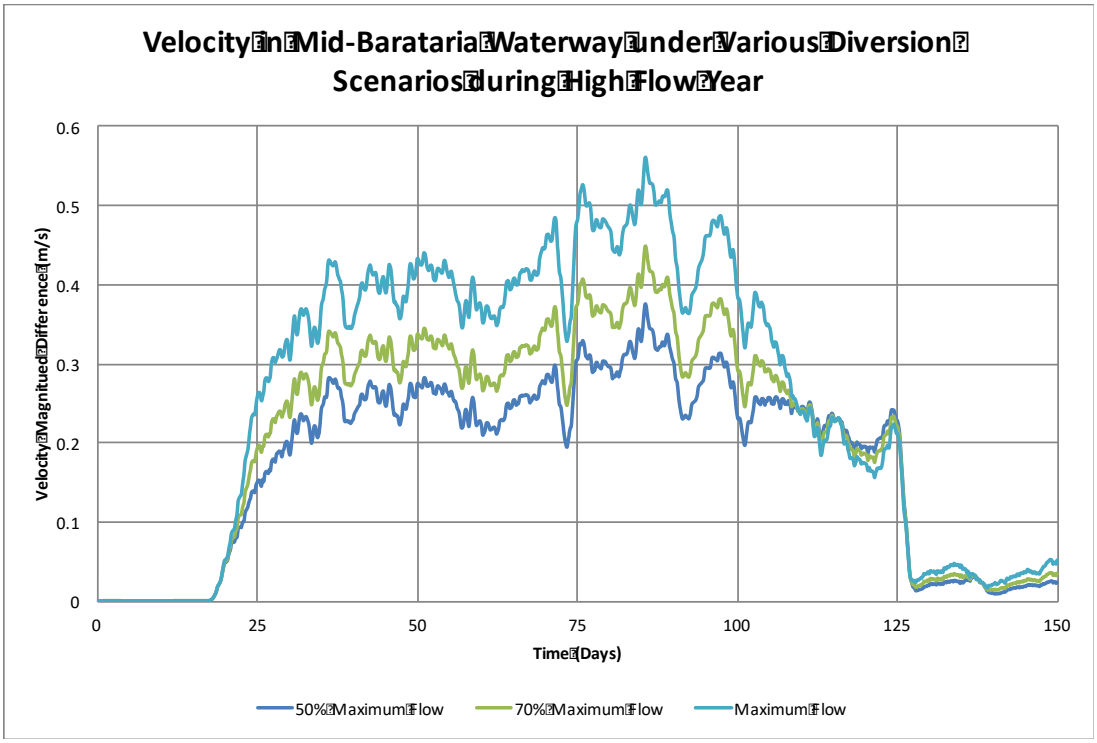

Figure 4.28: Depth averaged velocity due to different diversion operational strategies in Mid-Barataria Waterway during a high Mississippi River discharge year compared to the No Diversion scenario with a rolling 48-hour average filter applied to remove tidal differences.

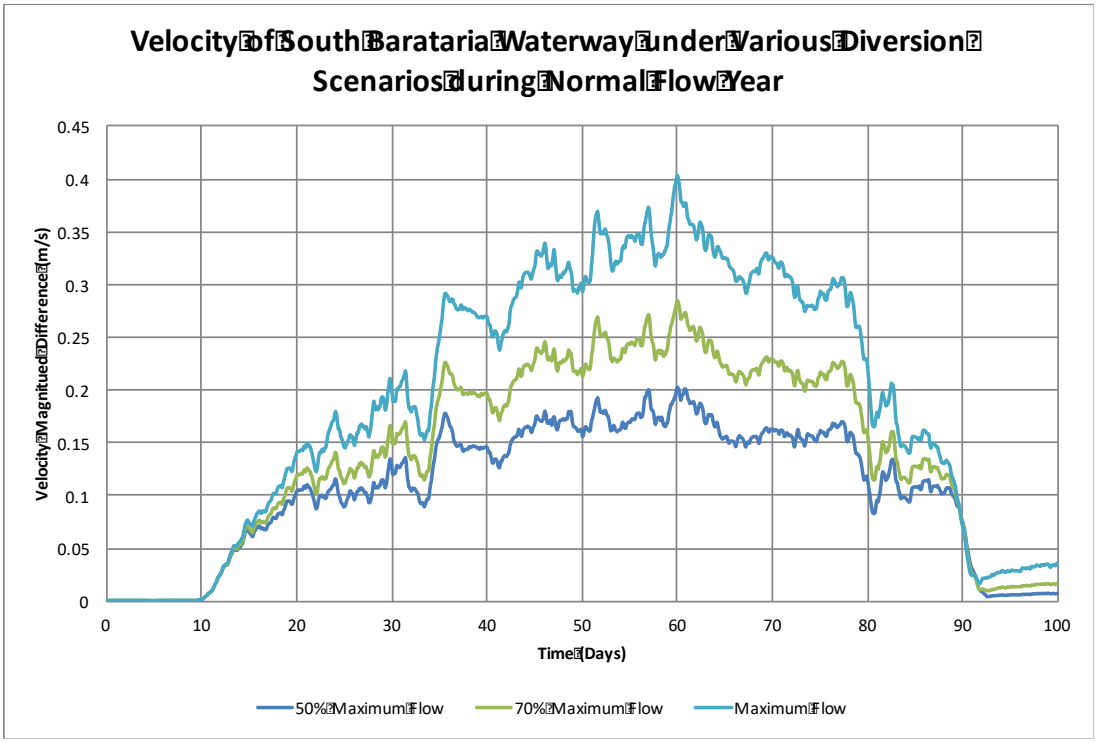

Figure 4.29: Depth averaged velocity due to different diversion operational strategies in South Barataria Waterway during a normal Mississippi River discharge year compared to the No Diversion scenario with a rolling 48-hour average filter applied to remove tidal differences.

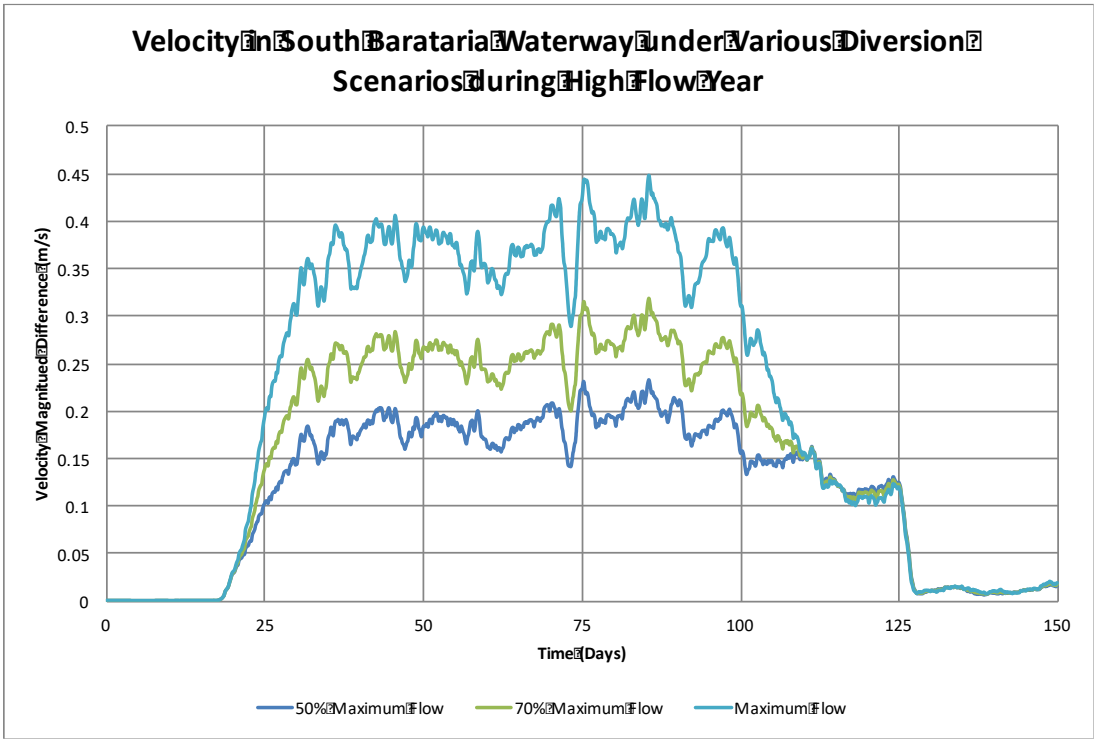

Figure 4.30: Depth averaged velocity due to different diversion operational strategies in South Barataria Waterway during a high Mississippi River discharge year compared to the No Diversion scenario with a rolling 48-hour average filter applied to remove tidal differences.

At Grand Bayou velocities also increase following the diversion operation. During the normal and high flow scenarios, the velocities can reach 0.4 m/s when the diversion is at full capacity. Running the diversion below capacity can reduce the velocity in the channel to up to 0.25 m/s (Figures 4.31 and 4.32).

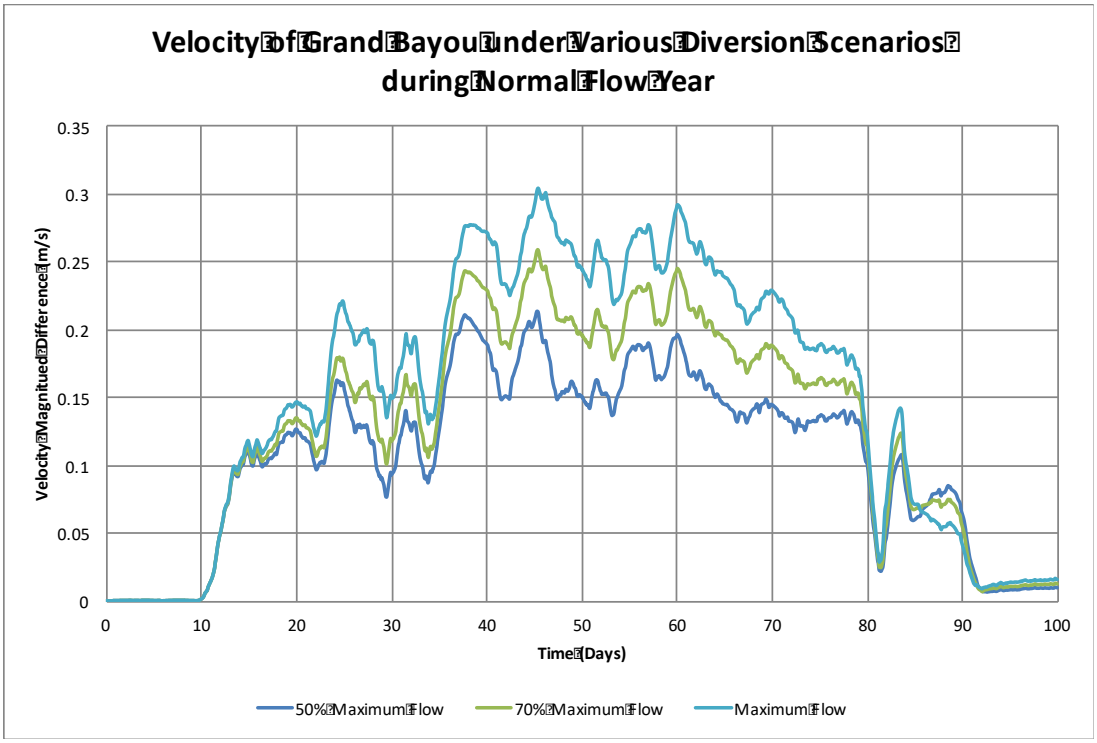

Figure 4.31: Depth averaged velocity due to different diversion operational strategies in Grand Bayou during a normal Mississippi River discharge year compared to the No Diversion scenario with a rolling 48-hour average filter applied to remove tidal differences.

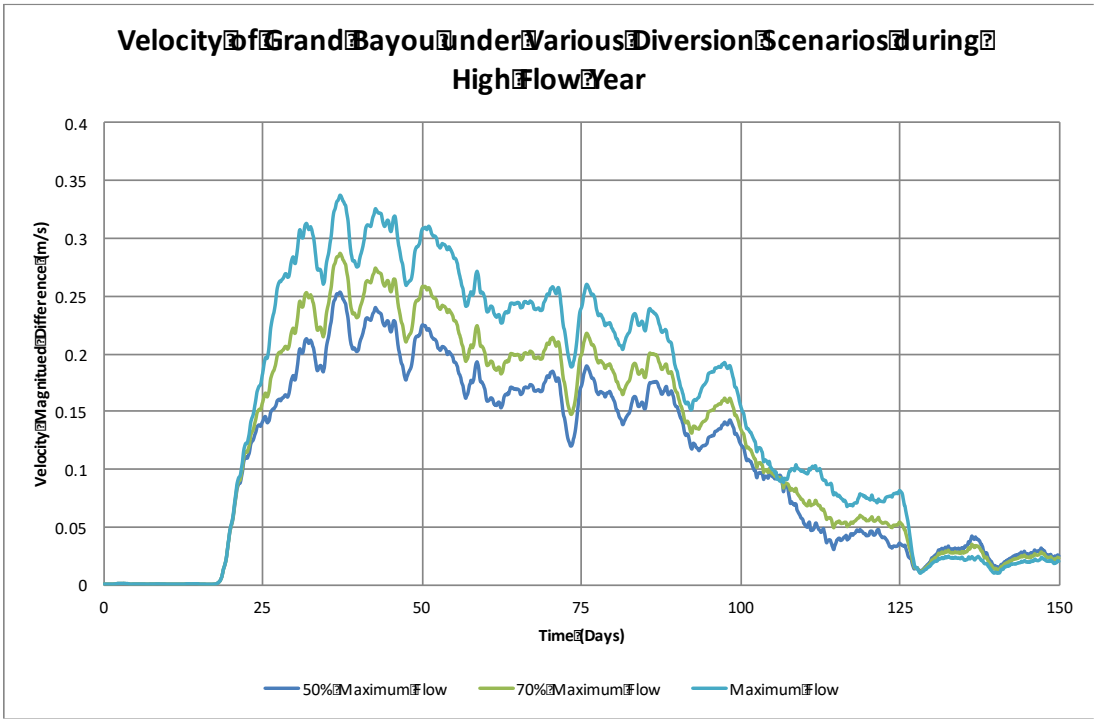

Figure 4.32: Depth averaged velocity due to different diversion operational strategies in Grand Bayou during a high Mississippi River discharge year compared to the No Diversion scenario with a rolling 48-hour average filter applied to remove tidal differences.

4.4 Geomorphology

4.4.1 Basin Wide

The diversion begins to scour a channel at the mouth of the diversion so that the flow can enter the basin (Figure 4.33). Immediately after opening of the diversion there is a strong southern current with a large eddy created south of the diversion and minimal movement of water to the north. As the flow through the diversion increases, the mouth of the diversion continues to erode forming a deeper channel at the mouth of the diversion. The strong southern current increases and the higher elevated land below the flooded surface begins to erode. Sediment is deposited in the counter rotating eddies just north and to the south of the diversion. Another portion of the flow goes west south west from the diversion making its way to Barataria Waterway. The area between this flow and the southern flow creates an area of nearly stagnate water southwest of the diversion where sediment is deposited (Figure 4.34).

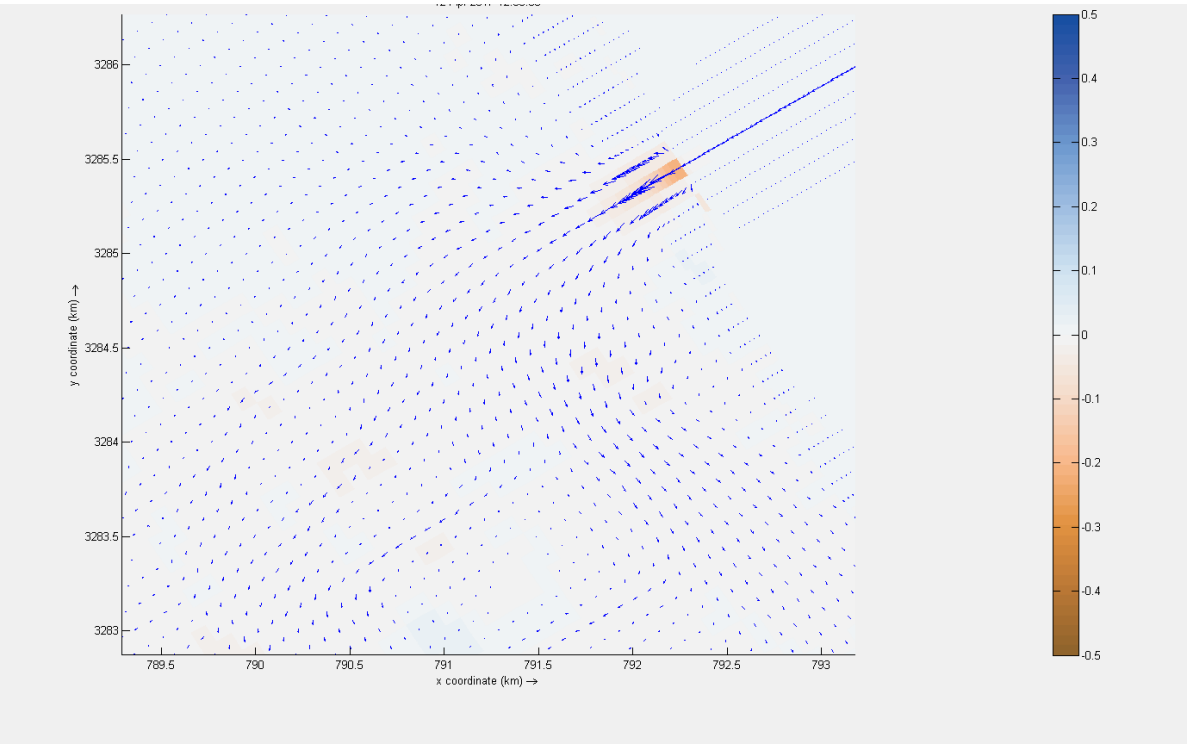

Figure 4.33: Erosion of the marshland two days after the diversion opened during a normal Mississippi River flow year with velocity vectors demonstrating flow paths. Blue is accumulation and brown is erosion in meters over a portion of the domain based on UTM Zone 15R.

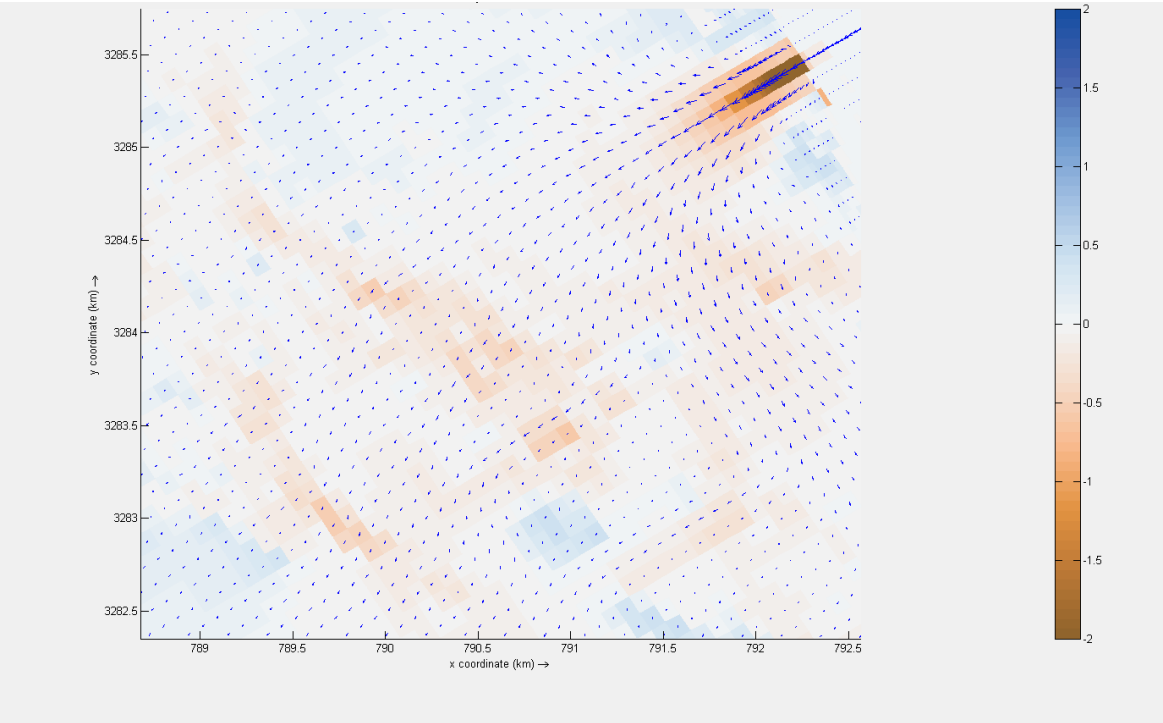

Figure 4.34: Erosion of the marshland when the diversion reaches maximum discharge during a normal Mississippi River flow year with velocity vectors demonstrating flow paths. Blue is accumulation and brown is erosion in meters over a portion of the domain in meters based on UTM Zone 15R.

When the diversion is beginning to close, the distributary routes have been firmly established. The strong southern velocity is still present but has reduced in magnitude and the overland flow to the south west continues. However, velocities to the north increased while the diversion was at capacity changing what started off a deposition area to one of net erosion as shown in Figure 4.35. This pattern is present in all operation scenarios during normal and high river flow.

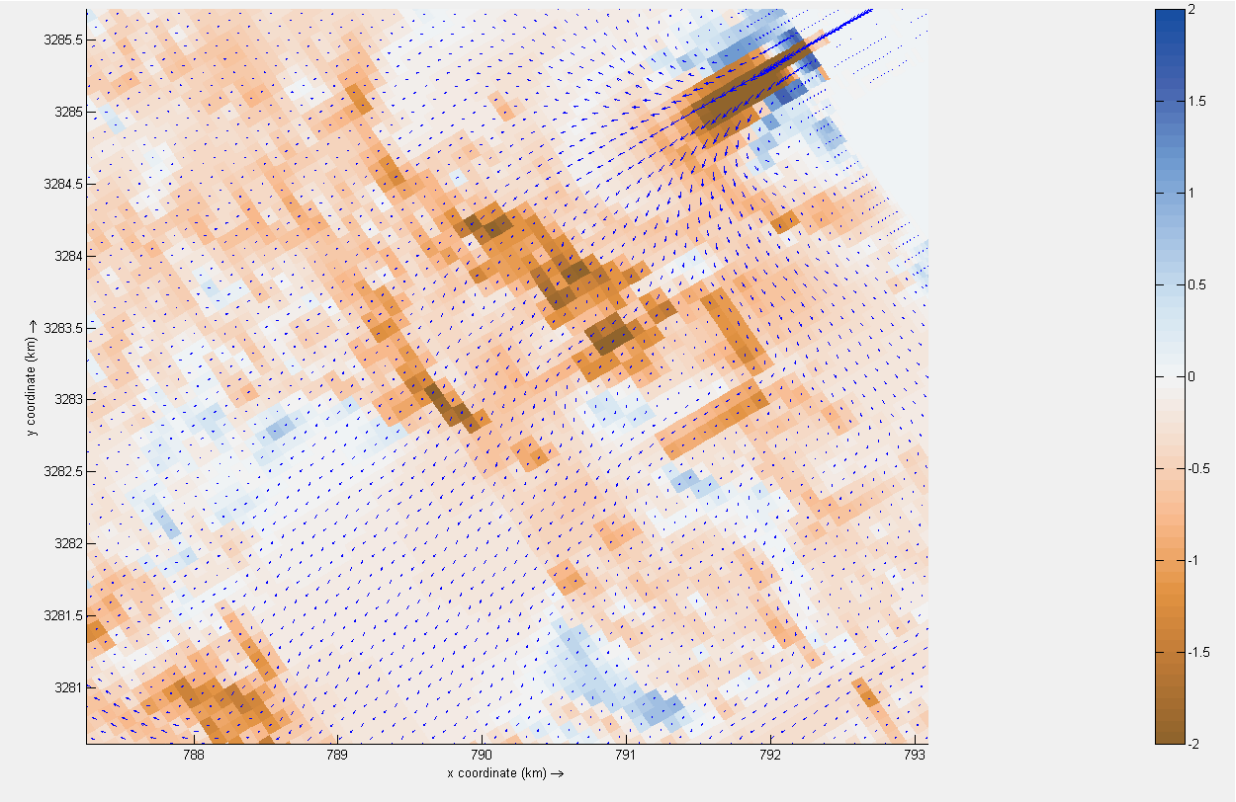

Figure 4.35: Erosion of the marshland when the diversion begins to reduce in discharge during a normal Mississippi River flow year with velocity vectors demonstrating flow paths. Blue is accumulation and brown is erosion in meters over a portion of the domain based on UTM Zone 15R.

Regardless of the Mississippi River Flow scenario when the diversion is opened, the receiving basin immediately begins to erode. First, the channel at the mouth of the diversion is scoured and the channels between open bodies of water begin to incise. Erosion occurs in the channel that connects Round Lake to Barataria Waterway, shown in Figure 4.36 and Figure 4.37, as the diversion is increasing in discharge during both river flow years. Once the diversion reaches maximum capacity the receiving basin immediately adjacent to the diversion erodes and accretes in an arced pattern showing that some large-scale eddies are forming from the diversion during both river flow years (Figure 4.38 and Figure 4.39). Sediment is deposited in large bodies of water like Round Lake and The Pen. A middle section of Barataria Waterway also experiences sediment deposition because of the channel conveys water from Round Lake to the northern part of Barataria Waterway and down through Bayou Rigolettes/Perot and Little Lake.

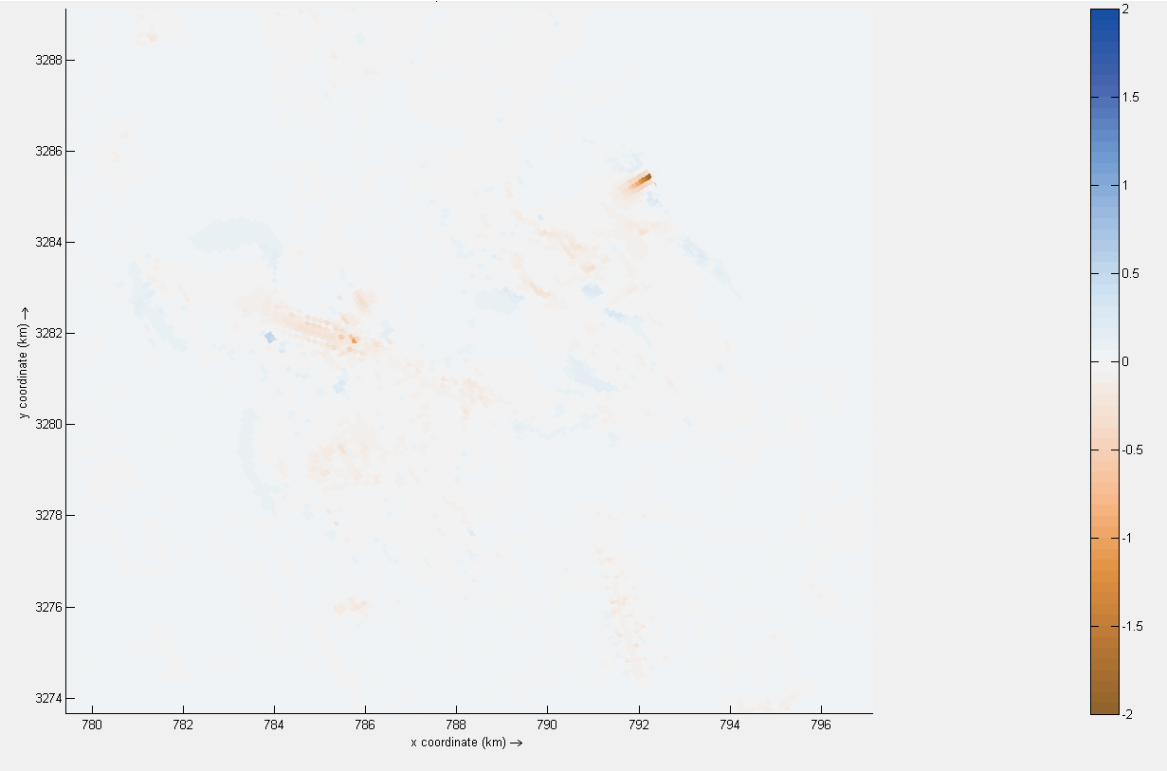

Figure 4.36: Erosion of the marshland when the diversion is increasing discharge during a normal Mississippi River flow year. Blue is accumulation and brown is erosion in meters over a portion of the domain based on UTM Zone 15R.

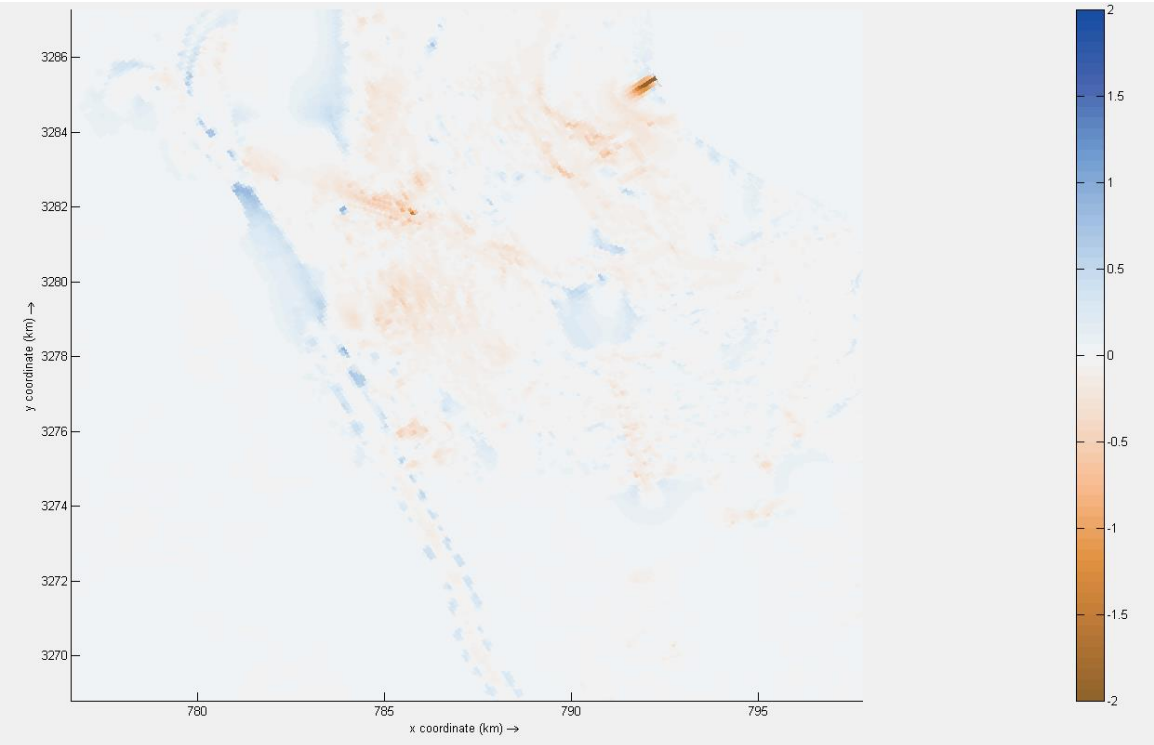

Figure 4.37: Erosion of the marshland when the diversion is increasing discharge during a high Mississippi River flow year. Blue is accumulation and brown is erosion in meters over a portion of the domain based on UTM Zone 15R.

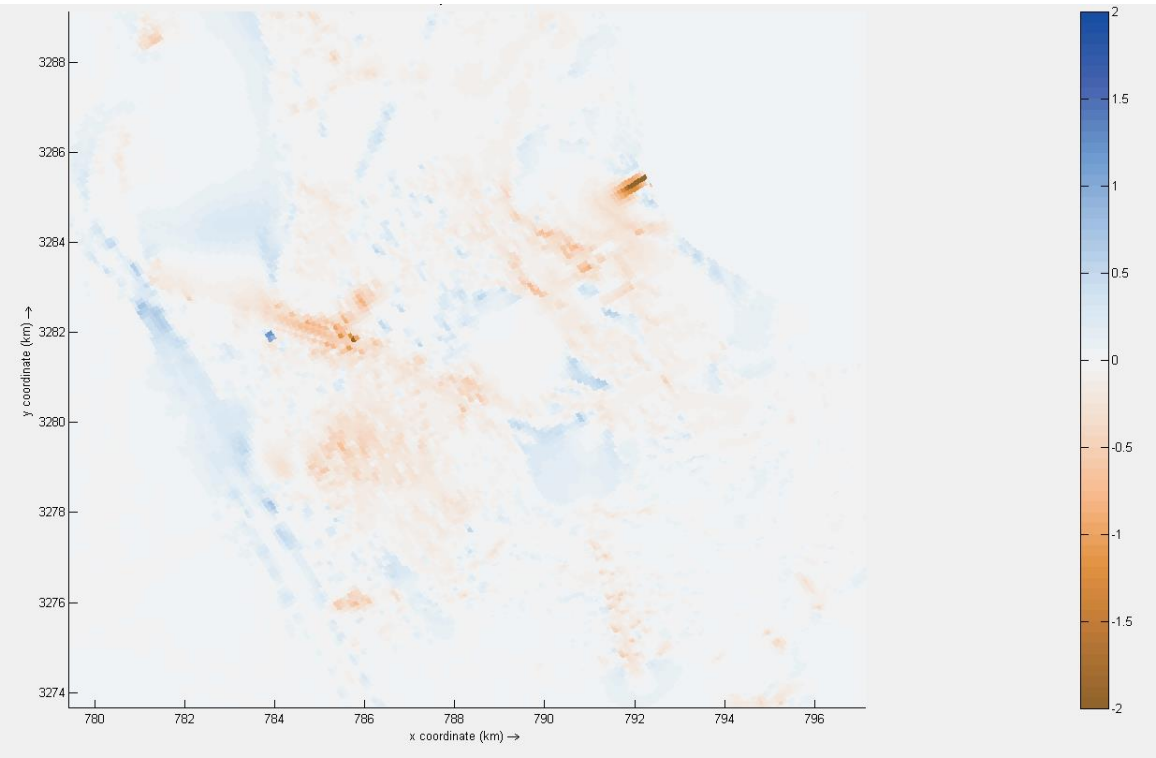

Figure 4.38: Erosion of the marshland when the diversion is at maximum discharge during a normal Mississippi River flow year. Blue is accumulation and brown is erosion in meters over a portion of the domain based on UTM Zone 15R.

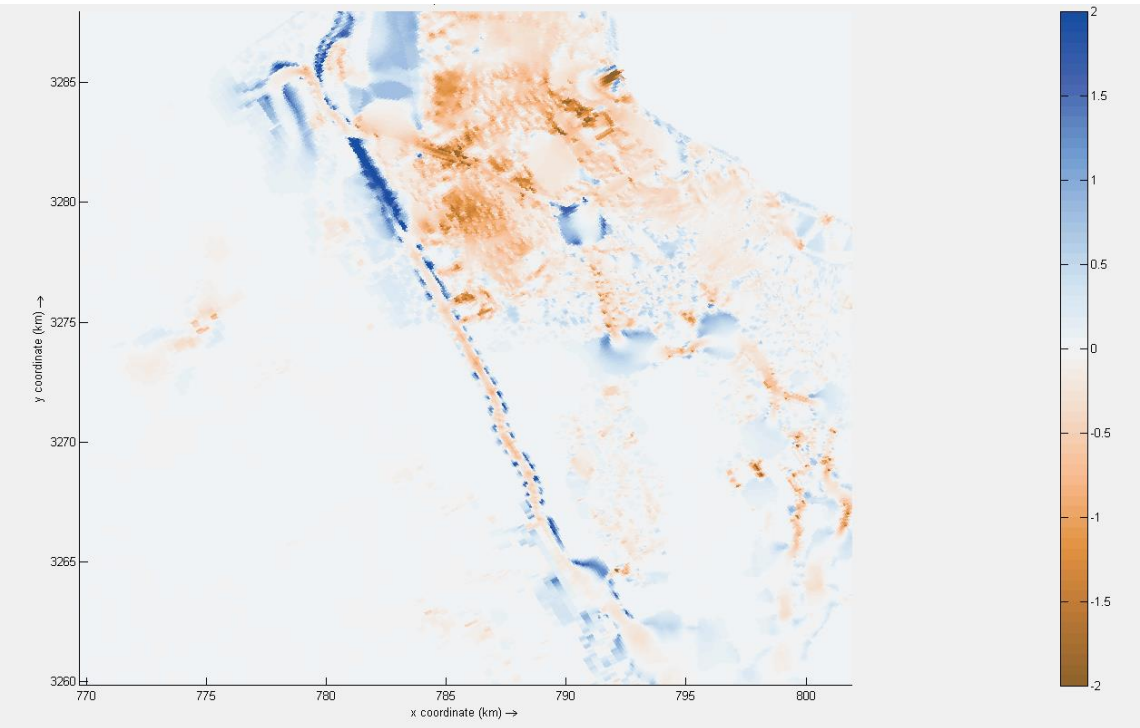

Figure 4.39: Erosion of the marshland when the diversion is increasing discharge during a high Mississippi River flow year. Blue is accumulation and brown is erosion in meters over a portion of the domain based on UTM Zone 15R.

By the time the diversion is closed this pattern of deposition in large water bodies and erosion in channels is well established. The mouth of the diversion has dug a distributary channel 6 to 8 m deep while creating natural levees of sediment deposits along the sides of it. Other deposition is present along the levee system near the diversion and the rest of the immediate receiving basin is eroded. The Pen, Bayou DuPont, Round Lake, and Lake Laurier all have significant sediment deposits. Barataria Waterway has an area of extreme sediment deposit between the Northern Path and Mid-Barataria Path. The latter of these flows travels south through the waterway and into Barataria Bay eroding the whole length of the waterway it travels through. On the edges sediment is deposited in a natural levee building process (Figure 4.40 and Figure 4.41)

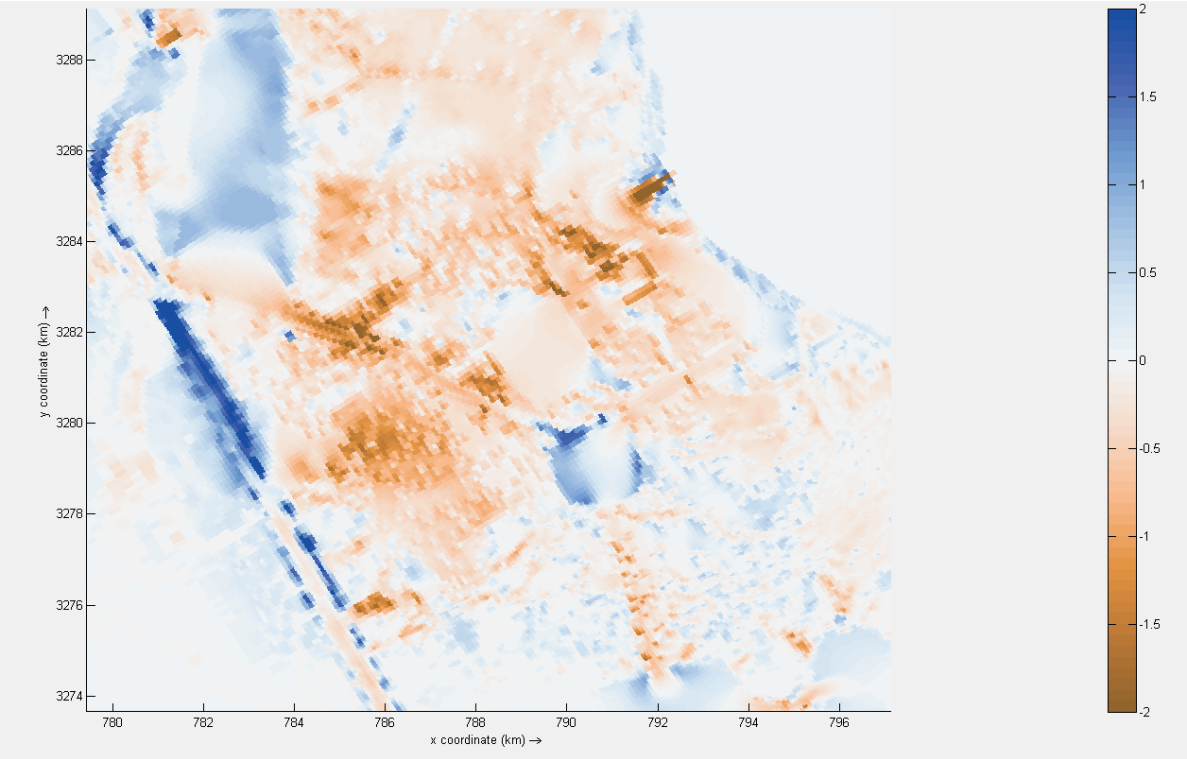

Figure 4.40: Erosion of the marshland when the diversion closes during a normal Mississippi River flow year. Blue is accumulation and brown is erosion in meters over a portion of the domain based on UTM Zone 15R.

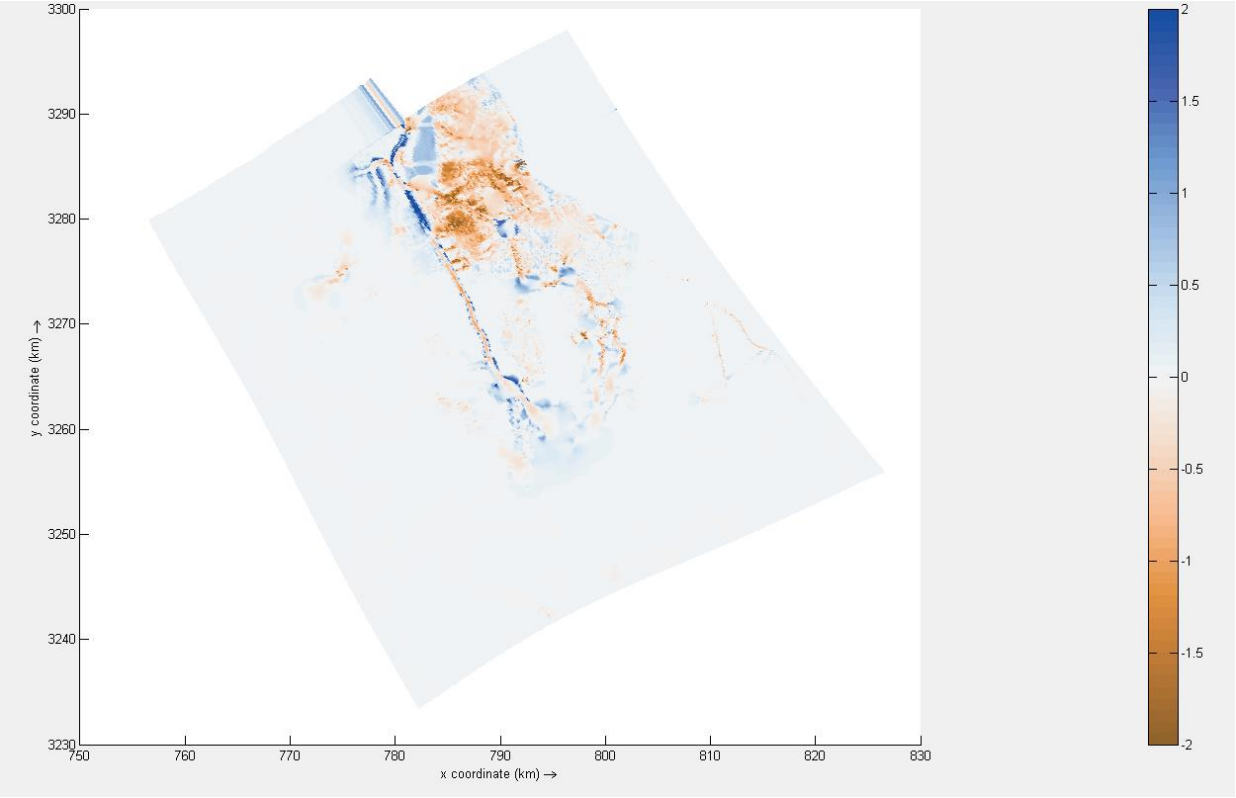

Figure 4.41: Erosion of the marshland when the diversion closes during a high Mississippi River flow year. Blue is accumulation and brown is erosion in meters over the entire domain based on UTM Zone 15R.

4.4.2 Localized Geomorphology

Overall the patterns of erosion in the receiving basin are similar during normal and high river flow and diversion operation, but some localized differences exist. At Bayou DuPont a linear erosion pattern occurs that differentiates based on diversion operation strategy (Figure 4.42). Starting at Day 10 of the normal flow scenario, which is the first day the diversion opens, erosion begins. It continues linearly until diversion begins to reduce its flow. The difference between operating the diversion at capacity versus 50% capacity changes the erosion by 0.1 m. A similar patter occurs during the high flow scenario except the diversion is open longer to allow for more erosion, up to 1.3 m, with a difference of 0.1 m between operating the diversion at capacity versus 50% capacity (Figure 4.43).

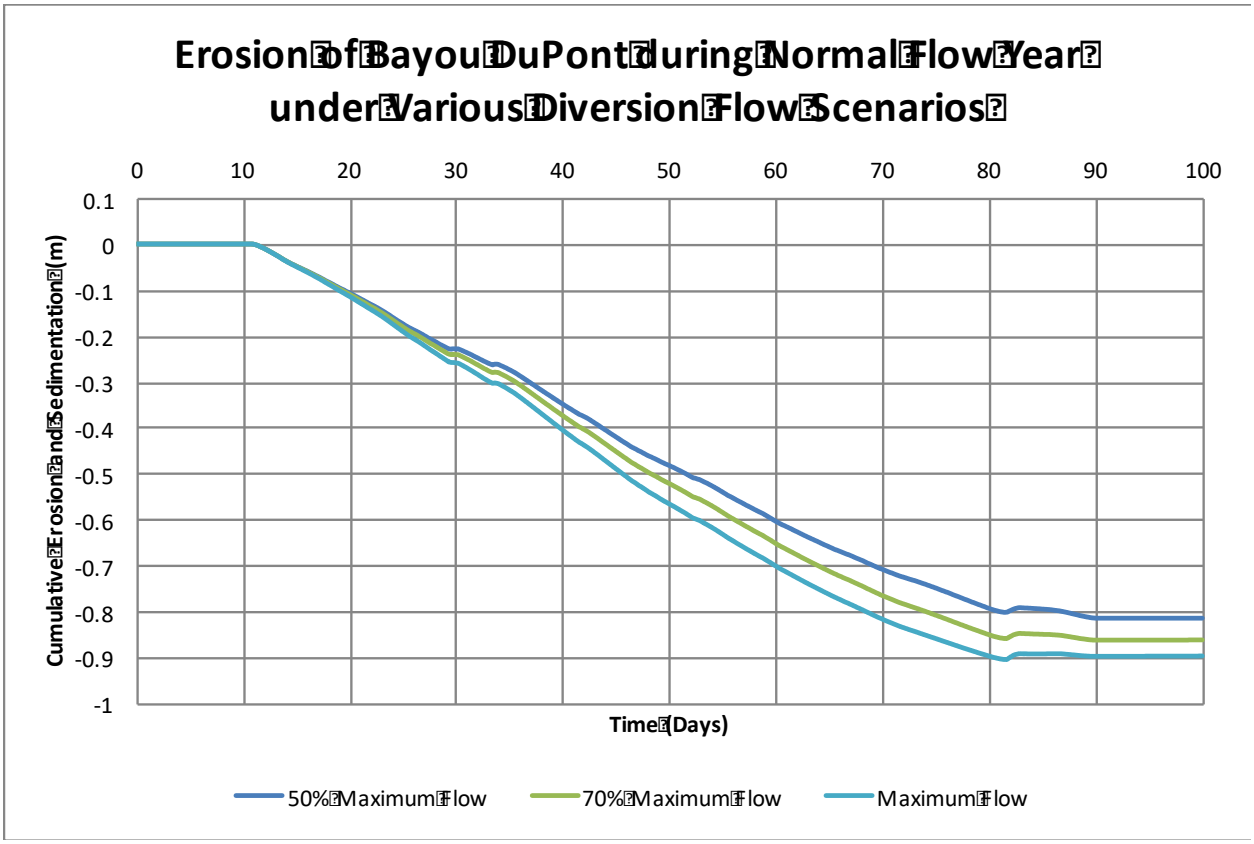

Figure 4.42: Erosion at Bayou DuPont due to the operational strategy of the diversion during a normal Mississippi River discharge year.

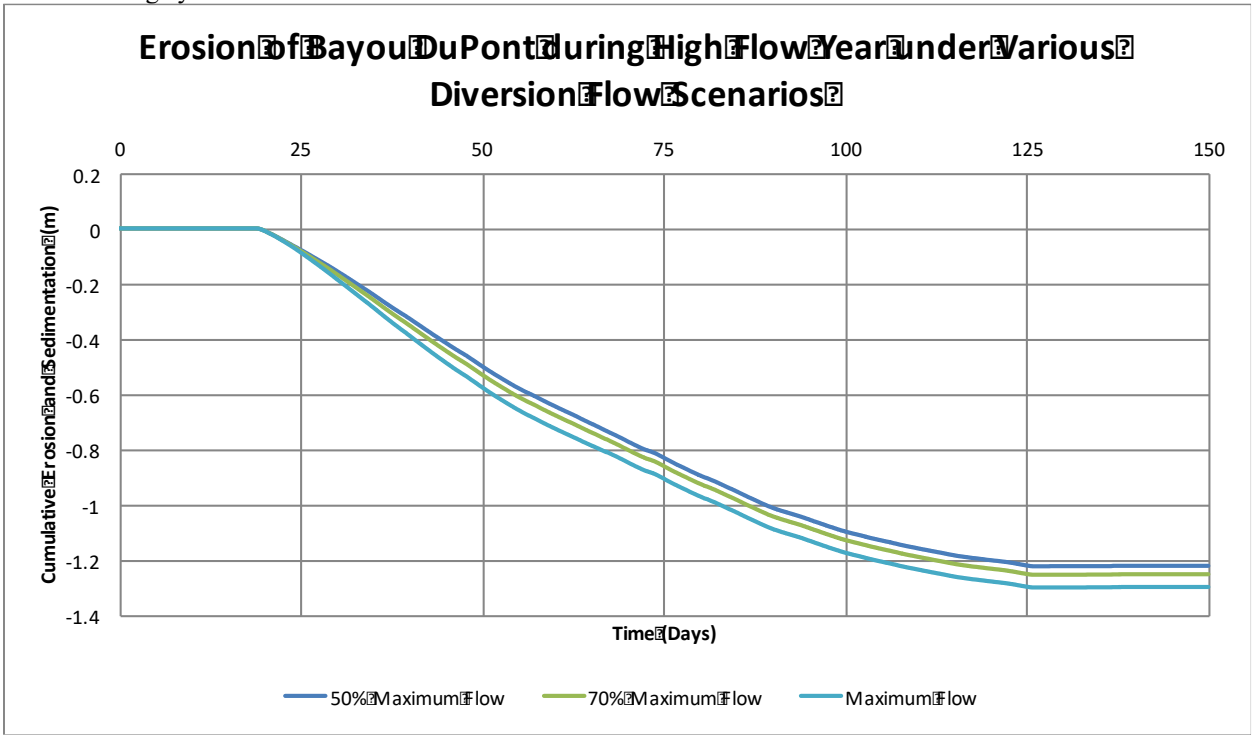

Figure 4.43: Erosion at Bayou DuPont due to the operational strategy of the diversion during a high Mississippi River discharge year.

Figure 4.44 shows that during a normal flow year erosion occurs in the channel at Grand Bayou, but it takes nearly 10 days after the diversion is opened for it to begin and tapers to nearly zero even before the diversion closes. Operating the diversion at 50% of the maximum flow will reduce the erosion in the channel at Grand Bayou by 0.08 m. During a high river flow year, Grand Bayou can erode over 0.2 m when the diversion is operated at capacity versus 0.05 m when it is operated at 50% capacity (Figure 4.45).

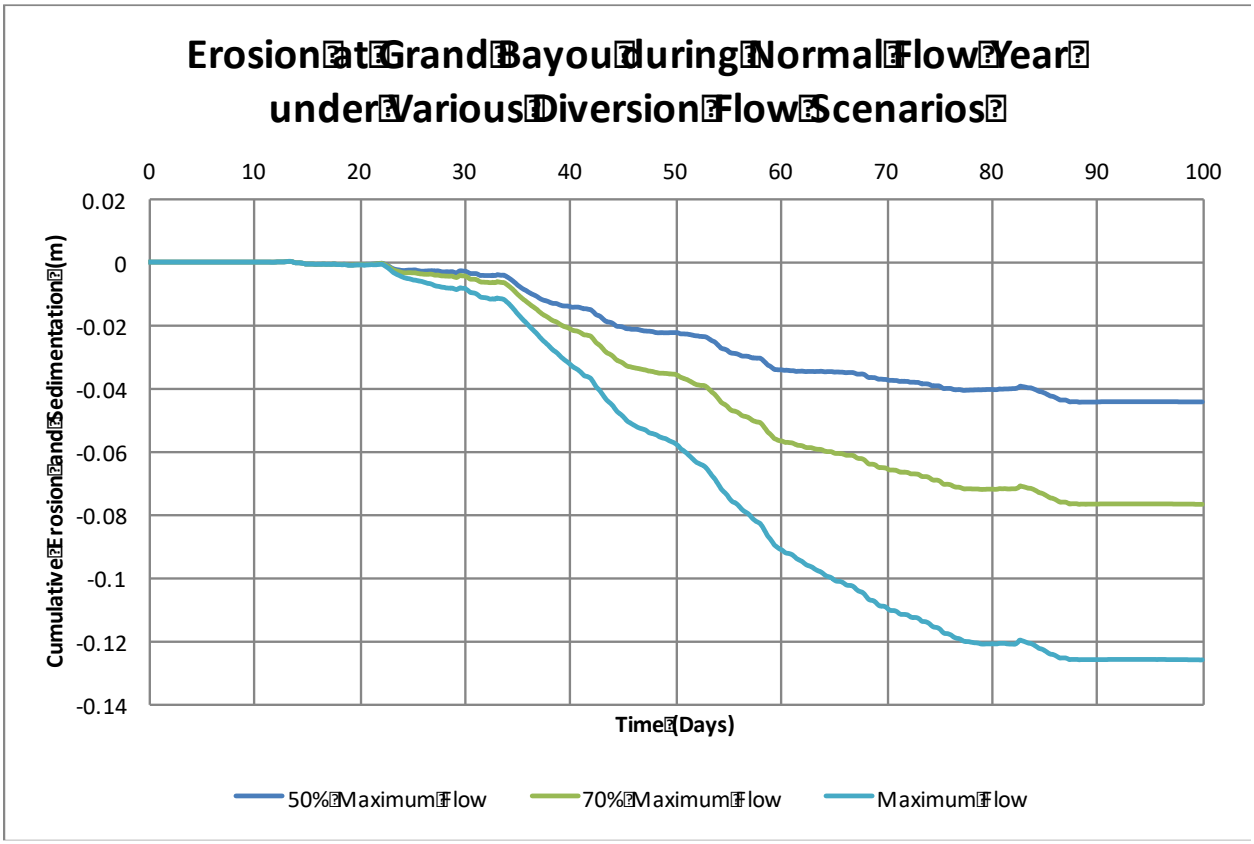

Figure 4.44: Erosion at Grand Bayou due to the operational strategy of the diversion during a normal Mississippi River discharge year.

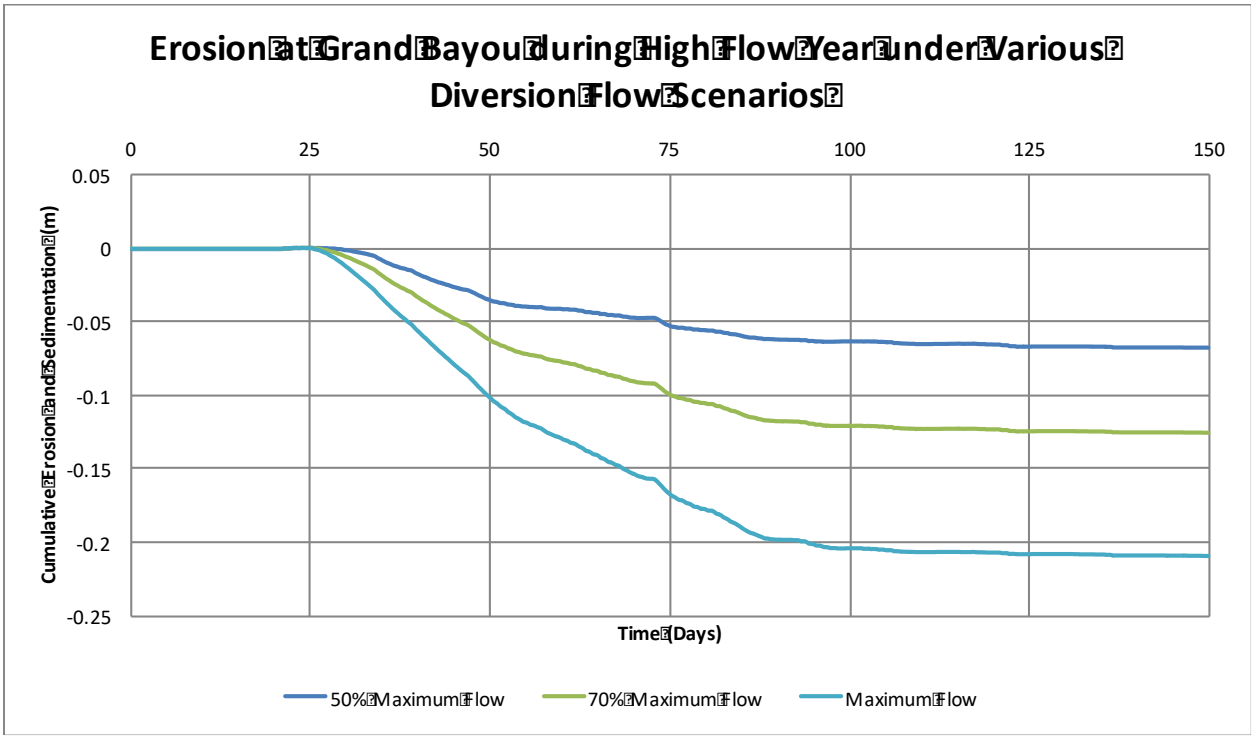

Figure 4.45: Erosion at Grand Bayou due to the operational strategy of the diversion during a high Mississippi River discharge year.

Up to 0.2 m of erosion occurs at the southern end of Barataria Waterway during the normal flow year (Figure 4.46) and 0.5 m during the high flow year (Figure 4.47). The central part of the waterway does not erode under the 50% maximum flow strategy but will erode almost 0.2 m during the maximum flow capacity during a normal river flow year (Figure 4.48). However, the 50% maximum flow strategy will erode this part of the channel 0.1 m during the high flow year and the diversion operated at capacity can cause up to 0.5 m of erosion (Figure 4.49). One of the only areas in a major channel in the domain that accumulates sediment is the northern part of Barataria Waterway (Figure 4.50). This sediment accumulates quickly adding 0.2 m under 50% maximum flow strategy to over 1.2 m when the diversion is operated at capacity. Sediment accumulation stops when the diversion begins to reduce its flow. The also occurs during the high flow year where almost 2 m of sediment is accumulated in the channel (Figure 4.51).

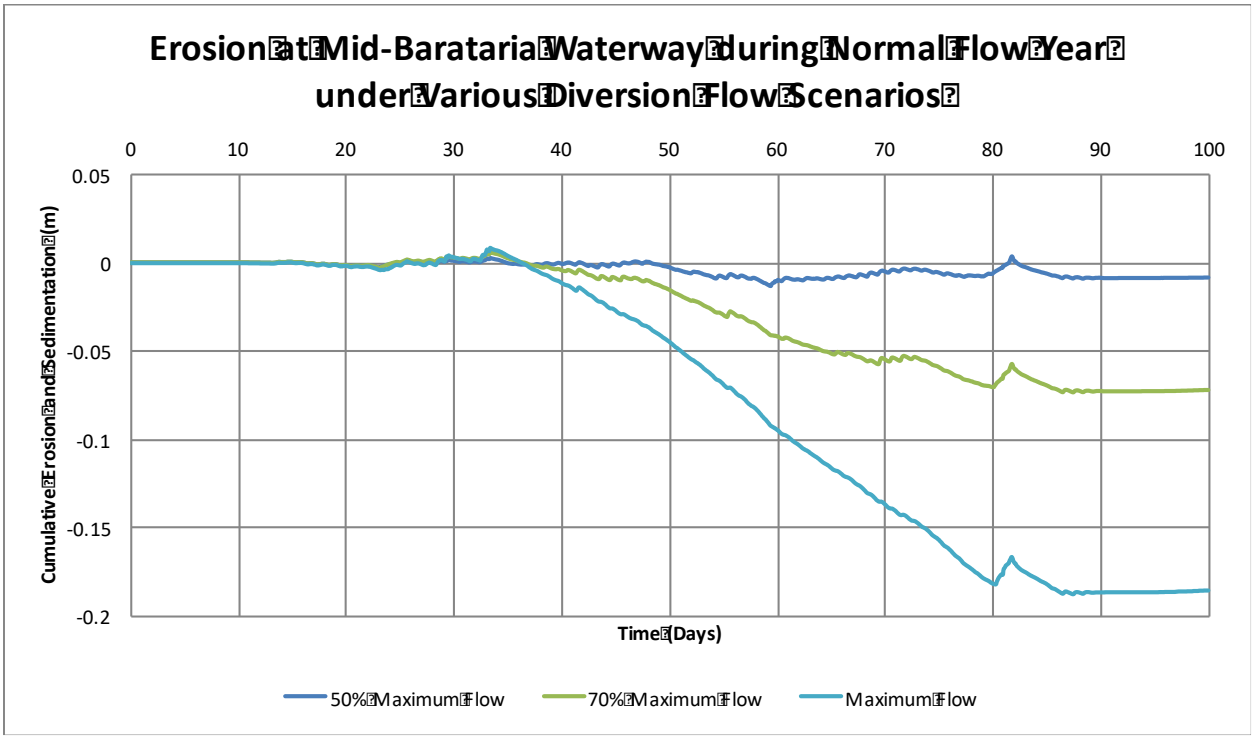

Figure 4.46: Erosion of the Mid-Barataria Waterway due to the operational strategy of the diversion during a normal Mississippi River discharge year.

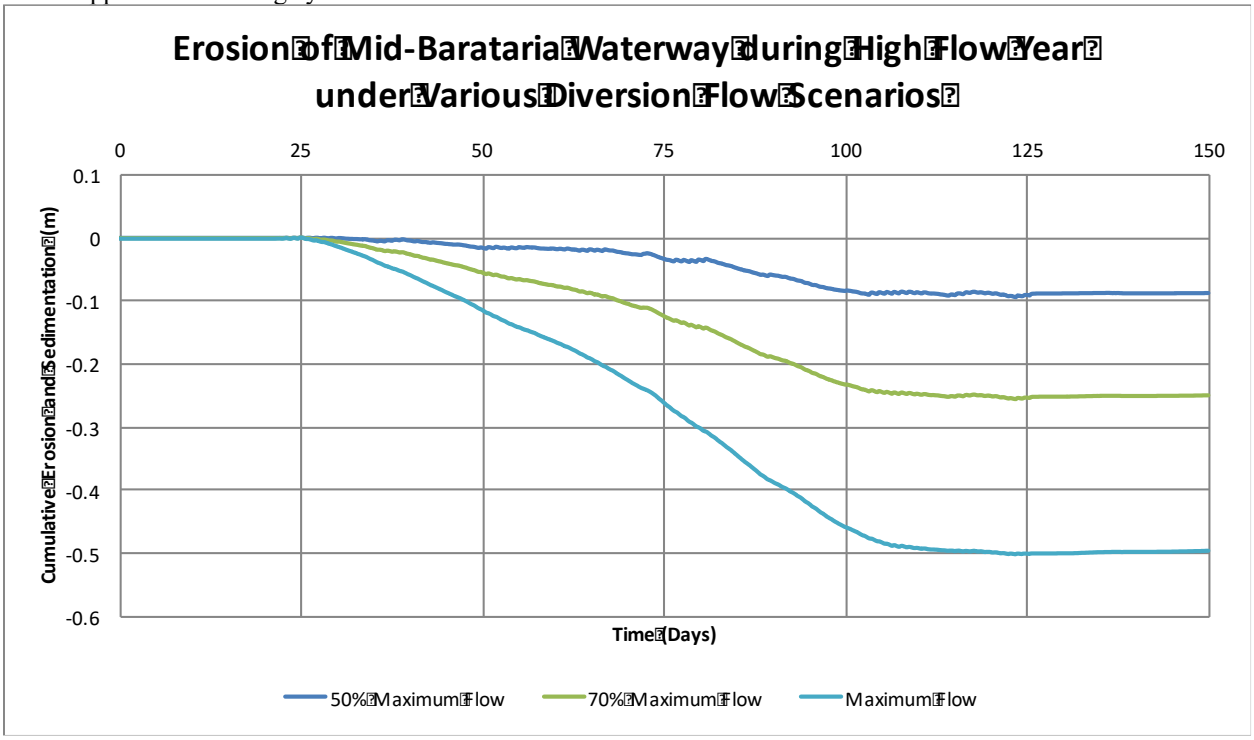

Figure 4.47: Erosion of the Mid-Barataria Waterway due to the operational strategy of the diversion during a high Mississippi River discharge year.

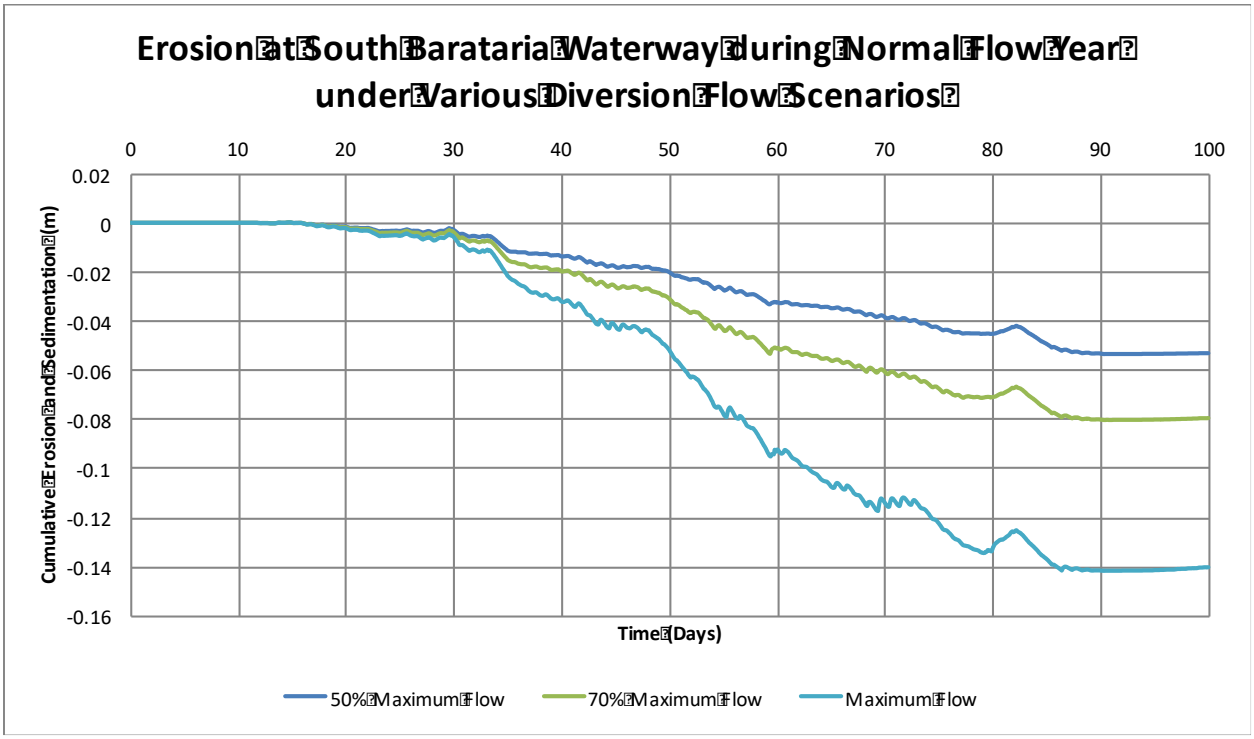

Figure 4.48: Erosion of the South Barataria Waterway due to the operational strategy of the diversion during a normal Mississippi River discharge year.

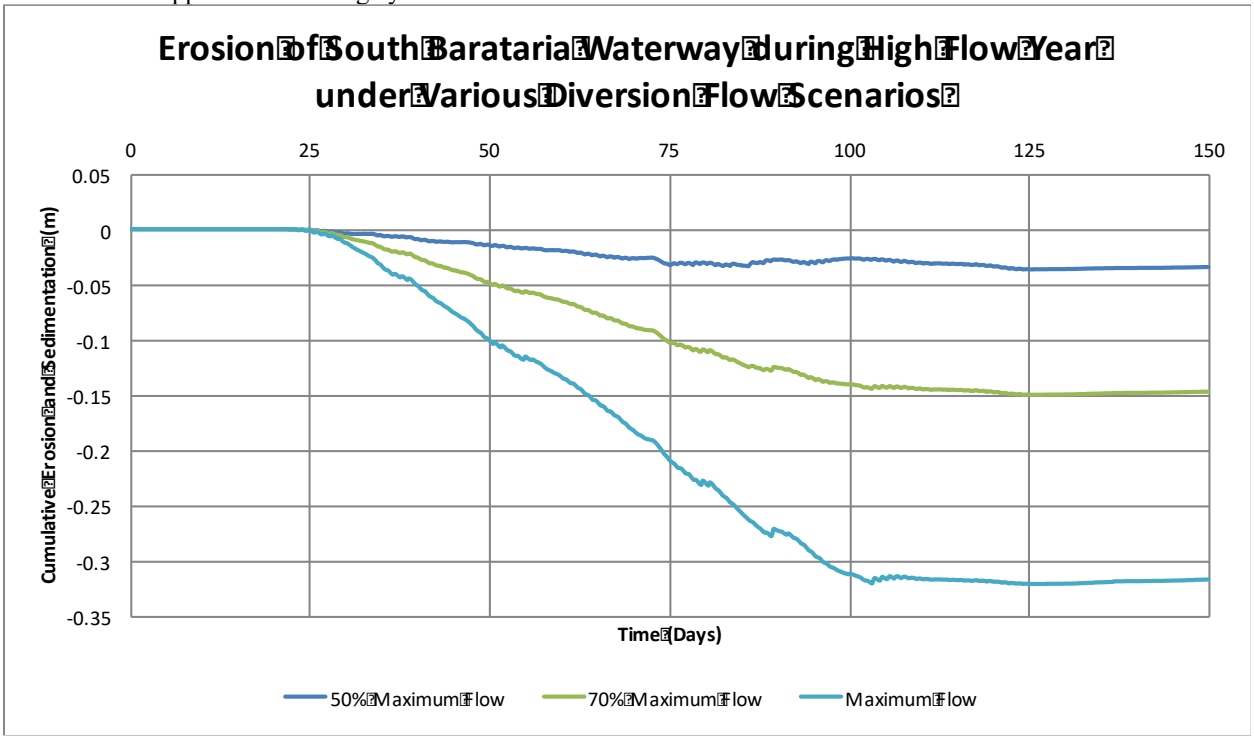

Figure 4.49: Erosion of the South Barataria Waterway due to the operational strategy of the diversion during a high Mississippi River discharge year.

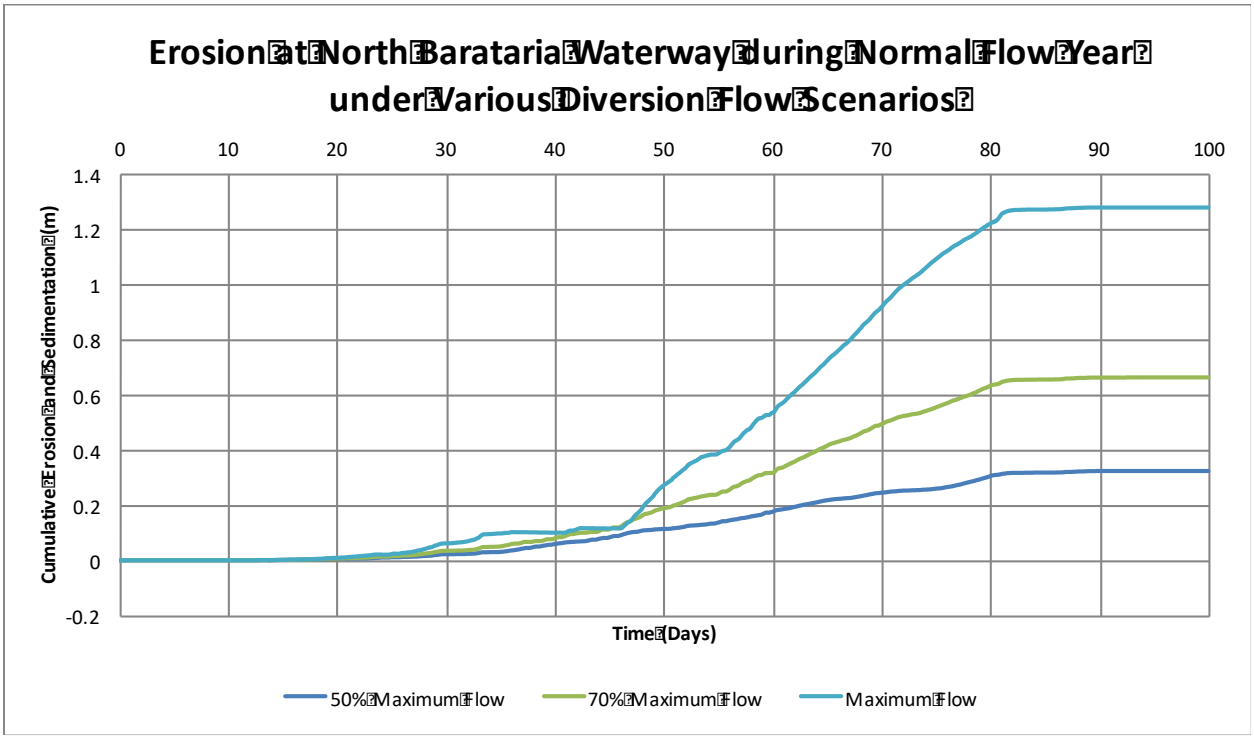

Figure 4.50: Accumulation in the North Barataria Waterway due to the operational strategy of the diversion during a normal Mississippi River discharge year.

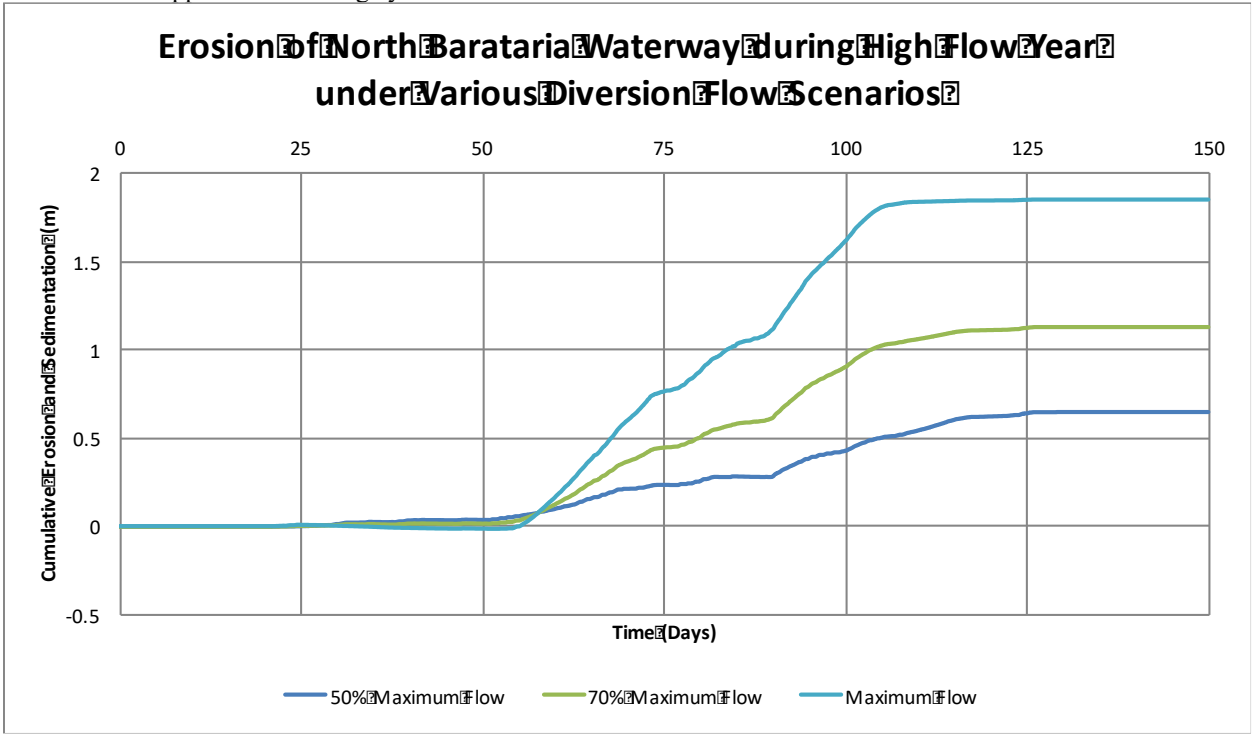

Figure 4.51: Accumulation in the North Barataria Waterway due to the operational strategy of the diversion during a high Mississippi River discharge year.

4.5 Sediment

When the diversion is first opened, velocities are not high enough to keep sand suspended in the flow until it reaches the receiving basin. Instead, it is deposited within the diversion channel. Once the velocity increases in the diversion, this sediment is re-suspended and transported out of the division into the receiving basin. As the diversion slows, more sediment is deposited. This final deposition is shown in Figure 4.52.

When the diversion enters the receiving basin the velocity slows. Eddies are created which deposit sand along the scour channel at the mouth of the diversion and along the back levee system. These deposits begin to extend into the receiving basin and consists of mainly sand and silt.

By the time the flow from the diversion reaches a monitoring stations within the domain, all of the suspended sand has deposited within the immediate receiving basin or is moving as bed load. Silt and clay still remain in suspension from the diversion and can be picked up from the erosion of the receiving basin. Localized sand can also be transported as bed load. Silt is deposited as water flow changes from narrow channels and bayous into larger bodies of water like Round Lake and The Pen. Silt concentrations in the water at various locations around the domain are shown in Table 4.1. It is noted that during the high diversion flows the silt and clay concentrations often exceed the concentrations in the diversion itself.

Average Silt Concentration during Peak Diversion Discharge (kg/m^3)						
	Normal Flow			High Flow		
Location	50% Maximum Flow	70% Maximum Flow	Maximum Flow	50% Maximum Flow	70% Maximum Flow	Maximum Flow
Diversion	0.09	0.09	0.09	0.08	0.08	0.08
North Barataria Waterway	0.13	0.37	0.72	0.61	0.87	1.26
South Barataria Waterway	0.17	0.49	1.03	0.44	0.79	1.31
The Pen	0.13	0.24	0.73	0.26	0.49	1.30
Round Lake	0.02	0.03	0.11	0.03	0.08	0.21
Grand Bayou	0.00	0.00	0.00	0.00	0.00	0.00

Table 4.1: Average silt concentration difference at various locations around the domain during peak discharge of the diversion under both Mississippi River flow scenarios.

Clay is transported through the diversion and more is picked up as the diversion erodes the receiving basin and the distributary channels. The diversion transported on average 0.07 kg/m^3 of clay at its peak discharge during a normal Mississippi River flow year and 0.03 kg/m^3 during the high flow year. As shown in Figure 4.52 and Figure 4.53, clay concentrations within Grand Bayou increases with the increase in diversion discharge but varies greatly depending on the river flow regime and the diversion operation.

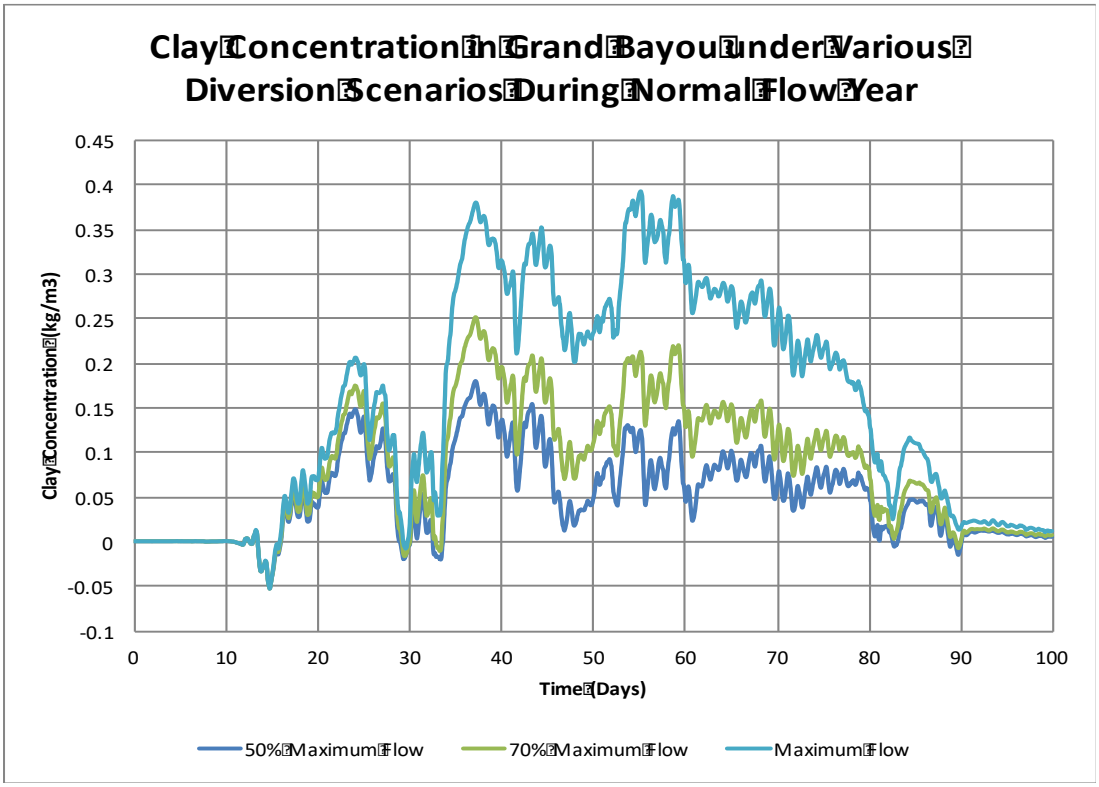

Figure 4.52: Concentration of clay in Grand Bayou due to the operational strategy of the diversion during a normal Mississippi River discharge year.

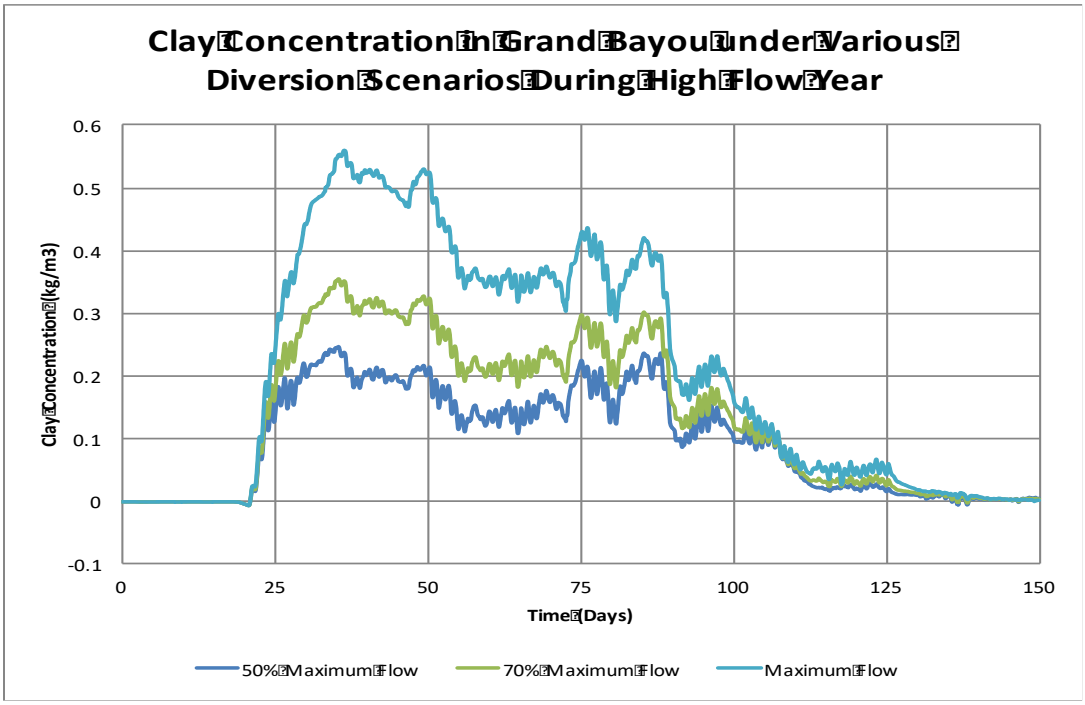

Figure 4.53 Clay concentration in Grand Bayou due to the operational strategy of the diversion during a high Mississippi River discharge year.

4.6 Salinity

Salinity within the basin drops rapidly when the diversion is opened. Within one week of the diversion opening, the salinity in northern Barataria Waterway drops to near zero (Figure 4.54). It takes a few more days for the salinity levels in Mid-Barataria Waterway and Grand Bayou to drop to zero (Figure 4.55 and 4.56). This happens regardless of operation scenario or level of Mississippi River flood. Lake Washington still retains some salinity when the diversion is open; the operation of the diversion causes a decrease of 5 to 10 ppt (Figure 4.57). The only place in the domain that the diversion has little effect (a drop of less than 2 ppt) is in the far southwestern corner of the domain (Figure 4.58). The normal versus high Mississippi River flow did not change the results of salinity therefore only the high flow year is shown.

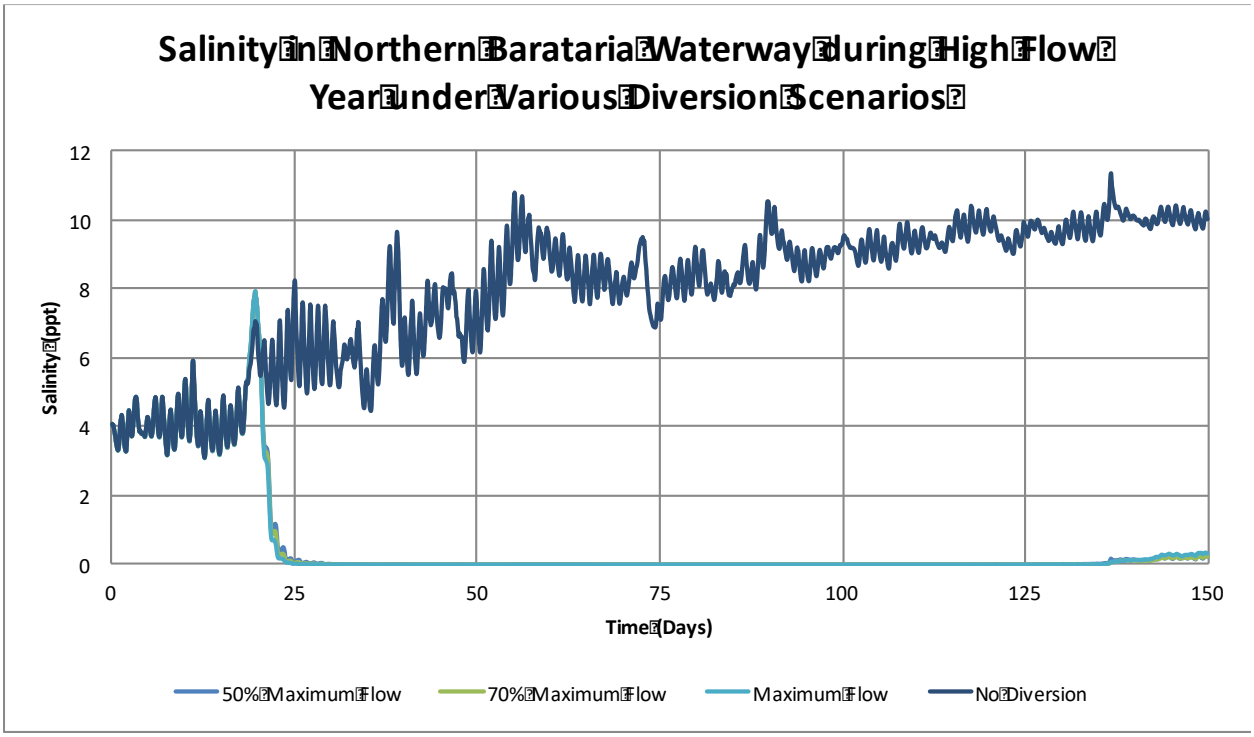

Figure 4.54: Salinity levels in the North Barataria Waterway due to the operational strategy of the diversion during a high Mississippi River discharge year as compared to the no diversion scenario.

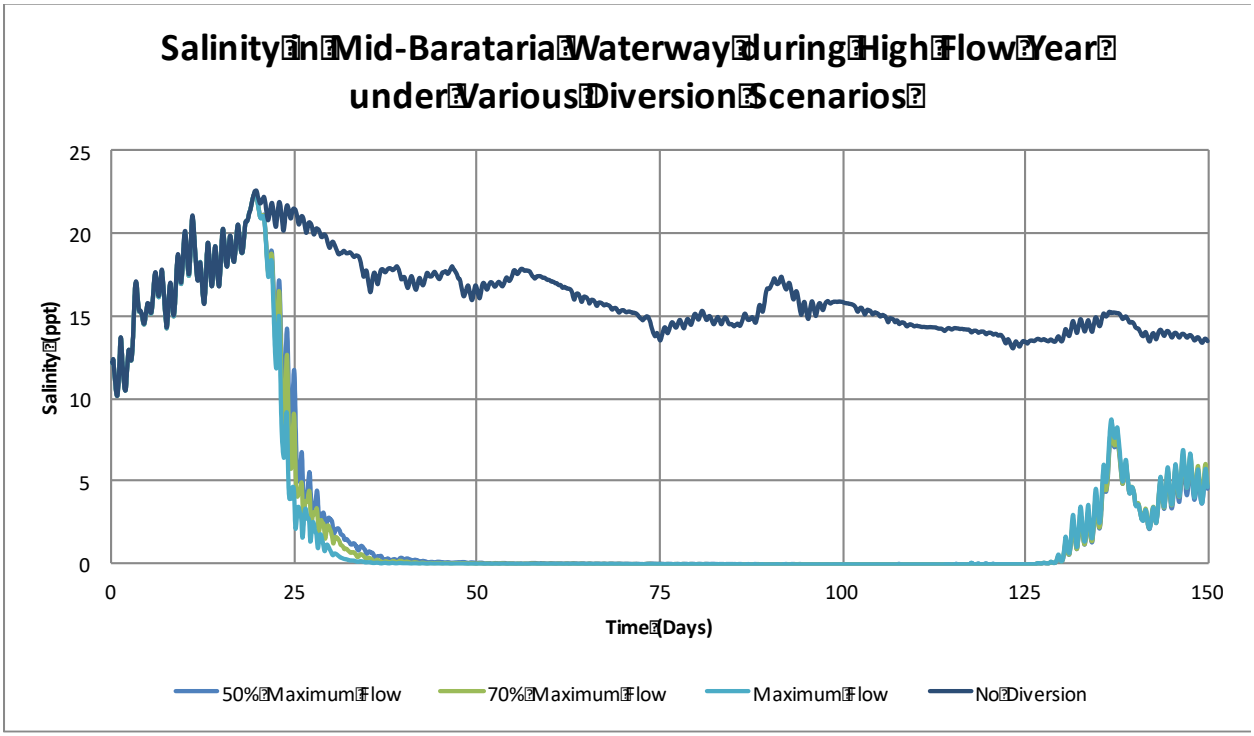

Figure 4.55: Salinity levels in the Mid-Barataria Waterway due to the operational strategy of the diversion during a high Mississippi River discharge year as compared to the no diversion scenario.

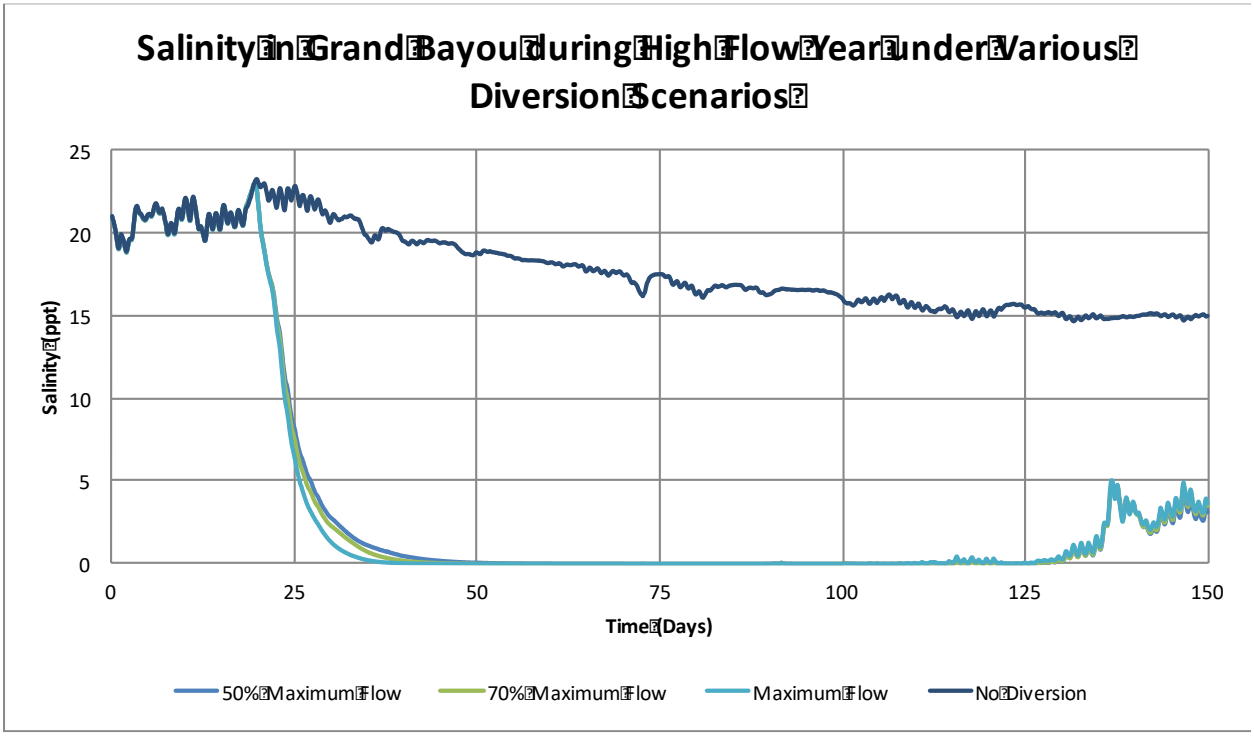

Figure 4.56: Salinity levels in Grand Bayou due to the operational strategy of the diversion during a high Mississippi River discharge year as compared to the no diversion scenario.

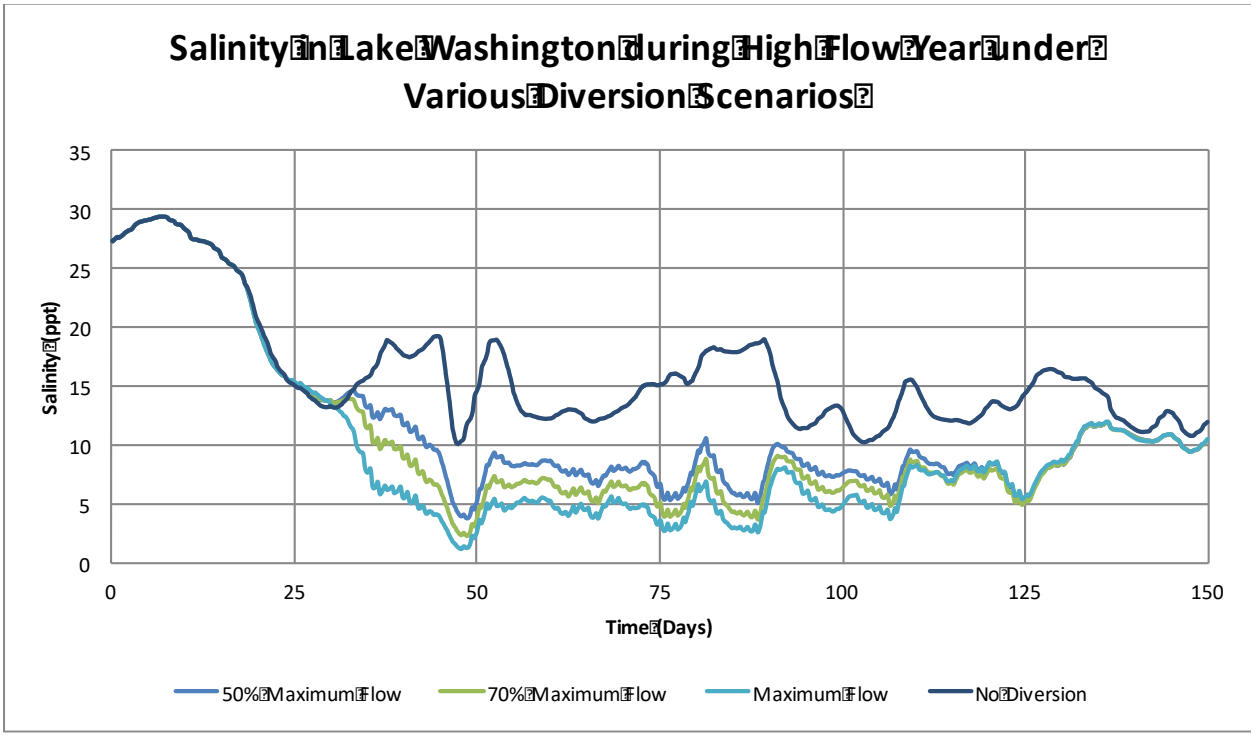

Figure 4.57: Salinity levels in Lake Washington due to the operational strategy of the diversion during a high Mississippi River discharge year as compared to the no diversion scenario.

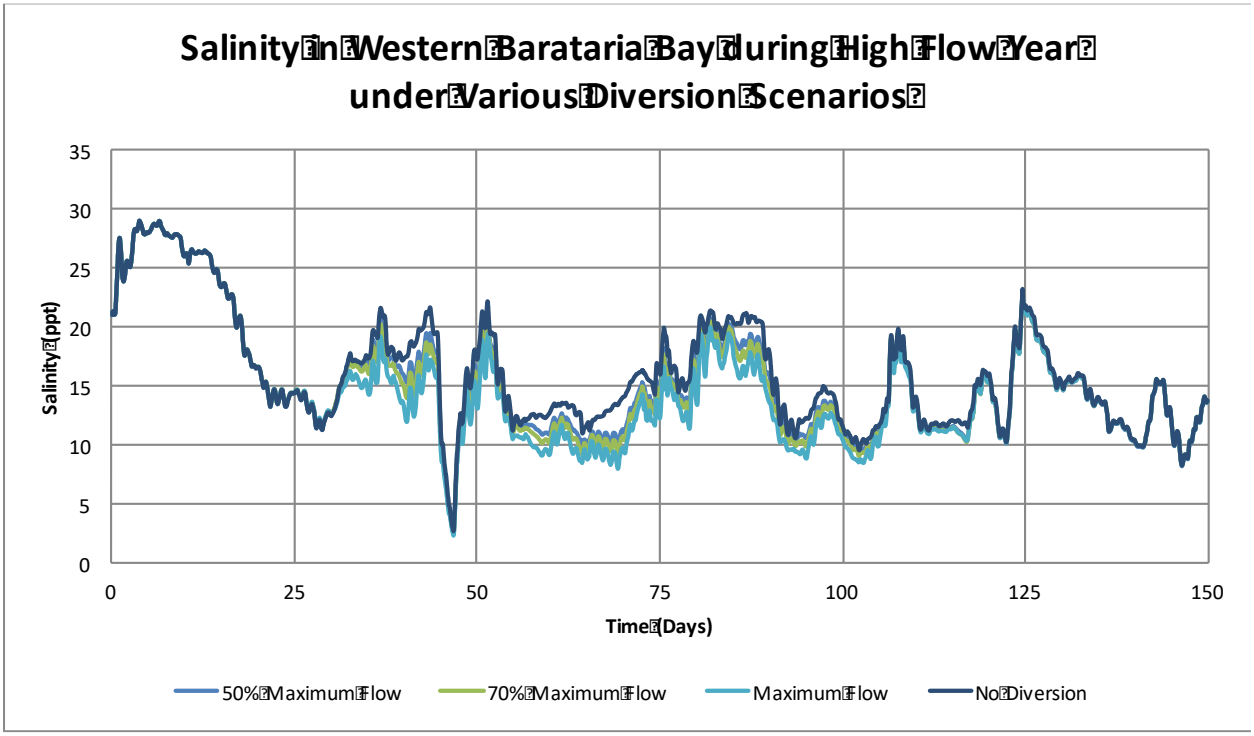

Figure 4.58: Salinity levels in western Barataria Bay due to the operational strategy of the diversion during a high Mississippi River discharge year as compared to the no diversion scenario.

Chapter 5: Discussion

5.1 Introduction

The model was calibrated for water levels and salinity over the course of a month for the years 2017 and 2018 at 6 locations representing a wide coverage of the domain. The model achieved acceptable water levels for the root mean square error, Pearson product-moment correlation coefficient, and bias error. While modeled water levels tracked closely with observed values there were higher errors in salinity. Salinity had to be calibrated using the daily average to filter out phase differences in the tidal signals with and without a diversion.

In the results, all data were compared to the No Diversion scenario. All figures represent the changes created by the diversion unless otherwise noted. The difference between the diversion and no diversion scenarios should have removed the tidal signal from the results, yet some remained.

5.2 Development of the Distributary System

5.2.1 Diversion Mouth

The water entering the receiving basin has the highest velocity measured in the domain because of the change in bed elevation from the diversion channel to the receiving basin. This change in elevation both increases the velocity and the water level. The high velocity of water scours a channel that reaches up to 8 m deep during the high flow year and the diversion operated with maximum flow. The normal flow year only produces a channel 6 m deep but more erosion would occur if the diversion was open longer. This means that the channel at the outlet of the diversion may not be fully formed within the first year of operation.

Once the water is free from the channel it spreads into the receiving basin and slows creating two eddies on either side of the diversion outlet. These produce depositions comprised of sand and silt. This is the goal of the sediment diversion and proves that some land creation will begin within the first year. This land will be adjacent to the back levees along the scour channel that the diversion creates.

Initially, flow from the diversion travels almost completely southward through the open water of the broken marshland. North of the diversion there is more continuous marshland than to the south which prevents the initial flow from moving in that direction. The slowing of water along this northern marsh boundary causes some deposition. Once the diversion increases to its maximum flow this area turns erosive as more distributary channels are needed to convey the increase in discharge. Overland flow erodes the marshland enhancing the channels within it and eroding more.

The receiving basin to the south is mainly open water but the sparse areas of land will begin to erode almost immediately. In some areas, erosion of up to 2 m can occur but this erosion begins to define distributary channels for the diversion. These channels are eroded into the bed of open

water areas and through the existing marshland immediately adjacent to the diversion. At roughly 2.5 miles from the diversion, the velocity of the water slows and begins to follow existing flow pathways. This is where the marshland becomes more continuous and only defined channels exist for the water to be transported through. The water flows through these channels elevating water levels downstream and increasing the velocity.

The highest velocity occurs southeast along the back levee through the existing open water in the present receiving basin. Most of this flow then makes a sharp turn to the southwest into the open pond in the middle of Bayou DuPont then follows the bayou south towards Round Lake. While the majority of the flow turns to enter Bayou DuPont, some water moves through the open water areas towards Grand Bayou.

Ultimately the diverted flow creates three main distributary routes that are discussed in the next sections of this thesis.

5.2.2 Southern Path

5.2.2.1 Round Lake

Flow from Bayou DuPont enters Round Lake (Figure 5.1), spreading out and slowing down. This deposits sediment contained within the water. From Round Lake most of the flow travels through Lake Laurier into Barataria Bay via Wilkinson Bayou. Some flow moves from Round Lake and into Mud Lake. This flow gradually develops as the diversion continues. Another flow of water happens just south of Lake Laurier towards Lake Judge Perez and down into Grand Bayou. This flow initially receives significant discharged but it is reduced to almost nothing even when the diversion is operating at capacity. This is due to the significant erosion that happens in the channel connecting Lake Laurier to Wilkinson Bayou, which allows more water to flow south to Barataria Bay. This is a much shorter flow path for the water comparted to the Grand Bayou outlet and therefore more optimal to receive flow due to the higher energy gradient. These results indicate that pre-dredging of Wilkinson Bayou or adding a structure to block flow down Grand Bayou could protect the people in the region from the worst of the flooding caused by the diversion.

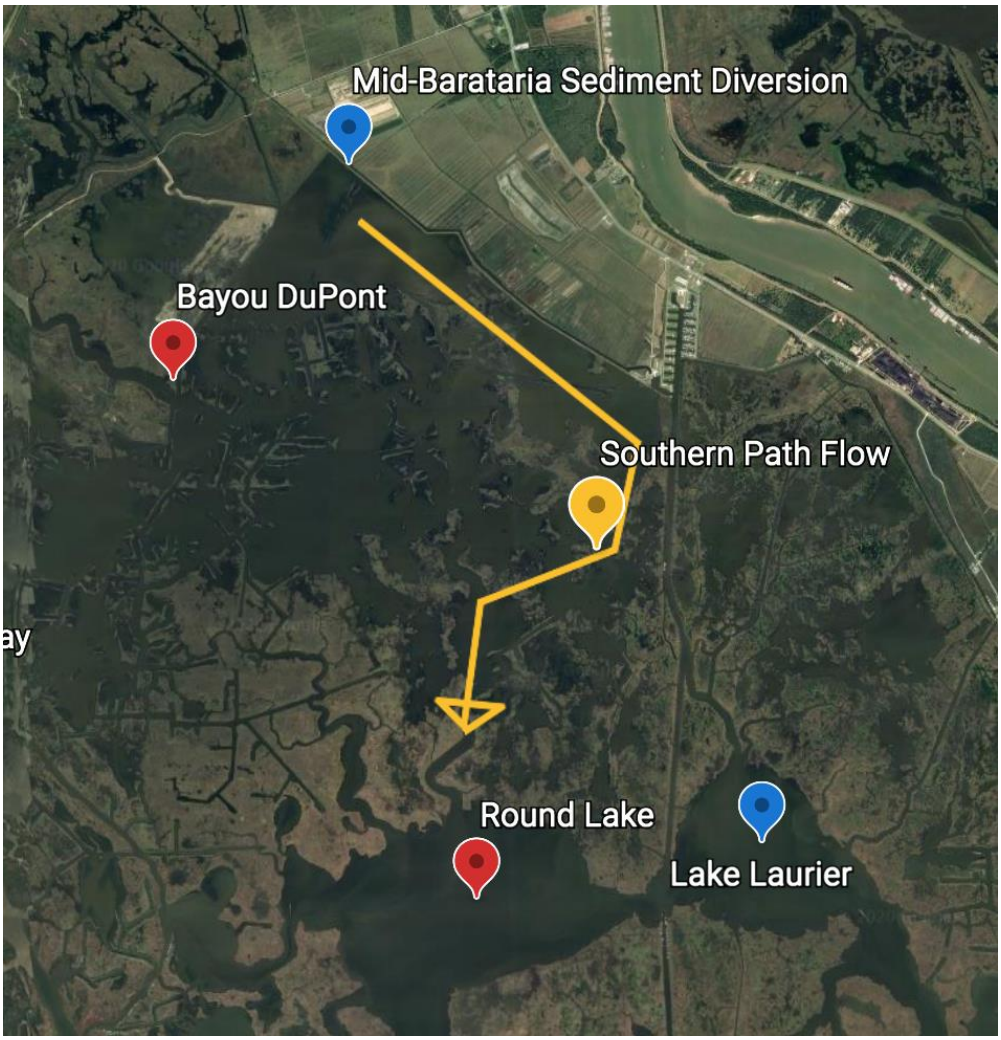

Figure 5.1: The Southern Path flows along the back level and into the southern part of Bayou DuPont flowing into Round Lake. Locations are labeled in blue, observation points in red, and flow paths in yellow.

5.2.2.2 Grand Bayou

One of the outlets originally from the Southern Path is Grand Bayou via Lake Laurier shown in Figure 5.2. Grand Bayou also receives flow through the broken marsh system immediately adjacent to the back levee which follows the flow of the diversion. The flow coming into Grand Bayou from Lake Laurier, however, does not follow the diversion hydrograph. This flow peaks before the diversion reaches maximum discharge and then reduces to almost nothing. That causes water levels in Grand Bayou peak just a few weeks after the diversion is opened before it reaches maximum discharge and then falls as the diversion continues to increase discharge. One explanation for this would be that the channels south of Lake Laurier begin to erode so they can receive a greater amount of water making them more hydraulically advantageous for water to flow south through Wilkinson Bayou instead of being diverted to the east through Grand Bayou. Discharge in Grand Bayou does reduce when the diversion reaches maximum for both the normal and high flow years.

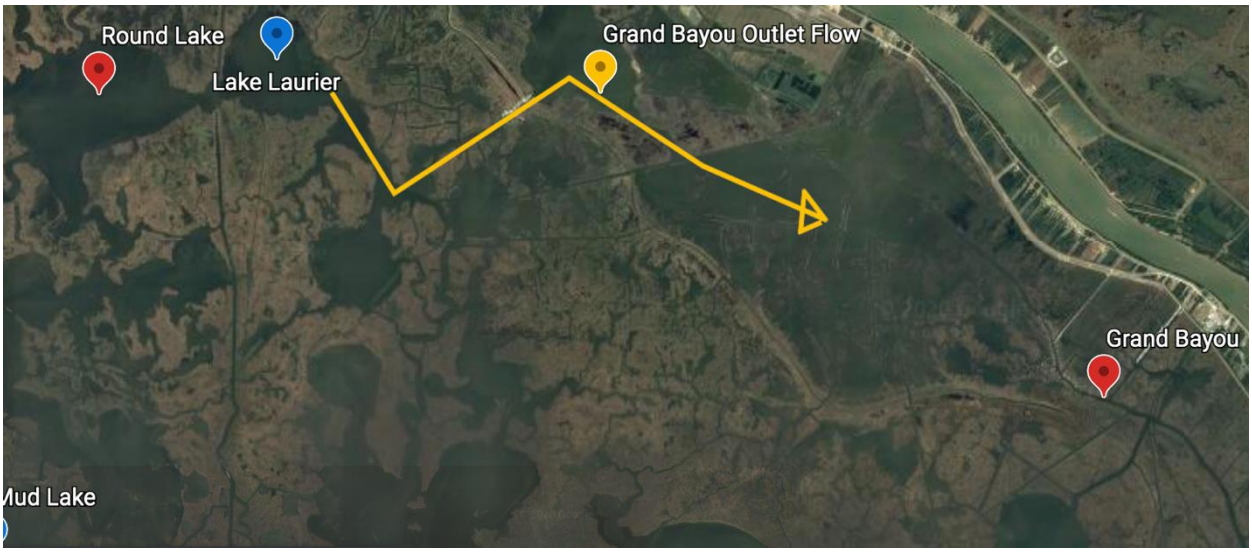

Figure 5.2: The Grand Bayou Outlet is a flow that comes from Lake Laurier and combines with overland flow along the back levee to enter into Grand Bayou. Locations are labeled in blue, observation points in red, and flow paths in yellow.

Grand Bayou itself also erodes. The erosion rates are highest two weeks after the diversion is opened and reaches an inflection point when velocities peak. Erosion occurs long after peak velocity and water levels but at a much lower rate. Depending on the river flow and the diversion operation scenario, Grand Bayou will erode 0.04 to 0.21 m.

5.2.3 Northern Path

Much of the immediate receiving basin of the diversion is open water but a few areas of marsh still remain. A combination of open water and overland flow comes together in Bayou DuPont and then turns northwest to connect with The Pen (Figure 5.3). Regardless of the flow year or operational strategy, flow velocity from the diversion is high enough to cause this part of Barataria Waterway to flow northward pushing water into Bayou Rigolettes (Figure 5.4), and into Lake Salvador. The flow that enters Bayou Rigolettes then travels through Little Lake into Barataria Basin. There is little deposition or accumulation within this part of the flow path but Bayou Rigolettes will have some silt deposition and the connection between this bayou and Little Lake will erode.

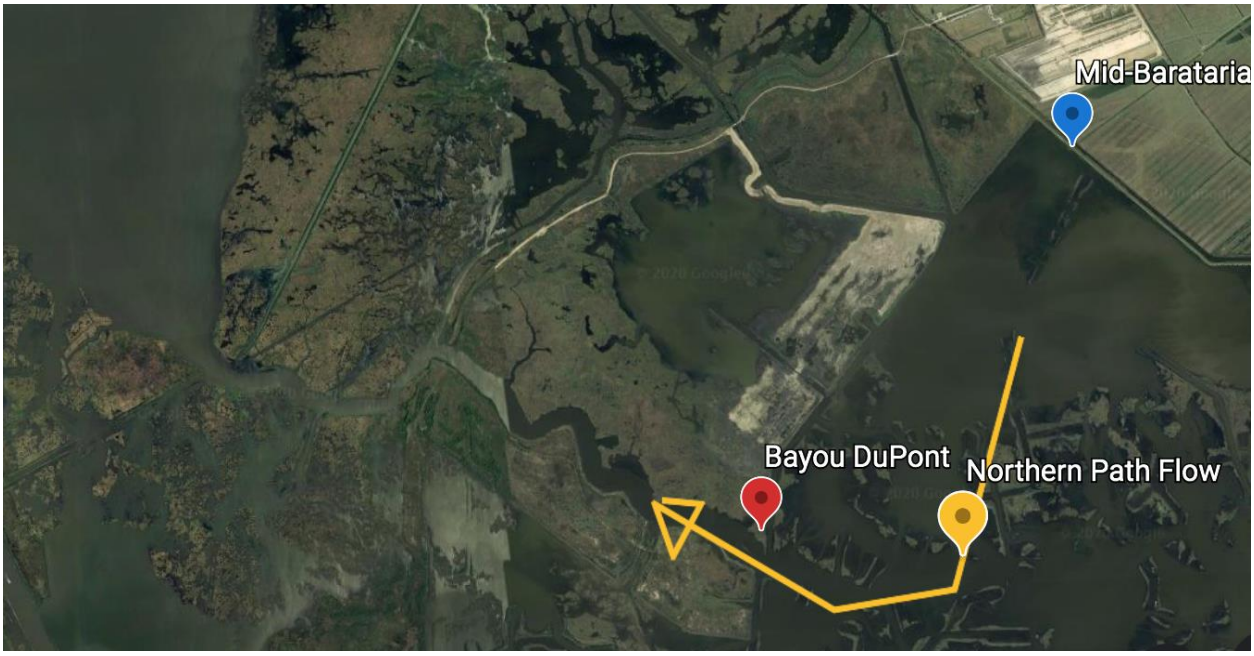

Figure 5.3: Bayou DuPont collects the flow through the open marshland and then it flows north into The Pen which is the start of the Northern Path. Locations are labeled in blue, observation points in red, and flow paths in yellow.

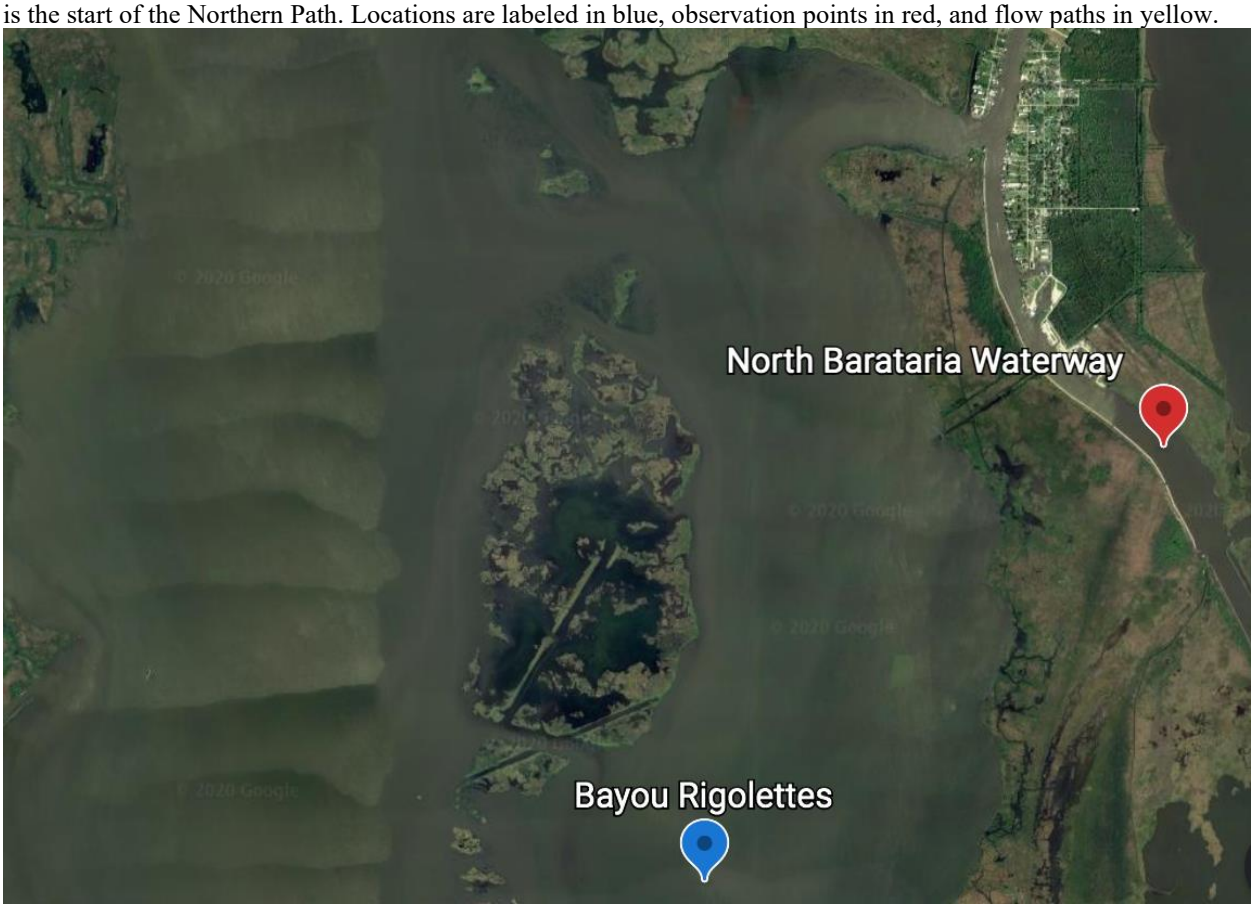

Figure 5.4: Northern opening that connects Bayou Rigolettes to North Barataria Waterway where the northern flow of Barataria Waterway enters the bayou creating the second transition in the Northern Path. Locations are labeled in blue and observation points in red.

Lake Salvador helps to damp the rate of change of this flow. Water levels in the lake follow the diversion hydrograph closely raising around 0.4 m while the diversion is operating at maximum flow and dropping quickly to zero when the diversion is not in operation. This is similar to what happens in North Barataria Waterway but it is clear by the difference in water levels between the two points that some of the flow enters Bayou Rigolettes at a fairly consistent percentage of the diversion induced flow.

5.2.4 Mid-Barataria Waterway Path

This path develops from many decentralized distributary channels already present within the marsh shown in Figure 5.5. Over the course of the diversion opening, these open water channels increase in velocity, transporting more water into Barataria Waterway. As the diversion increases discharge, these channels erode becoming deeper and allowing more flow into the waterway. This is also an energy efficient pathway due to the high flow capacity of the Barataria Waterway.

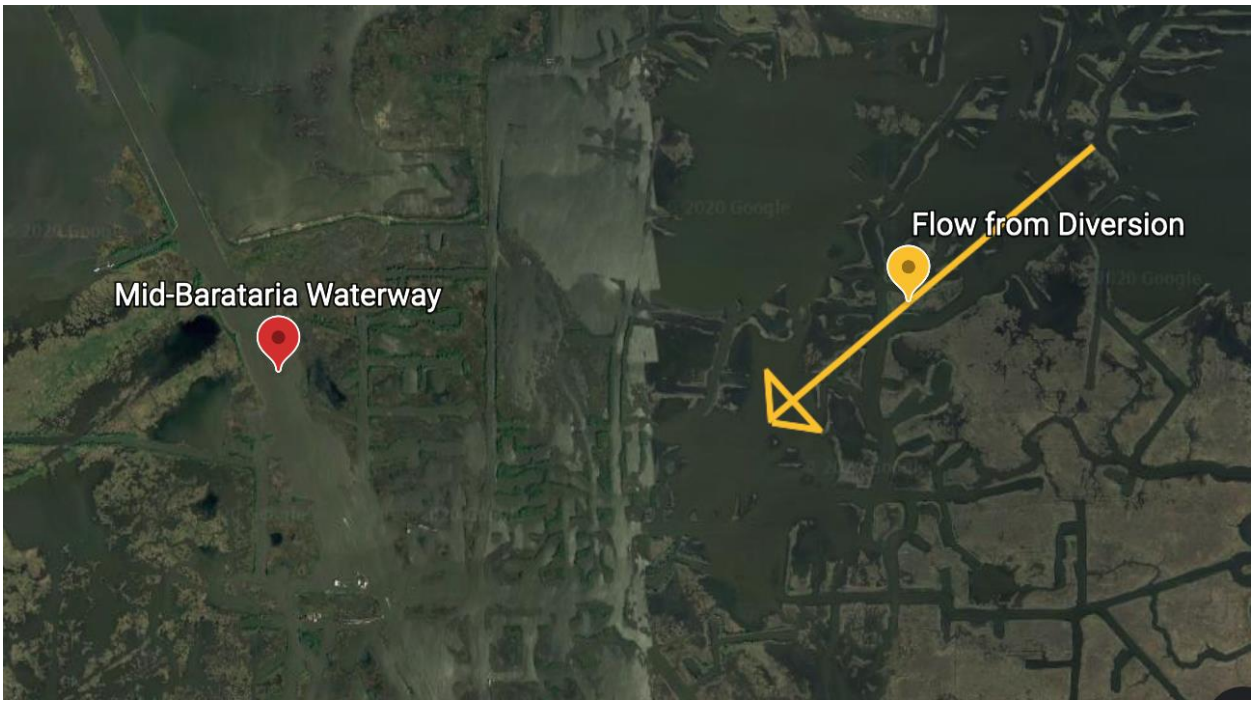

Figure 5.5: Open water distributaries that when combined increase the flow in the Barataria Waterway flowing south to create the Mid-Barataria Waterway diversion distributary channel. Observation points in red and flow paths in yellow.

Erosion continues at this point until the diversion discharge ends and is one of the areas with the highest erosion in the domain. Velocity within the waterway stays high which not only prevents sediment deposition in the middle of the channel but also erodes the waterway. During the maximum flow operation scenario in a high flow year, up to 0.5 m of erosion can occur in the channel while operating the diversion at 50% Maximum Flow during a normal river flow year causes negligible erosion.

5.3 Flood Levels

5.3.1 Water Level Filter

Water levels showed signs of tidal variation even within the difference files; this was attributed to phase changes that may have occurred due to a change in the tidal prism or cross-sectional area that the tides move through or the interaction of the tides and currents in the tidal passes. To reduce this tidal variation, the data were filtered to remove any signal with a frequency below 48 hours using a two-day moving average. For example, Figure 5.6 shows the unfiltered water levels difference at the southern terminus of Barataria Waterway, which is influenced by both tide and flow from the diversion. Differencing the diversion operation water levels with the No Diversion case should have removed this signal. It did not. Once the two-day moving average filter was applied, this signal was removed as indicated by the solid blue line in Figure 5.6.

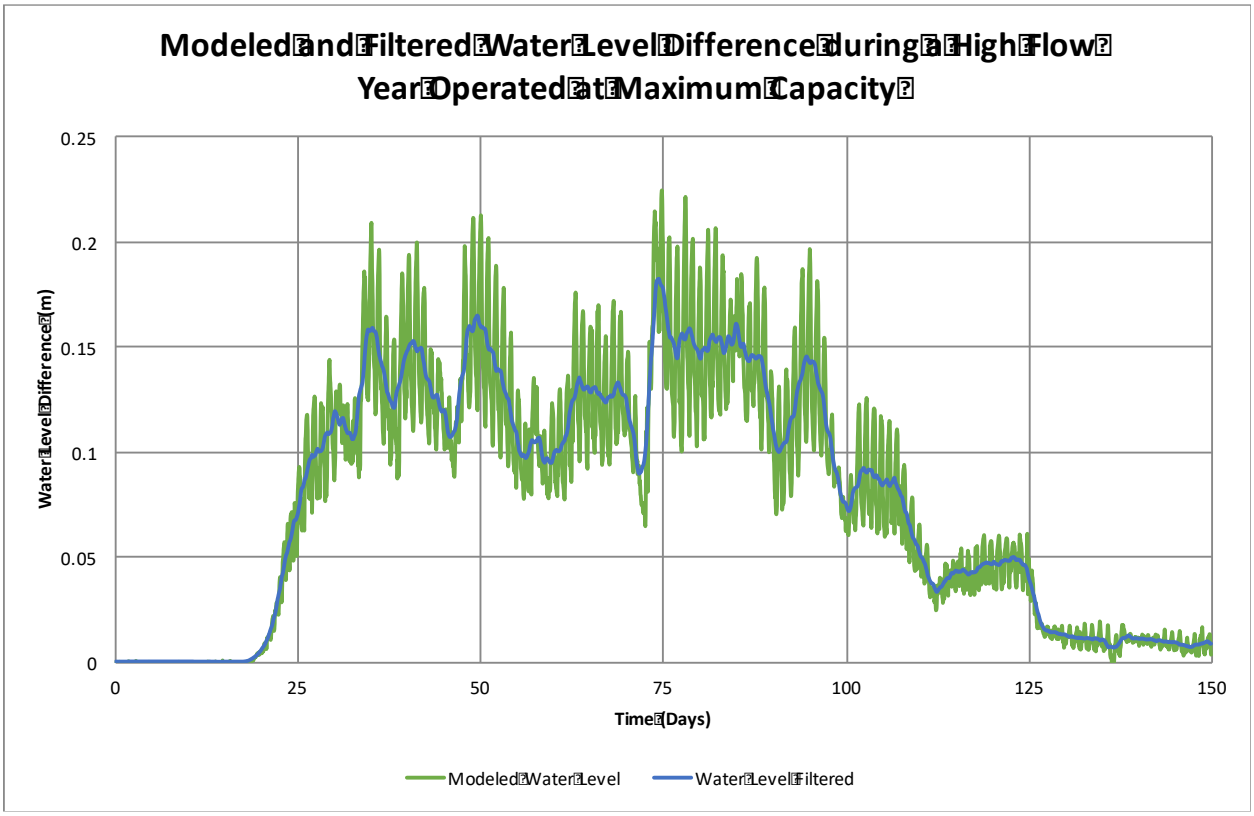

Figure 5.6: Water level difference at South Barataria Waterway during a high flow year when the diversion is operated at maximum capacity displaying raw and two-day moving averaged data.

5.3.2 Receiving Basin

At Bayou DuPont and Round Lake, water levels increase along with the increase in diversion discharge. Water levels at these sites react very quickly to the change in the diversion. When the diversion opens, water levels increase sharply over the first day and then follow the gradual rise of the increasing diversion discharge. Water levels at both locations peak early in the diversion discharge and begin to decrease even when the diversion is at maximum flow. This is due to the undeveloped distributary channels in the receiving basin including at the mouth of the diversion.

The mouth of the diversion is not initially deep enough to pass the amount of water released by the diversion without a significant increase in the water level. As this channel and the channels in the receiving basin begin to erode water levels no longer has to be as high to pass the discharge from the diversion. Once the diversion discharge is no longer changing, the erosion of the receiving basin continues, which reduces water levels to pass the same amount of discharge. This is demonstrated by the difference in peak water levels between the high and low flow year. During the high flow year, the diversion ramps from a flow of 500 m^3/s to peak discharge in a shorter period of time than during the normal flow year, which allows less time for the distributary channels to erode. The result is increased water levels. At Bayou DuPont and Round Lake during the high flow year, water levels peak at 0.2 m higher than during the normal flow years.

Water levels decrease while the diversion is at maximum discharge but then begin to decrease sharply as the diversion discharge is reduced. Within a day of the diversion closing, the water levels return to the levels of the No Diversion scenario. This is because the distributary channels have developed to the point of carrying the maximum discharge from the diversion. Once this is reduced water easily drains from this area as shown in Figure 5.7.

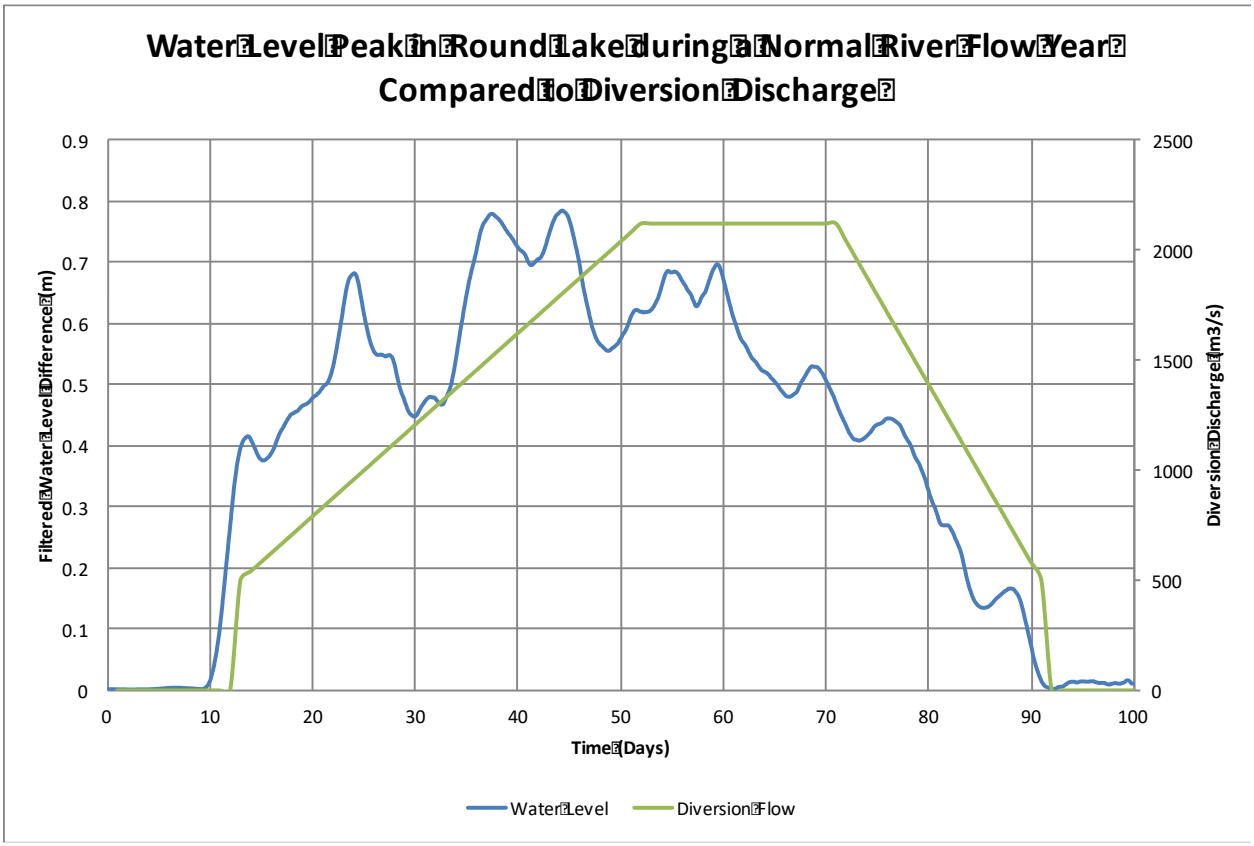

Figure 5.7: Water level peak in comparison to diversion discharge during a normal Mississippi River flow year at Round Lake.

Round Lake receives most of its flow from the diversion through Bayou DuPont (to the north) as shown in. The high flow of water into Round Lake increases water levels causing extreme flooding in the marsh surrounding the lake.

When the diversion is operating at capacity water levels remain over 0.5 m higher than the No Diversion scenario. Running the diversion at 50% Maximum Flow can reduce water levels by 0.2 m for both the normal and high flow years. This suggests that operation of the diversion can reduce flooding by 20% while distributary channels are forming.

During the first year, the length of time the diversion is in operation will determine the duration of flood levels for the receiving basin. Since there is so much open water between these points it makes sense that flow is minimally restricted. The operation of the diversion changes the flood levels by a maximum of 0.25 m based on the operational strategy used.

5.3.3 Barataria Waterway

There are two different flows within the Barataria Waterway. One migrating north towards Bayou Rigolettes and the other south to Barataria Basin. There were three observation points within the Barataria Waterway; The North Barataria Waterway observation point is at the entrance of Bayou Rigolettes; The Mid-Barataria observation point is south of the broken marshland that consolidates flow into the Mid-Barataria Path, and the South Barataria point is just before the flow enters Barataria Basin.

Water levels in North Barataria Waterway remains fairly constant while the diversion is at maximum capacity during the high flow year except when a large storm drains Lake Salvador and the entire Barataria Waterway. During the normal flow year, water levels increase until they peak in the middle of when the diversion is operating at capacity (Figure 5.8). The constant rise and near constant water levels while the diversion is at maximum is because the Barataria Waterway is already a developed channel that can transmit the flow from the diversion. Some erosion does occur which reduces water levels right at the end of the maximum flow from the diversion. This could indicate that the channel has incised enough to allow the full flow from the diversion and less erosion will occur in year two.

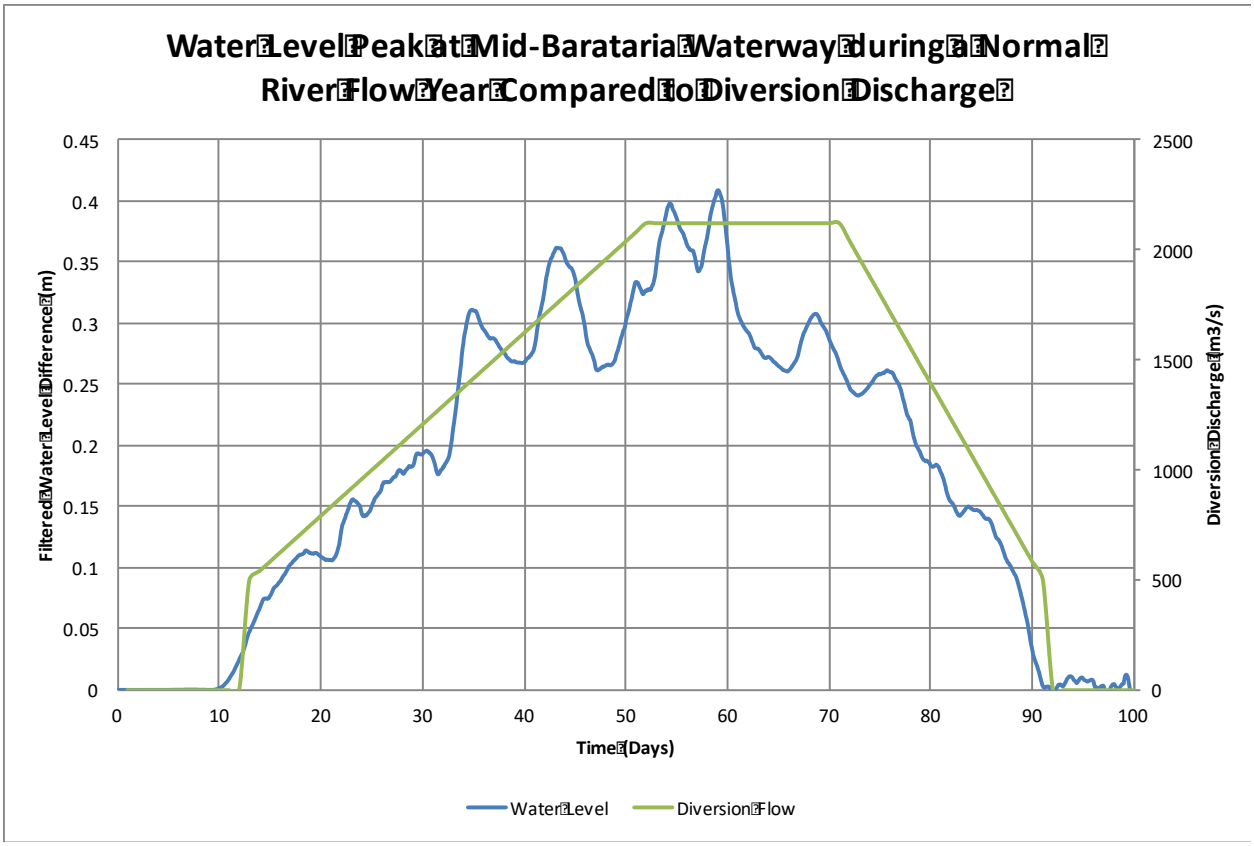

Figure 5.8: Water level peak in comparison to diversion discharge during a normal Mississippi River flow year at Mid-Barataria Waterway.

Lake Salvador water levels follow the pattern in Northern Barataria Waterway but have reduced values. Lake Salvador provides storage for some of the flow in the Northern Path. Once the diversion discharge is reduced the water level in Lake Salvador does not drop as fast as the Northern Barataria Waterway point. Once the diversion is close, the water level in Lake Salvador does not return to the No Diversion scenario. It remains slightly elevated as it slowly drains the stored water.

The Mid-Barataria Waterway has similar water levels to the northern observation point. Water levels increase up to 0.4 m during the normal river flow year and 0.5 m during the high flow year. This will flood the landscape creating overland paths out of the waterway as well. By the time the flow reaches Southern Barataria Waterway, water levels have dropped but still follow the same pattern as the other two observation points. This drop in water level could be due to some flow being lost to Little Lake and Mud Lake.

5.3.4 Grand Bayou

On average the diversion increased water levels within Grand Bayou 0.25 m while it is in operation for both normal and high flow years with maximum levels of 0.45 and 0.55 m respectively. These elevated water levels will flood much of the marsh surrounding the bayou

but this water level is not static. Initially water levels in Grand Bayou increase greatly and then reduce remaining below 0.2 m for over half the time the diversion is in operation.

During the high flow year, water levels reach 0.45 m and stay above 0.4 m for three weeks. This is due to the flow from Lake Laurier peaking around this time. During a normal flow year, water levels above 0.4 m occur for two weeks but happen one month after the diversion is opened as shown in Figure 5.9. This is because the flow of the water has less time to erode the channel of Grand Bayou. Water levels drop off here for two reasons. Grand Bayou erodes to a level that allows for the diversion flow to pass through it with minimal increases in water level and that discharge from Lake Laurier reduces over the course of the diversion flow. This is due to erosion in Wilkinson Bayou that increases discharge through that path.

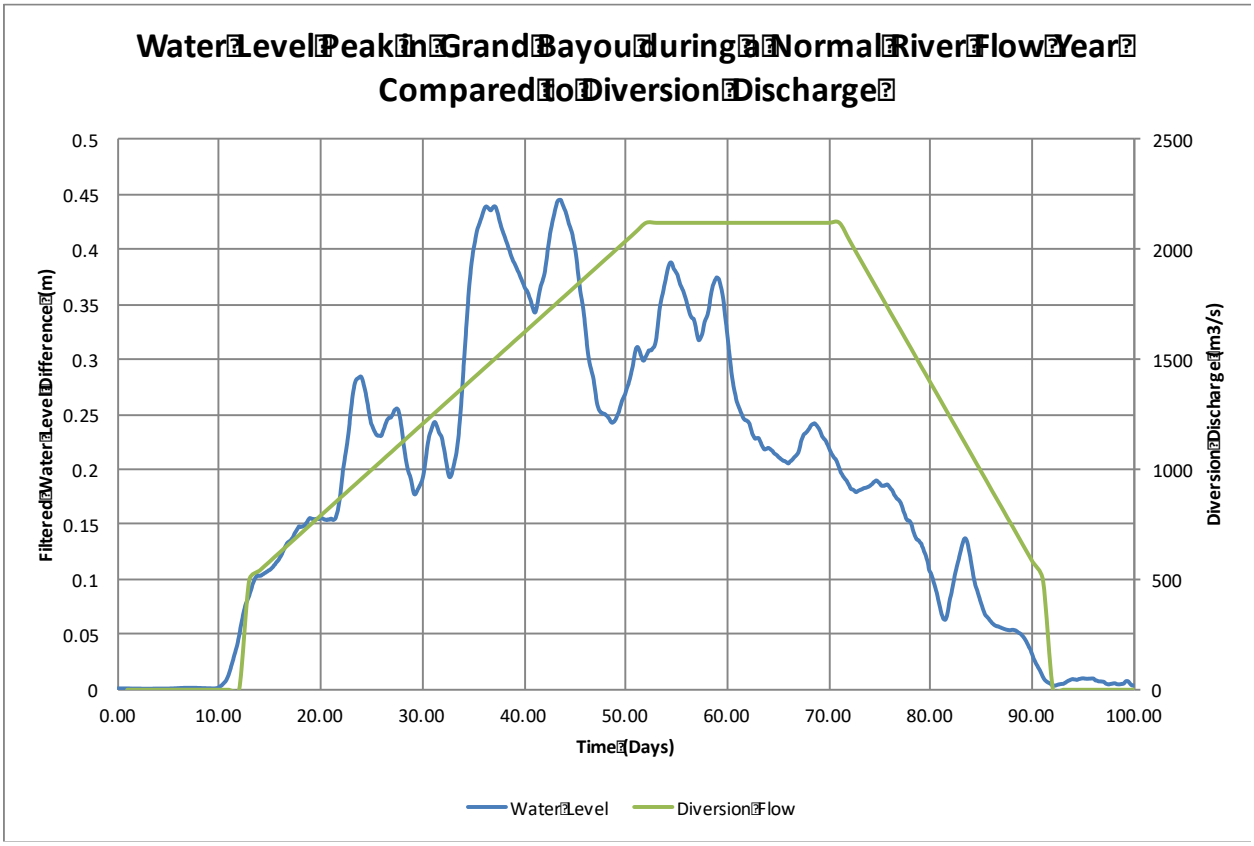

Figure 5.9: Water level peak in comparison to diversion discharge during a normal Mississippi River flow year at Grand Bayou.

5.4 Velocity

5.4.1 Velocity Filter

There are low velocity regions within larger bodies of water such as Round Lake. Here the water velocity at slack water would be close to zero regardless of whether the diversion is operating. The velocity of the diversion and the tide would counteract during flood tide damping the results as seen in the raw difference files and would enhance the flow during ebb tide. The tidal

signature for the maximum flow scenario during a high flow year is shown in Figure 5.10. To remove this a 48-hour filter was applied to the data. Any signals greater than two days will still show within the data.

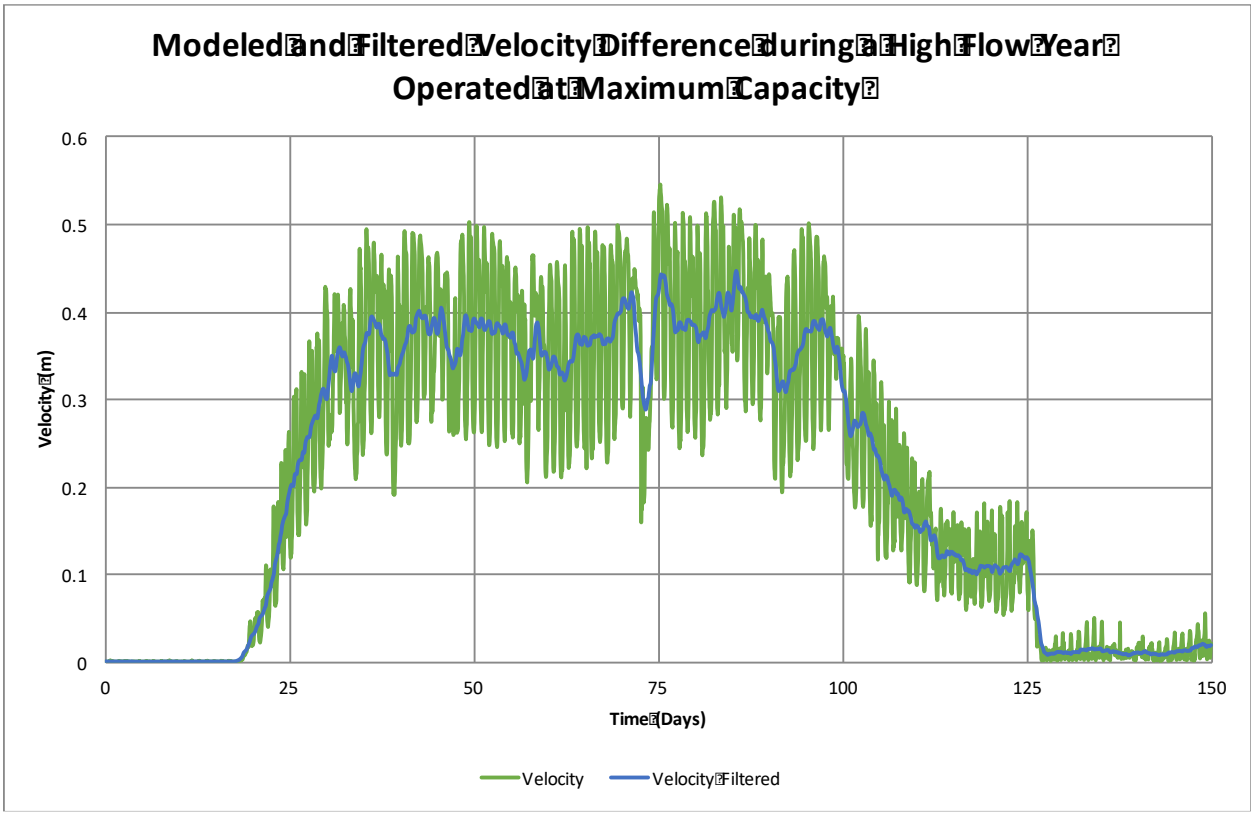

Figure 5.10: Velocity difference at South Barataria Waterway during a high flow year when the diversion is operated at maximum capacity displaying raw and two-day moving averaged data.

5.4.2 Receiving Basin

When the diversion is first opened the velocity, i.e. shear stress in the channel is not enough to keep sand entrained, so some of the sand gets deposited in the channel. As the diversion approaches its peak discharge, velocity through the diversion increases up to 1.8 m/s which is sufficient to resuspend the sand. This not only resuspends but transports sand into the receiving basin. Most of the deposited sand is resuspended within the channel during the rising limb. When the discharge of the diversion is reduced, sediment is again deposited in the channel.

5.4.3 Barataria Waterway

Velocities in the Northern Barataria Waterway increase by 0.2 m/s during the normal flow year and 0.27 m/s during a high flow year. This area has high levels of deposition (up to 1.2 m) which alters the velocity within the waterway. As the flow splits, some entering Bayou Rigolettes and some continuing north into Lake Salvador. The velocity into Bayou Rigolettes is much greater than the flow north into Lake Salvador. The observation point is in the slower flow. At Day 45 during the normal flow year the deposition in North Barataria Waterway begins to differentiate.

This is when velocity differences reach a maximum, but soon after the velocity becomes little differentiated between the operation scenarios. At Day 55 during the high flow year, velocities actually begin to reverse patter with the 50% scenario having the highest velocities.

When the diversion is operating at maximum there is more sediment within the water to be deposited. When the velocities of the various diversion operations are the same more sediment will be deposited from the maximum flow scenario because there is a greater quantity of it in suspension. More deposition in North Barataria Bay leads to more flow being diverted into Bayou Rigolettes reducing velocity in the waterway north of the turn. This leads to more deposition within the channel creating a feedback loop.

Once the diversion is closed, the water that was stored in Lake Salvador begins to drain. This water must move past the section of Barataria Waterway that has filled with silt thus increasing the velocity to maintain discharge. Dredging the receiving basin before the diversion is opened for the first time could prevent much high concentrations of silt from getting into Barataria Waterway and being deposited when the velocity slows.

Since there are no major outlets around the middle and southern observations points on Barataria Waterway, they do not have similar results. In Mid-Barataria Waterway the diversion can increase the velocity by 0.55 m/s when the diversion is operating at maximum flow during a high river flow year and 0.45 m/s during the normal flow year. In South Barataria Waterway the diversion can increase velocity by 0.45 m/s. Peaking when the diversion is operating at full capacity. Velocity in the channel remains elevated even after the diversion begins to decrease in discharge as shown in Figure 5.11. This delayed response could be from the draining of Bayou DuPont and Lake Salvador. By the time the diversion closes it waterway drops to near No Diversion levels within a day. This signifies that most of the receiving basin has been drained by the time the diversion is closed. Lake Salvador still has slightly elevated water levels and continues to drain after the diversion closes, which could explain the difference in velocity once the diversion is closed.

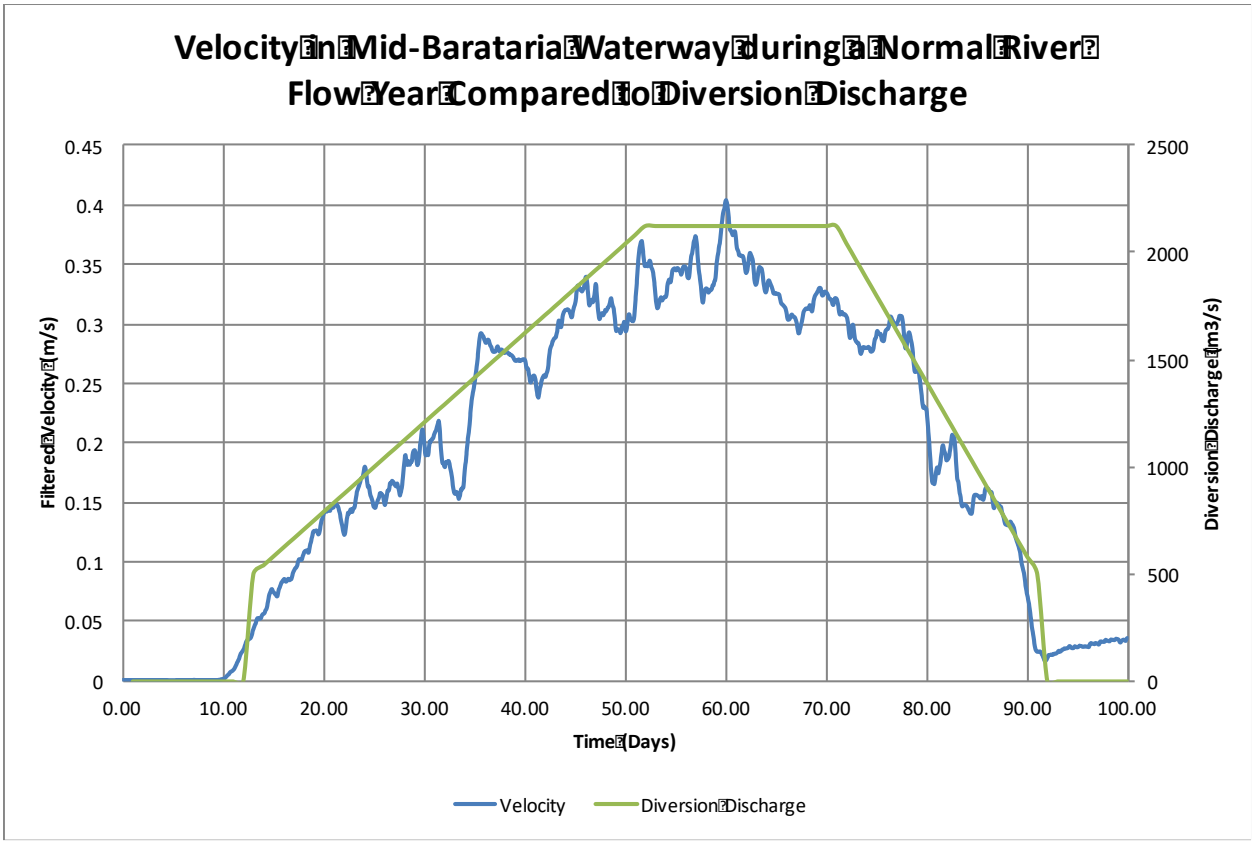

Figure 5.11: Velocity peak in comparison to diversion discharge during a normal Mississippi River flow year at Mid-Barataria Waterway.

5.4.4 Grand Bayou

Velocity in Grand Bayou follows the pattern of elevated water levels for normal and high flow years. The peak velocity during the normal flow year is 0.3 m/s and occurs one month after the diversion is open and just before it reaches maximum discharge as shown in Figure 5.12. The high flow year has a peak discharge of 0.34 m/s occurring three weeks after the diversion is opened. Both flow regimes increase the velocity within Grand Bayou by an average 0.2 m/s while the diversion is in operation. The decrease in water levels and decrease in velocity without a major increase in the depth of the channel shows that discharge entering Grand Bayou is reduced before the diversion's flow is reduced.

Once the diversion is closed. Velocity in Grand Bayou does not return to No Diversion levels. This is because water that traveled to Grand Bayou from the path along the back levee and from Lake Judge Perez is still draining.

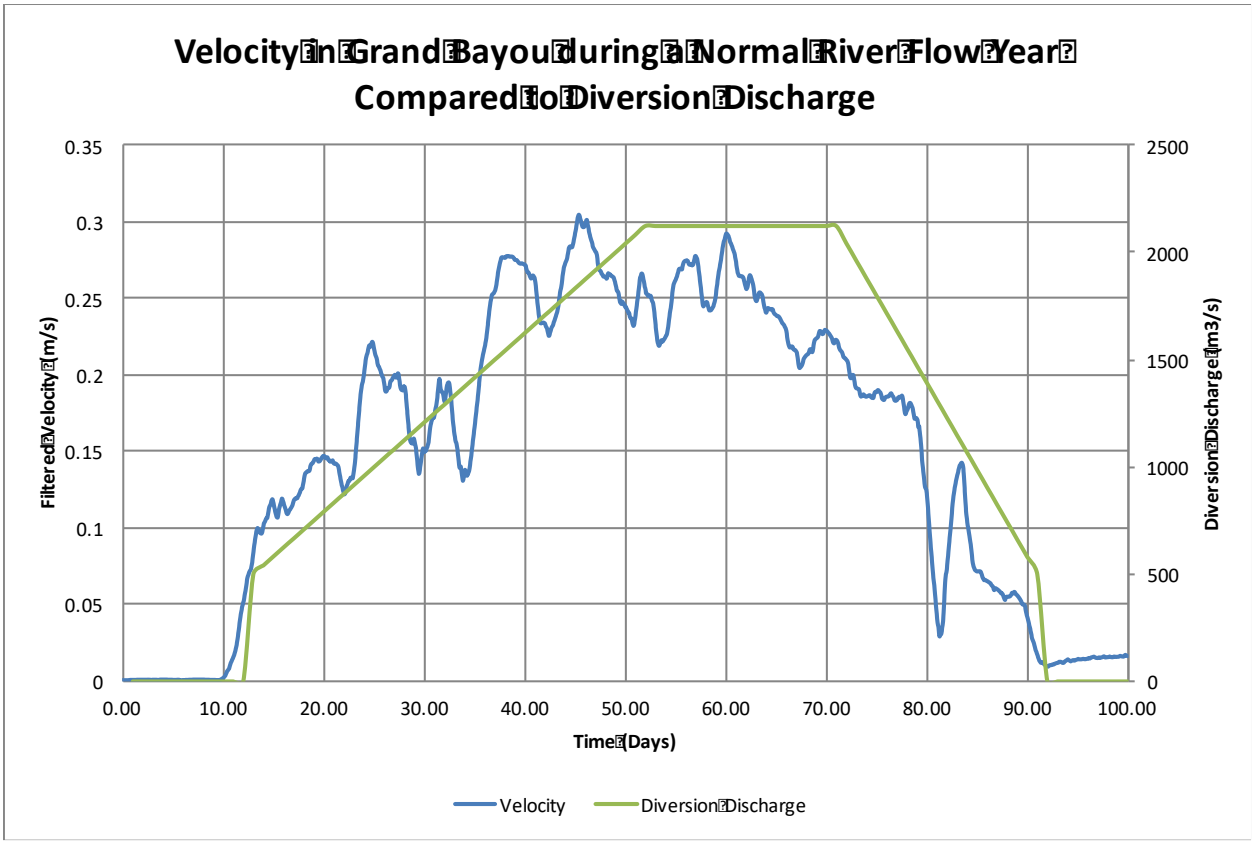

Figure 5.12: Velocity peak in comparison to diversion discharge during a normal Mississippi River flow year in Grand Bayou.

5.5 Sediment

5.5.1 Receiving Basin

Sediment concentration in this water varies greatly based on diversion operational scenarios. While higher amounts of sediment are brought into the receiving basin when the diversion is operated at maximum flow versus 50% the concentration remains the same in the model. What does change is the erosion of the receiving basin. The mouth of the diversion can erode up to 8 m when the diversion is operated at maximum flow in the first year increasing the sediment in the water.

Sand settles out of the water column quickly, depositing on the sides of the channel created at the mouth of the diversion and along the levee system due to the eddies coming out of the diversion. Even the sand that is picked up while scouring the channel at the mouth of the diversion is quickly deposited. Outside of the mouth of the diversion, the velocity of water is not fast enough to keep sand in suspension. Some sand can move as bed load, however this is very small.

Silt leaves the diversion at a concentration of just under 0.1 kg/m^3. The souring at the mouth of the diversion and continued erosion of the immediate receiving basin increases the silt concentration. By the time the flow reaches The Pen, concentrations in the water have increased

by up to 1.3 kg/m^3. When the flow is operated at 50% maximum flow during the high flow year, the silt concentration increases by 0.26 kg/m^3. This means that much of the silt is entrained during the initial scour at the mouth of the diversion and the continued erosion of the receiving basin.

The initial time to peak discharge also plays a role in how much silt enters The Pen. At maximum flow, the difference in concentration between the normal and high flow years is almost 0.6 kg/m^3. This corresponds with a 2 m increase in the depth of the channel at the mouth of the diversion.

Round Lake has much lower concentrations of silt. When the diversion is operated at maximum flow during a high flow year the average concentration of silt is 0.21 kg/m^3 but run at 50% it is 0.03 kg/m^3. This is because the cannel into Round Lake is more established that the flow entering The Pen so less erosion occurs. Also, much of the flow entering The Pen goes through the northern portion of Bayou DuPont with no areas of deposition. The flow into Round Lake comes through the southern portion of Bayou DuPont which travels through an open water section slowing velocities and depositing much of the silt before it reaches Round Lake.

Clay follows a similar pattern to silt however less is deposited. Once the flow picks up clay from the receiving basin it stays in suspension until the flow enters Barataria Bay and beyond. This is partially due to the fact that salinity within the basin drops to zero just days after the diversion is open which reduces the flocculation of the clay particles in the water.

5.5.2 Barataria Waterway

Velocities entering The Pen are high enough to cause erosion along the bottom half of this area. Some flow escapes north into the nearly still water; Velocities slow and silt is deposited. As the flow enters Barataria Waterway velocities continue to slow and more silt is deposited. By the time the flow reaches the observation point at North Barataria Waterway, some sediment has been lost since The Pen but silt levels are still as high as 1.26 kg/m^3 during the high flow year which is 15 times the concentration of silt entering the through the diversion. At the turn into Bayou Rigolettes this silt is deposited as the velocity of the water continues to slow. This can deposit as much as 1.2 m of silt in the waterway, which would be a problem for transpiration in the channel. This sediment will have to be dredged to allow for ships to continue through the waterway unhindered. More research will have to be done to determine if this silt will deposit within the waterway every year or will this deposition slow as the distributary channels become more defined. If the latter is the case, the receiving basin could be dredged before the diversion is opened to reduce the amount of erosion that will occur in the diversions first year.

Silt concentrations at the southern terminus of Barataria Waterway is the highest out of any observation point during the Maximum flow but is less than at North Barataria Waterway during reduced maximum flow scenarios. The northern and southern flow in Barataria Waterway start with similar concentrations. As the flow travels south down the waterway silt is deposited along the edges as the middle of the channel erodes. During the maximum flow scenarios, this channel can erode up to 0.5 m adding more silt to the water column but when the diversion is operated at

50% maximum flow the waterway has minimal erosion. This explains why there is much less silt when the diversion is operated at a reduced maximum flow.

5.5.3 Grand Bayou

Sand and silt that came through the diversion is deposited before the flow reaches Grand Bayou. Round Lake and Lake Laurier both have large silt deposits that take most of the silt out of suspension. Clay concentrations increased within the water range from 0.2 to 0.55 kg/m^3 depending on operational strategy. During the high flow year, the diversion had a lower concentration of clay than during the high flow year yet the concentration of silt in Grand Bayou during the high flow year had a concentration of 0.15 kg/m^3 greater than that of the normal flow year. This is because of the erosion happening within the receiving basin during the high flow year with its quicker time to peak discharge.

Clay has little impact on the geomorphology of Grand Bayou because the velocities within the bayou are too high for the clay to settle out and there is limited flocculation while the salinity is at zero. However, the increased turbidity of the water reduces the light available for photosynthesis, which alters oxygen levels within the water. Increased turbidity can harm fish spawning and increase pollution levels in the area so working to reduce this concentration would be beneficial.

5.6 Salinity

The diversion causes salinity levels to drop to zero over much of the domain. The area around Bayou DuPont, Round Lake, and Barataria Waterway become fresh just days after the diversion is open and recovery is slow once the diversion is closed. In North Barataria Waterway, salinity rebound is negligible but could change if the silt restricting some of the flow is dredged. Then it would probably similar to the salinity in Mid-Barataria Waterway which shows modest recovery after the diversion is closed. If that rate of recovery were to continue, it would take over a month for salinity levels to return to normal.

The salinity within Grand Bayou falls to 0 ppt within the first two weeks of the diversion opening. This prevents flocculation of sediment. The bayou remains purely fresh water until the diversion is closed. Then it slowly begins to increase in salinity levels. This recovery is not nearly as rapid as the decline and will take months to return to normal levels if the rate stays the same.

Lake Washington has salinity levels as low as 5 ppt when the diversion is operated at maximum flow. This area is far south of the diversion but is fed by Grand Bayou. When the diversion is open it has fresh water entering from the north and salt water coming in from Bay Long to the south. This large tidal influence is why Lake Washington retains some salinity while the diversion is in operation. The area west of Lake Washington is the central Barataria Bay which receives a large influx of fresh water from Barataria Waterway but gets salt water from inlets near Grand Isle and Grand Terre Islands. For that reason, the eastern part of the bay has similar responses to the diversion. Once the diversion closes salinity levels rebound to near No Diversion levels however freshwater drainage from the rest of the basin could be slowing the

complete return to these levels. Even salinity changes of this much could affect a lot of species that require higher salinity levels to survive.

The western part of Barataria Bay has even less direct fresh water input. The closest flow path created by the diversion is the Northern Path that enters Barataria Bay through Little Lake which is to the east of the Western Barataria Bay observation point. Due to mixing of the bay some of this water coming from the northern path reduces the salinity that is present during the No Diversion scenario but this was minimal when the diversion is at peak discharge and there is no difference after the diversion begins to decrease discharge.

5.7 Model Sensitivity

There are multiple sources of error that could occur within the model. One source is that there are a range of values determined by previous studies that could be used in the model. Precedence from previous models was used to determine these values. When that was not immediately available a best approximation was used to determine model values based on literature analysis. In addition to value ranges between students, many are spatially variable as well. Simplifications were made to reduce the number of spatially varying possibilities.

The critical shear stress of the bed was modeled as 0.1 Pa, which is on the lower side of critical shears stresses tested in Barataria Basin. This value was chosen because this is the critical shear stress of newly deposited sediment within the basin. The sediment deposited by the diversion would likely have an initial critical shear stress less than this value but sediment that was in the basin prior to the diversion construction would have a larger value. Studies have shown that the critical shear stress increases to 0.2 Pa within 6 months of sediment deposition in the basin. Vegetation also increases the critical shear stress of soil yet no vegetation was modeled in this study. A higher average critical shear stress in the marsh areas of the basin would lead to reduced marsh erosion and increased incising of the open water pathways.

Critical shear stress is not the only value that determines erosion in the model. The velocity and, in turn, the shear stress of the flow is determined based on the Manning's roughness. Three different Manning's roughness were used in the model increasing from the center of the channel, to the marsh edge and center. The higher roughness in the middle of the marsh was used to approximate the roughness due to vegetation that reduces the velocity and shear stress caused by the flow. This roughness dampens erosion in the basin. These values were determining through literature and the model calibration. However, any under estimate in these values would also lead to an over prediction of erosion.

The sediment composition of the bed determines how easy it is eroded. There were five layers of the bed each chosen to be 2 m deep. The sand percentage ranged from 5 – 20% through the layers from top to bottom. This was chosen based on literature values. These layers were assumed to be constant throughout the domain and were only differentiated between the marsh (elevation 0 m and above) and the channels (elevation below 0 m) in layer thickness. In reality, sediment fractions in the basin would vary. However, this would cost computational time so the simplification was made. More sand in these layers would make the bed harder to erode reducing the erosion determined by the model. The critical shear for sand is based on the Shields Curve.

The final parameter that determines erosion and deposition is settling velocity. For sand, the settling velocity was determined using the van Rijn equations based on an average sediment diameter determined from literature. For silt and clay, both the settling velocity and average particle size were determined from literature. Any under estimation in settling velocity would increase the net erosion values especially in the immediate receiving basin since slow settling velocities would cause particles to remain in suspension longer moving away from the diversion.

5.8 Recommendations

The results show that dredging a channel at the mouth of the diversion is needed to reduce increased turbidity in the water and silt deposition in Round Lake, The Pen, and Barataria Waterway. Dredging of the three major distributary pathways within the receiving basin could further reduce erosion and prevent high concentrations of sediment in the water. This would also result in a more control evolution of the distributary system and would help reduce the maximum flood levels. The depth and duration of marsh flooding may also be reduced by pre-dredging the main distributary channels.

Grand Bayou could be protected through the addition of a flood diverting structure or pre-dredging of Wilkinson Bayou. This bayou eventually erodes enough to receive the majority of the flow from the Southern Path but it takes time of this channel to develop. Pre-dredging this path would immediately reduce the flood waters in Grand Bayou protecting the native populations along its banks.

A combination of pre-dredged channels, slowly ramping the diversion up to peak discharge, and operating the diversion at reduced flow in the initial years could prevent flooding within the basin while still developing the distributary pathway needed to move the full diversion flow. Also, timing of the diversion opening is critical. If the diversion is only operated off of the Mississippi River hydrograph, the diversion could cause much of the basin to be completely fresh water late into June when the peak discharge is late for example in the modeled normal river flow scenario. Some years the maximum sediment building capacity will need to be balanced against the salinity needs of oyster and other fisheries that cannot handle the fresh water during warm water periods in the spring and summer months.

Chapter 6: Conclusions

The Barataria Basin model was successfully developed, calibrated, and applied to simulate tides, diversion flow, wind forcing, sediment, and salinity. As the diversion enters the receiving basin the mouth of the diversion is scoured creating a deep channel with sediment depositing on either side in a natural levee building process. However, the majority of the immediate receiving basin experiences erosion with large amounts of silt and clay being resuspended with a consequent increase in the sediment concentration in the water.

Three major pathways were created by the diversion out of the immediate receiving basin. The southern path through Round Lake that initially pushes flow through Grand Bayou until Wilkinson Bayou erodes enough to take a large portion of the flow. The Mid-Barataria Waterway path that enters Barataria Waterway through the broken mashes west of Bayou DuPont. Finally, the Northern Path that moves water north through Barataria Waterway into Bayou Rigolettes. These pathways distribute fresh water that reduces salinity levels to near zero and floods the marshes around them. When the velocity slows in large bodies of water like The Pen and Round Lake silt deposits are built. This also occurs in the area of nearly stagnate water between the northern and southern flow of water in Barataria Waterway. Pre-dredging of the receiving basin will reduce the amount of silt resuspension and subsequent deposition and reduce the turbidity of the water. If Wilkinson Bayou is dredged before the diversion is operated, Grand Bayou could be spared the worst of the flooding.

The operation of the diversion will determine the impact that the diversion has on the landscape. The diversion should have a slow ramp up to peak discharge to allow channel development. The length of time that the diversion is open is directly proportional to the length of time water levels are elevated, so even if pre-dredging is utilized, peak discharge should be shortened during the first year to reduce the duration of major flooding while channels are developing to their full capacity. Finally, timing of the diversion opening cannot be solely based on the Mississippi River hydrograph. The model showed that during the simulated normal flow year much of the basin would be fresh water into June possibly damaging the oyster harvest for the year.

More research needs to be done to test the effectiveness of some of the recommendations in Chapter 5. The model could be run again using the final bathymetry generated during this one season scenario to see if the channels have fully developed during the first year or if more erosion should be expected in year two and possibly beyond. The model could also be used to text how much pre-dredging of the channels before the diversion is opened would needed to achieve the optimum benefits such as reducing excessive erosion, high silt concentrations and subsequent deposition in Barataria Waterway. Further model work could be done to determine the best way to operate the diversion in subsequent years to maximize land building and minimize erosion while reducing other impacts on the receiving basin.

References

Allison, M. A., Demas, C., Ebersole, B., Kleiss, B., Little, C., Meselhe, E., Powell, J., Pratt, T., & Vosburg, B. (2012). A Water and Sediment Budget for the Lower Mississippi–Atchafalaya River in Flood Years 2008–2010: Implications for Sediment Discharge to the Oceans and Coastal Restoration in Louisiana. *Journal of Hydrology, 432–433*, 84–97.

Allison, M. A., Ramirez, M. T., & Meselhe, E. A. (2014). Diversion of Mississippi River water downstream of New Orleans, Louisiana, USA to maximize sediment capture and ameliorate coastal land loss. *Water resources management*, *28*(12), 4113-4126.

Allison, M. A., & Meselhe, E. A. (2010). The use of large water and sediment diversions in the lower Mississippi River (Louisiana) for coastal restoration. *Journal of Hydrology*, *387*(3-4), 346-360.

Amer, R., Kolker, A. S., & Muscietta, A. (2017). Propensity for erosion and deposition in a deltaic wetland complex: Implications for river management and coastal restoration. *Remote Sensing of Environment*, *199*, 39-50.

Amini, Sina (2014) Hydrodynamics and Salinity of Pontchartrain Estuary during Hurricanes, Master of Science Thesis, Civil and Environmental Engineering, University of New Orleans, New Orleans, LA.

Adrus, T. M., & Bentley, S. J. (2007). Sediment flux and fate in the Mississippi River Diversion at West Bay: Observation study. *Coastal Sediments, 07,* 722-735.

Barras, J., Beville, S., Britsch, D., Hartley, S., Hawes, S., Johnston, J., Kemp, P., Kinler, Q., Martucci, A., Porthouse, J., Reed, D., Roy, K., Sapkota, S., & Suhayda, J. (2003). Historical and projected coastal Louisiana land changes: 1978-2050. *USGS Open File Report 03-334*, 39.

Barras, J. A. (2006). Land area change in coastal Louisiana after the 2005 hurricanes—a series of three maps. *U.S. Geological Survey Open-File Report 06-1274*.

Barras, J. A., Padgett, W. C., & Sanders, C. B. (2009). Aerial and Bathymetric Spatial Change Analysis of the West Bay Sediment Diversion Receiving Area, Louisiana for US Army Engineer District, New Orleans (MVN) Report. *US Army Eng. Res. Dev. Cent., Environ. Lab, Baton Rouge, La*.

Barras, J. A. (2010). Hurricane-induced failure of low salinity wetlands. *Proceedings of the National Academy of Sciences*, *107*(32), 14014 LP-14019.

Batker D., Mack S., Sklar F., Nuttle W., Kelly M., Freeman A. (2014) The Importance of Mississippi Delta Restoration on the Local and National Economies. In: Day J., Kemp G., Freeman A., Muth D. (eds) Perspectives on the Restoration of the Mississippi Delta. Estuaries of the World. Springer, Dordrecht

Baker, A., Henkel, T., Lopez, J. & Boyd, E. (2011). A Project of the Lake Pontchartrain Basin Foundation and the Coalition to Restore Coastal Louisiana. Lake Pontchartrain Basin Foundation.

Bauman, R. H., Day, J. W., & Miller, C. A. (1984). Mississippi Deltaic Wetland Survival: Sedimentation Versus Coastal Submergence. *Science*, *224*(4653), 1093 LP-1095.

Bevington, A. E., & Twilley, R. R. (2018). Island edge morphodynamics along a chronosequence in a prograding deltaic floodplain wetland. *Journal of Coastal Research*, *34*(4), 806-817.

Bianchi, T. S., & Allison, M. A. (2009). Large-river delta-front estuaries as natural "recorders" of global environmental change. *Proceedings of the National Academy of Sciences*, *106*(20), 8085-8092

Blankespoor, B., Dasgupta, S., & Laplante, B. (2012). Sea-level rise and coastal wetlands. *Policy Research Working Paper (WPS6277), World Bank*.

Blum, M. D., & Roberts, H. H. (2009). Drowning of the Mississippi Delta due to insufficient sediment supply and global sea-level rise. *Nature Geoscience*, *2*, 488.

Boesch, D., Josselyn, M., Mehta, A., Morris, J., Nuttle, W., Simenstad, C., & Swift, D. (1994). Scientific Assessment of Coastal Wetland Loss, Restoration and Management in Louisiana. *Journal of Coastal Research,* I-103.

Britsch, L. D., & Kemp III, E. B. (1990). Land loss rates: Mississippi River deltaic plain (No. WES/TR/GL-90-2). Army Engineer Waterways Experiment Station, Vicksburg, MS.

Brown, S., Couvillion, B., Conzelmann, C., de Mutsert, K., Fischbach, J., Hunnicutt, C., McKelvy, M., Quibodeaux, P., Roberts, H., Rodrigue, M., Schindler, J., Suir, K., Thomson, G., Visser, J., & White, E. (2017). 2017 Coastal Master Plan: Appendix C: Modeling Chapter 3 - Modeling Components and Overview. Version Final. (p. 72). Baton Rouge, Louisiana: Coastal Protection and Restoration Authority

Brown, G., McAlpin, J., Pevey, K., Loung, P., Price, C., & Kleiss, B. (2019). Mississippi River Hydrodynamic and Delta Management Study: Delta Management Modeling. *US Army Corps of Engineers Coastal and Hydraulics Laboratory.* TR-19-2.

Buttles, J., Mohrig, D., Nittrouer, J., McElroy, B., Baitis, E., Allison, M., & Kim, W. (2007). Partitioning of water discharge by distributary channels in the prograding, Wax Lake Delta, coastal Louisiana, USA. *AGU*.

Cahoon, D. R., & Reed, D. J. (1995). Relationships among marsh surface topography, hydroperiod, and soil accretion in a deteriorating Louisiana salt marsh. *Journal of Coastal Research*, 357-369.

Cao, S., & Knight, D.W. (2002) Review of regime theory of alluvial channels. *Journal of Hydrodynamics, 3*, 1–3.

Carle, M. V., Sasser, C. E., & Roberts, H. H. (2015). Accretion and vegetation community change in the Wax Lake Delta following the historic 2011 Mississippi River flood. *Journal of Coastal Research*, *31*(3), 569-587.

Carle, M. V., & Sasser, C. E. (2016). Productivity and resilience: long-term trends and storm-driven fluctuations in the plant community of the accreting Wax Lake Delta. *Estuaries and coasts*, *39*(2), 406-422.

Coastal Protection and Restoration Authority of Louisiana. (2012). Louisiana's Coastal Master Plan for a Sustainable Coast; Coastal Protection and Restoration Authority of Louisiana: Baton Rouge, LA, USA.

Coastal Protection and Restoration Authority of Louisiana. (2017) Louisiana's Coastal Master Plan for a Sustainable Coast; Coastal Protection and Restoration Authority of Louisiana: Baton Rouge, LA, USA.

Coleman, J.M., Roberts, H., & Stone, G. (1998) Mississippi River Delta: an Overview. *Journal of Coastal Research, 14(3),* 698-716.

Conner, W., Nuttle, W. K., Brinson, M. M., Cahoon, D., Callaway, J. C., Christian, R. R., & Lynch, C. (1997). Conserving Coastal Wetlands Despite Sea Level Rise. *Eos, Transactions, American Geophysical Union*.

Couvillion, B. R., Beck, H., Schoolmaster, D., & Fischer, M. (2017). *Land area change in coastal Louisiana (1932 to 2016)* (No. 3381). US Geological Survey.

Das, A., Justic, D., Inoue, M., Hoda, A., Huang, H., & Park, D. (2012). Impacts of Mississippi River diversions on salinity gradients in a deltaic Louisiana estuary: Ecological and management implications. *Estuarine, Coastal and Shelf Science*, *111*, 17-26.

Day Jr, J. W., Martin, J. F., Cardoch, L., & Templet, P. H. (1997). System functioning as a basis for sustainable management of deltaic ecosystems. *Coastal Management*, *25*(2), 115-153.

Day, J. W., Britsch, L. D., Hawes, S. R., Shaffer, G. P., Reed, D. J., & Cahoon, D. (2000). Pattern and process of land loss in the Mississippi Delta: a spatial and temporal analysis of wetland habitat change. *Estuaries*, *23*(4), 425-438.

Day Jr, J. W., Barras, J., Clairain, E., Johnston, J., Justic, D., Kemp, G. P., & Templet, P. (2005). Implications of global climatic change and energy cost and availability for the restoration of the Mississippi delta. *Ecological Engineering*, *24*(4), 253-265.

Day, J. W., Boesch, D. F., Clairain, E. J., Kemp, G. P., Laska, S. B., Mitsch, W. J., & Whigham, D. F. (2007). Restoration of the Mississippi Delta: Lessons from Hurricanes Katrina and Rita. *Science*, *315*(5819), 1679-1684.

Day, J. W., Christian, R. R., Boesch, D. M., Yáñez-Arancibia, A., Morris, J., Twilley, R. R., & Schaffner, L. (2008). Consequences of climate change on the ecogeomorphology of coastal wetlands. *Estuaries and Coasts*, *31*(3), 477-491.

Day, J. W., Cable, J. E., Cowan Jr, J. H., DeLaune, R., De Mutsert, K., Fry, B., & Rick, J. (2009). The impacts of pulsed reintroduction of river water on a Mississippi Delta coastal basin. *Journal of Coastal Research*, 225-243.

Day, J.W., Christian, R.R., & Boesch, D.M. (2012). Consequences of Climate Change on the Ecogeomorphology of Coastal Wetlands. *Climatic Change, 110*, 297.

Day, J., Lane, R., Moerschbaecher, M., DeLaune, R., Mendelssohn, I., Baustian, J., & Twilley, R. (2013). Vegetation and soil dynamics of a Louisiana estuary receiving pulsed Mississippi River water following Hurricane Katrina. *Estuaries and coasts*, *36*(4), 665-682.

Day, J. W., Cable, J. E., Lane, R. R., & Kemp, G. P. (2016). Sediment deposition at the Caernarvon crevasse during the great Mississippi flood of 1927: implications for coastal restoration. *Water*, *8*(2), 38.

DeLaune, R. D., Baumann, R. H., & Gosselink, J. G. (1983). Relationships among vertical accretion, coastal submergence, and erosion in a Louisiana Gulf Coast marsh. *Journal of Sedimentary Research*, *53*(1), 147-157.

DeLaune, R. D., Jugsujinda, A., Peterson, G. W., & Patrick Jr, W. H. (2003). Impact of Mississippi River freshwater reintroduction on enhancing marsh accretionary processes in a Louisiana estuary. *Estuarine, Coastal and Shelf Science*, *58*(3), 653-662.

DeLaune, R. D., & White, J. R. (2012). Will coastal wetlands continue to sequester carbon in response to an increase in global sea level?: a case study of the rapidly subsiding Mississippi river deltaic plain. *Climatic Change*, *110*(1-2), 297-314.

DeLaune, R. D., Kongchum, M., White, J. R., & Jugsujinda, A. (2013). Freshwater diversions as an ecosystem management tool for maintaining soil organic matter accretion in coastal marshes. *Catena*, *107*, 139-144.

Deltares. (2013) Ch. 11: Sediment transport and morphology. In: Delft3D-FLOW – Simulation of multi-dimensional hydrodynamic flows and transport phenomena, including sediments – User Manual – Hydro-Morphodynamics, version 3.15.30059.

Dokka, R. K. (2006). Modern-day tectonic subsidence in coastal Louisiana. *Geology*, *34*(4), 281–284.

Donnelly, J. P., Hawkes, A. D., Lane, P., MacDonald, D., Shuman, B. N., Toomey, M. R., & Woodruff, J. D. (2015). Climate forcing of unprecedented intense-hurricane activity in the last 2000 years. *Earth's Future*, *3*(2), 49-65.

Esposito, C. R., Georgiou, I. Y., & Kolker, A. S. (2013). Hydrodynamic and geomorphic controls on mouth bar evolution. *Geophysical Research Letters*, *40*(8), 1540-1545.

Falloon, P. D., & Betts, R. A. (2006). The impact of climate change on global river flow in HadGEM1 simulations. *Atmospheric Science Letters*, *7*(3), 62-68.

Fisk, H. N. (1944). Geological investigations of the alluvial valley of the lower Mississippi River: US Army Corps of Engineers. *Mississippi River Commission, Vicksburg, Mississippi*.

Fisk, H. N. (1952). Geological investigation of the Atchafalaya Basin and the problem of Mississippi River diversion, Vol. 1. *US Corps of Engineers Waterways Experiment Station, Vicksburg, Mississippi*.

Gagliano, S.M., Culley, P., Earle, D.W., Jr., King, P., Latiolas, C., Light, P., & Rowland, A. (1973). Environmental Atlas and Multiuse Management Plan for South Central Louisiana. *Louisiana State University: Baton Rouge, LA, USA,*

Gagliano, S. M., Kwon, H. J., & Van Beek, J. L. (1970). Deterioration and restoration of coastal wetlands. *Coastal Engineering,* 1767-1781.

Gagliano, S. M., Meyer-Arendt, K. J., & Wicker, K. M. (1981). Land loss in the Mississippi River deltaic plain. *Gulf Coast Association of Geological Societies Transactions, 31*, 295-300.

Gaweesh, A., & Meselhe, E. (2016). Evaluation of sediment diversion design attributes and their impact on the capture efficiency. *Journal of Hydraulic Engineering*, *142*(5)

Georgiou, I.Y, McCorquodale, J.A., Neupani, J., Howes, N., Hughes, Z., FitzGerald, D.M., Schindler, J.K. (2010) Modeling the Hydrodynamics of diversion into Barataria Basin, Final report submitted to the Lake Pontchartrain Basin Foundation, Pontchartrain Institute for Environmental Sciences, University of New Orleans, New Orleans, LA, 102 pp.

Ghose Hajra, M., McCorquodale, A., Mattson, G., Jerolleman, D., and Filostrat, J. (2014). "Effects of salinity and particle concentration on sediment hydrodynamics and critical bed-shear-stress for erosion of fine grained sediments used in wetland restoration projects," Proceedings, Sediment Dynamics from the Summit to the Sea, ICCE/IAHS International Symposium, December 11-14, 2014, New Orleans, LA

Hiatt, M., & Passalacqua, P. (2015). Hydrological connectivity in river deltas: The first-order importance of channel-island exchange. *Water Resources Research*, *51*(4), 2264-2282.

Hiatt, M., & Passalacqua, P. (2017). What controls the transition from confined to unconfined flow? Analysis of hydraulics in a coastal river delta (Doctoral dissertation, American Society of Civil Engineers).

Horowitz, A. J. (2010). A quarter century of declining suspended sediment fluxes in the Mississippi River and the effect of the 1993 flood. *Hydrological Processes: An International Journal*, *24*(1), 13-34.

Horton, B. P., Rahmstorf, S., Engelhart, S. E., & Kemp, A. C. (2014). Expert assessment of sea-level rise by AD 2100 and AD 2300. *Quaternary Science Reviews*, *84*, 1-6.

Howes, N. C., FitzGerald, D. M., Hughes, Z. J., Georgiou, I. Y., Kulp, M. A., Miner, M. D., ... & Barras, J. A. (2010). Hurricane-induced failure of low salinity wetlands. *Proceedings of the National Academy of Sciences*, *107*(32), 14014-14019.

Kearney, M. S., Riter, J. A., & Turner, R. E. (2011). Freshwater river diversions for marsh restoration in Louisiana: Twenty-six years of changing vegetative cover and marsh area. *Geophysical Research Letters*, *38*(16).

Keogh, M. E., Kolker, A. S., Snedden, G. A., & Renfro, A. A. (2019). Hydrodynamic controls on sediment retention in an emerging diversion-fed delta. *Geomorphology*, *332*, 100-111.

Kesel, R. H. (1988). The decline in the suspended load of the lower Mississippi River and its influence on adjacent wetlands. *Environmental Geology and Water Sciences*, *11*(3), 271-281.

Khan, N. S., Horton, B. P., McKee, K. L., Jerolmack, D., Falcini, F., Enache, M. D., & Vane, C. H. (2013). Tracking sedimentation from the historic AD 2011 Mississippi River flood in the deltaic wetlands of Louisiana, USA. *Geology*, *41*(4), 391-394.

Kim, W., Mohrig, D., Twilley, R., Paola, C., & Parker, G. (2009). Is it feasible to build new land in the Mississippi River Delta?. *Eos, Transactions American Geophysical Union*, *90*(42), 373-374.

Knutson, T. R., McBride, J. L., Chan, J., Emanuel, K., Holland, G., Landsea, C., & Sugi, M. (2010). Tropical cyclones and climate change. *Nature geoscience*, *3*(3), 157-163.

Kolb, C. R., & Van Lopik, J. R. (1966). Depositional environments of the Mississippi River deltaic plain—southeastern Louisiana. *Deltas in Their Geologic Framework,* 17-61.

Kolker, A. S., Miner, M. D., & Weathers, H. D. (2012). Depositional dynamics in a river diversion receiving basin: The case of the West Bay Mississippi River Diversion. *Estuarine, Coastal and Shelf Science*, *106*, 1-12.

Lake Pontchartrain Basin Foundation. (2018). Hydrocoast Map – Salinity. Saveourlake.org.

Lane, R. R., Day, J. W., & Day, J. N. (2006). Wetland surface elevation, vertical accretion, and subsidence at three Louisiana estuaries receiving diverted Mississippi River water. *Wetlands*, *26*(4), 1130-1142.

Lane, R. R., Day Jr, J. W., Marx, B. D., Reyes, E., Hyfield, E., & Day, J. N. (2007). The effects of riverine discharge on temperature, salinity, suspended sediment and chlorophyll a in a Mississippi delta estuary measured using a flow-through system. *Estuarine, Coastal and Shelf Science*, *74*(1-2), 145-154.

Lacey, G. (1930). Stable Channels in Alluvium *Minutes of the Proceedings of the Institution of Civil Engineers* (Vol. 229, No. 1930, pp. 259-292). Thomas Telford-ICE Virtual Library.

Legates, D.R., & McCabe, G.J., Jr. (1999). Evaluating the use of "goodness-of-fit" measures in hydrologic and hydroclimatic model validation. Water Resources Research, 35(1), 233-241

Leonardi, N., Defne, Z., Ganju, N. K., & Fagherazzi, S. (2016). Salt marsh erosion rates and boundary features in a shallow Bay. *Journal of Geophysical Research: Earth Surface*, *121*(10), 1861-1875.

Lezina, B., & Barth, B. (2019, December). Mid-Barataria Sediment Diversion Modeling Data. *Coastal Protection and Restoration Authority Board Meeting.* Baton Rouge, LA.

Lopez, J.; Henkel, T.; Moshogianis, A.; Baker, A.; Boyd, E.; Hillman, E.; Batker, D. (2014a) Evolution of Mardi Grad Pass within the Bohemia Spillway of the Mississippi Delta in Southeast Louisiana: March 2012 through December 2013; Lake Pontchartrain Basin Foundation: New Orleans, LA, USA.

Lopez, J. & Henkel, T. & Moshogianis, A. & Baker, A. & Boyd, E. & Hillmann, Eva & Connor, P. & Baker, D.B.. (2014b). Examination of deltaic processes of Mississippi River outlets-Caernarvon Delta and Bohemia Spillway in Southeast Louisiana. *Gulf Coast Assoc. Geol. Sci. Trans, 64*, 707-708.

Louisiana Coastal Wetlands Conservation and Restoration Task Force and the Wetlands Conservation and Restoration Authority (LCWCRTF). (1998). Coast 2050: Toward a Sustainable Coastal Louisiana; Louisiana Department of Natural Resources: Baton Rouge, LA, USA.

McCorquodale, A., Couvillion, B., Dortch, Freeman, A., M., Meselhe, E., Reed, D., Roth, B., Shelden, J., Snedden, G., Wang, H., & White, E. (2017). 2017 Coastal Master Plan: Attachment C3-1: Sediment Distribution. Version Final. (pp. 1-56). Baton Rouge, Louisiana: Coastal Protection and Restoration Authority.

Meade, R. H., & Moody, J. A. (2010). Causes for the decline of suspended-sediment discharge in the Mississippi River system, 1940–2007. *Hydrological Processes: An International Journal*, *24*(1), 35-49.

Melillo, J.M.; Richmond, T.C.; Yohe, G.W. (2014). Climate Change Impacts in the United States: The Third National Climate Assessment. *U.S. Glob. Chang. Res. Program, 841*

Mendelsohn, R., Emanuel, K., Chonabayashi, S., & Bakkensen, L. (2012). The impact of climate change on global tropical cyclone damage. *Nature Climate Change*, *2*, 205.

Meselhe, E. A., Georgiou, I., Allison, M. A., & McCorquodale, J. A. (2012). Numerical modeling of hydrodynamics and sediment transport in lower Mississippi at a proposed delta building diversion. *Journal of Hydrology*, *472*, 340-354.

Meselhe E. A., & Rodrigue, M.D. (2013). Models Performance Assessment Metrics and Uncertainty Analysis. Final Report. Prepared for the Louisiana Coastal Protection and Restoration Authority.
Meselhe, E.A., Baustian, M.M., Allison, M.A. (2015). Basin-wide model development for the Louisiana Coastal Area Mississippi River hydrodynamic and delta management study. The Water Institute of the Gulf, Baton Rouge, Louisiana.

Meselhe, E. A., Sadid, K. M., & Allison, M. A. (2016). Riverside morphological response to pulsed sediment diversions. *Geomorphology*, *270*, 184-202.

Michener, W. K., Blood, E. R., Bildstein, K. L., Brinson, M. M. & Gardner, L. R. (1997), Climate Change, Hurricanes and Tropical Storms, and Rising Sea Level in Coastal Wetlands. *Ecological Applications, 7*, 770-801.

Mikeš, D., and Manning, A. (2010). Assessment of Flocculation Kinetics of Cohesive Sediments from the Seine and Gironde Estuaries, France, through Laboratory and Field Studies. Journal of Waterway, Port, Coastal and Ocean Engineering, 136(6), 306-318.

Morton, R. A., Buster, N. A., & Krohn, M. D. (2002). Subsidence controls on historical subsidence rates and associated wetland loss in southcentral Louisiana, *Gulf Coast Association of Geological Societies Transactions, 52*, 767-778

Morton, R., & Asbury H. Sallenger Jr. (2003). Morphological Impacts of Extreme Storms on Sandy Beaches and Barriers. *Journal of Coastal Research, 19*(3), 560-573.

Morton, R. A., Bernier, J. C., & Barras, J. A. (2006). Evidence of regional subsidence and associated interior wetland loss induced by hydrocarbon production, Gulf Coast region, USA. *Environmental Geology*, *50*(2), 261.

Mossa, J., & Roberts, H. H. (1990). Synergism of riverine and winter storm-related sediment transport processes in Louisiana's coastal wetlands. *Transactions of the Gulf Coast Association of Geological Societies, 40*, 635-642.

Nakaegawa, T., Kitoh, A., & Hosaka, M. (2013). Discharge of major global rivers in the late 21st century climate projected with the high horizontal resolution MRI-AGCMs. *Hydrological Processes*, *27*(23), 3301-3318.

Nicholls, R. J., Hoozemans, F. M., & Marchand, M. (1999). Increasing flood risk and wetland losses due to global sea-level rise: regional and global analyses. *Global Environmental Change*, *9*, S69-S87.

Nittrouer, J. A., Best, J. L., Brantley, C., Cash, R. W., Czapiga, M., Kumar, P., & Parker, G. (2012). Mitigating land loss in coastal Louisiana by controlled diversion of Mississippi River sand. *Nature Geoscience*, *5*(8), 534-537.

Nyman, J. A., DeLaune, R. D., & Patrick Jr, W. H. (1990). Wetland soil formation in the rapidly subsiding Mississippi River deltaic plain: Mineral and organic matter relationships. *Estuarine, Coastal and Shelf Science*, *31*(1), 57-69.

Nyman, J., DeLaune, R., Roberts, H., & Patrick, W. (1993). Relationship between vegetation and soil formation in a rapidly submerging coastal marsh. *Marine Ecology Progress Series, 96*(3), 269-279.

Pandoe, W. W., and Edge, B. L. (2008). Case Study for a Cohesive Sediment Transport Model for Matagorda Bay, Texas, with Coupled ADCIRC 2D-Transport and SWAN Wave Models. Journal of Hydraulic Engineering, 134(3), 303-314.

Paola, C., Twilley, R. R., Edmonds, D. A., Kim, W., Mohrig, D., Parker, G., & Voller, V. R. (2011). Natural processes in delta restoration: Application to the Mississippi Delta. *Annual review of marine science*, *3*, 67-91.

Parker, G., & Sequeiros, O. (2006). Large scale river morphodynamics: Application to the Mississippi Delta. In *River Flow 2006: Proceedings of the International Conference on Fluvial Hydraulics* (pp. 3-11). London: Taylor and Francis.

Penland, S., Boyd, R., & Suter, J. R. (1988). Transgressive depositional systems of the Mississippi Delta plain; a model for barrier shoreline and shelf sand development. *Journal of Sedimentary Research*, *58*(6), 932-949.

Penland, S., Connor, P., Beall, A., Fearnley, S., & Williams, S. (2005). Changes in Louisiana's Shoreline: 1855–2002. *Journal of Coastal Research,* 7-39.

Penland, S., & Ramsey, K. E. (1990). Relative sea-level rise in Louisiana and the Gulf of Mexico: 1908-1988. *Journal of Coastal Research*, 323-342.

Peyronnin, N., Caffey, R., Cowan, J., Justic, D., Kolker, A., Laska, S., & Visser, J. (2017). Optimizing sediment diversion operations: working group recommendations for integrating complex ecological and social landscape interactions. *Water*, *9*(6), 368.

Plitsch, E. (2017). 2016 Operations, Maintenance, and Monitoring Report for West Bay Sediment Diversion (MR-03), Coastal Protection and Restoration Authority of Louisiana, New Orleans, Louisiana.

Ramirez, M. T., & Allison, M. A. (2013). Suspension of bed material over sand bars in the Lower Mississippi River and its implications for Mississippi delta environmental restoration. *Journal of Geophysical Research: Earth Surface*, *118*(2), 1085-1104.

Reed, D. J. (2002). Sea-level rise and coastal marsh sustainability: geological and ecological factors in the Mississippi delta plain. *Geomorphology*, *48*(1-3), 233-243.

Rivera-Monroy, V. H., Branoff, B., Meselhe, E., McCorquodale, A., Dortch, M., Steyer, G. D., & Wang, H. (2013). Landscape-level estimation of nitrogen removal in coastal Louisiana

wetlands: Potential sinks under different restoration scenarios. *Journal of Coastal Research*, *67*(sp1), 75-87.

Roberts, H. H., Adams, R. D., & Cunningham, R. H. W. (1980). Evolution of sand-dominant subaerial phase, Atchafalaya Delta, Louisiana. *AAPG Bulletin*, *64*(2), 264-279.

Roberts, H. H. (1997). Dynamic changes of the Holocene Mississippi River delta plain: the delta cycle. *Journal of Coastal Research*, 605-627.

Roberts, H. H. (1998). Delta switching: early responses to the Atchafalaya River diversion. *Journal of Coastal Research*, *14*(3).

Russell, R. J. (1936). *Physiography of lower Mississippi River delta*. Louisiana Geological Survey

Russell, R. J. (1939). Louisiana stream patterns. *AAPG Bulletin*, *23*(8), 1199-1227.

Russell, R. J. (1940). Quaternary history of Louisiana. *Bulletin of the Geological Society of America*, *51*(8), 1199-1233.

Sadid, K., Messina, F., Jung, H., Yuill, B., & Meselhe, E. (2018). TO51: Basinwide Model Version 3 - Basinwide Model for Mid-Breton Sediment Diversion Modeling. Baton Rouge, LA: The Water Institute of the Gulf. Funded by the Coastal Protection and Restoration Authority under Task Orders 51.

Sha, X., Xu, K., Bentley, S. J., & Robichaux, P. A. (2018). Characterization and modeling of sediment settling, consolidation, and suspension to optimize coastal Louisiana restoration. *Estuarine, Coastal and Shelf Science*, *203*, 137-147.

Shaw, J. B., Mohrig, D., & Whitman, S. K. (2013). The morphology and evolution of channels on the Wax Lake Delta, Louisiana, USA. *Journal of Geophysical Research: Earth Surface*, *118*(3), 1562-1584.

Shaw, J. B., & Mohrig, D. (2014). The importance of erosion in distributary channel network growth, Wax Lake Delta, Louisiana, USA. *Geology*, *42*(1), 31-34.

Shaw, J. B., Mohrig, D., & Wagner, R. W. (2016). Flow patterns and morphology of a prograding river delta. *Journal of Geophysical Research: Earth Surface*, *121*(2), 372-391.

Simas, T., Nunes, J. P., & Ferreira, J. G. (2001). Effects of global climate change on coastal salt marshes. *Ecological Modelling*, *139*(1), 1-15.

Smith, J. E., Bentley, S. J., Snedden, G. A., & White, C. (2015). What role do hurricanes play in sediment delivery to subsiding river deltas?. *Scientific reports*, *5*(1), 1-8.

Snedden, G. A., Cable, J. E., Swarzenski, C., & Swenson, E. (2007). Sediment discharge into a subsiding Louisiana deltaic estuary through a Mississippi River diversion. *Estuarine, Coastal and Shelf Science*, *71*(1-2), 181-193.

Snedden, G. A., & Steyer, G. D. (2013). Predictive occurrence models for coastal wetland plant communities: Delineating hydrologic response surfaces with multinomial logistic regression. *Estuarine, Coastal and Shelf Science*, *118*, 11-23.

Syvitski, J. P., Kettner, A. J., Correggiari, A., & Nelson, B. W. (2005). Distributary channels and their impact on sediment dispersal. *Marine Geology*, *222*, 75-94.

Tao, B., Tian, H., Ren, W., Yang, J., Yang, Q., He, R., & Lohrenz, S. (2014). Increasing Mississippi river discharge throughout the 21st century influenced by changes in climate, land use, and atmospheric CO2. *Geophysical Research Letters*, *41*(14), 4978-4986.

Teal, J. M., Best, R., Caffrey, J., Hopkinson, C. S., McKee, K. L., Morris, J. T., & Orem, B. (2012). Mississippi River freshwater diversions in Southern Louisiana: effects on wetland vegetation, soils, and elevation. *Final report to the state of Louisiana and the US army corps of engineers through the Louisiana coastal area science & technology program*.

Ian L. Turner, Bruce P. Coates, & R. Ian Acworth. (1997). Tides, Waves and the Super-elevation of Groundwater at the Coast. *Journal of Coastal Research, 13*(1), 46-60.

Turner, R. E. (1997). Wetland loss in the northern Gulf of Mexico: multiple working hypotheses. *Estuaries*, *20*(1), 1-13.

Turner, R. E., Swenson, E. M., & Milan, C. S. (2002). Organic and inorganic contributions to vertical accretion in salt marsh sediments. *Concepts and controversies in tidal marsh ecology* 583-595.

Turner, R. E., Layne, M., Mo, Y., & Swenson, E. M. (2019). Net land gain or loss for two Mississippi River diversions: Caernarvon and Davis Pond. *Restoration Ecology*, *27*(6), 1231-1240.

Van Wijnen, H. J., & Bakker, J. P. (2001). Long-term surface elevation change in salt marshes: a prediction of marsh response to future sea-level rise. *Estuarine, Coastal and Shelf Science*, *52*(3), 381-390.

Viparelli, E., Shaw, J., Bevington, A., Meselhe, E., Holm, G. O., Mohrig, D., & Parker, G. (2011). Inundation model as an aid for predicting ecological succession on newly-created deltaic land associated with Mississippi River diversions: Application to the Wax Lake delta. *World Environmental and Water Resources Congress 2011: Bearing Knowledge for Sustainability*. 2340-2349.

Visser, J. M. (1989). The impact of vertebrate herbivores on primary production of Sagittaria marshes in the Wax Lake Delta, Atchafalaya Bay, Louisiana. LSU Historical Dissertations and Theses. 4816.

Visser, J. M., & Sandy, E. R. (2009). The effects of flooding on four common Louisiana marsh plants. *Gulf of Mexico Science*, *27*(1), 3.

Vörösmarty, C. J., & Meybeck, M. (2004). Responses of continental aquatic systems at the global scale: new paradigms, new methods. *Vegetation, water, humans and the climate*, 375-413.

Walker, H. J., Coleman, J. M., Roberts, H. H., & Tye, R. S. (1987). Wetland loss in Louisiana. *Geografiska Annaler: Series A, Physical Geography*, *69*(1), 189-200.

Wang, H., Steyer, G. D., Couvillion, B. R., Rybczyk, J. M., Beck, H. J., Sleavin, W. J., & Rivera-Monroy, V. H. (2014). Forecasting landscape effects of Mississippi River diversions on elevation and accretion in Louisiana deltaic wetlands under future environmental uncertainty scenarios. *Estuarine, Coastal and Shelf Science*, *138*, 57-68.

Wellner, R., Beaubouef, R., Van Wagoner, J., Roberts, H., & Sun, T. (2005). Jet-plume depositional bodies—the primary building blocks of Wax Lake Delta. *Gulf Coast Assoc. Geol. Soc. Trans., 55*, 867–909.

Wells, J. T., & Coleman, J. M. (1987). Wetland loss and the subdelta life cycle. *Estuarine, Coastal and Shelf Science*, *25*(1), 111-125.

Wilson, C. A., & Allison, M. A. (2008). An equilibrium profile model for retreating marsh shorelines in southeast Louisiana. *Estuarine, Coastal and Shelf Science*, *80*(4), 483-494.

Wolanski, E., & Gibbs, R. J. (1995). Flocculation of suspended sediment in the Fly River estuary, Papua New Guinea. *Journal of Coastal Research*, 754-762.

Wright, L. D. (1977). Sediment transport and deposition at river mouths: a synthesis. *Geological Society of America Bulletin*, *88*(6), 857-868.

Xu, K., Bentley, S. J., Robichaux, P., Sha, X., & Yang, H. (2016). Implications of texture and erodibility for sediment retention in receiving basins of coastal Louisiana diversions. *Water*, *8*(1), 26.

Young, B. M., & Harvey, E. L. (1996). A spatial analysis of the relationship between mangrove (Avicennia marinavar. australasica) physiognomy and sediment accretion in the Hauraki Plains, New Zealand. *Estuarine, Coastal and Shelf Science*, *42*(2), 231-246.

Yuill, B. T., Khadka, A. K., Pereira, J., Allison, M. A., & Meselhe, E. A. (2016). Morphodynamics of the erosional phase of crevasse-splay evolution and implications for river sediment diversion function. *Geomorphology*, *259*, 12-29.

Zwiers F.W. et al. (2013) Climate Extremes: Challenges in Estimating and Understanding Recent Changes in the Frequency and Intensity of Extreme Climate and Weather Events. In: Asrar G., Hurrell J. (eds) Climate Science for Serving Society. Springer, Dordrecht

Appendix A

MDF File Example

```
Ident  = #Delft3D-FLOW 3.56.29165#
Commnt =
Runtxt = #2018 River Operation#
Filcco = #nola_30m_extendedgrid.grd#
Anglat =  2.9000000e+001
Grdang =  0.0000000e+000
Filgrd = #nola_30m.enc#
MNKmax = 562 902 1
Thick  =  1.0000000e+002
Commnt =
Fildep = #nola latest_30m resolutiondiversion_onecell_SalvadorAdd.dep#
Commnt =
Commnt =              no. dry points: 0
Commnt =              no. thin dams: 2
Filtd  = #Diversion.thd#
Commnt =
Itdate = #2018-02-01#
Tunit  = #M#
Tstart =  0.0000000e+000
Tstop  =  2.1594000e+005
Dt     = 1
Tzone  = 0
Commnt =
Sub1   = #S W #
Sub2   = # C #
Namc1  = #SedimentSand       #
Namc2  = #SedimentSilt       #
Namc3  = #SedimentClay       #
Commnt =
Wnsvwp = #N#
Filwnd = #Wind2018.wnd#
Wndint = #Y#
Commnt =
Commnt =              initial conditions from initial conditions file
Filic  = #initialwithsed2018.ini#
Commnt =
Commnt =              no. open boundaries: 2
Filbnd = #DiversionOpen.bnd#
FilbcT = #Diversion2018.bct#
FilbcC = #Final.bcc#
Rettis =  0.0000000e+000
```

0.0000000e+000
Rettib = 0.0000000e+000
0.0000000e+000
Commnt =
Ag = 9.8100000e+000
Rhow = 1.0000000e+003
Tempw = 1.5000000e+001
Salw = 3.1000000e+001
Wstres = 6.3000000e-004 0.0000000e+000 7.2300000e-003 1.0000000e+002 7.2300000e-003 1.0000000e+002
Rhoa = 1.0000000e+000
Betac = 5.0000000e-001
Equili = #N#
Ktemp = 0
Fclou = 0.0000000e+000
Sarea = 0.0000000e+000
Temint = #Y#
Commnt =
Roumet = #M#
Filrgh = #roughness_marsh_edge_bed2.rgh#
Xlo = 0.0000000e+000
Vicouv = 1.0000000e+000
Dicouv = 6.0000000e+001
Htur2d = #N#
Irov = 0
Filsed = #testingsand.sed#
Filmor = #InitialMor.mor#
Commnt =
Iter = 2
Dryflp = #YES#
Dpsopt = #MAX#
Dpuopt = #MOR#
Dryflc = 1.0000000e-001
Dco = -9.9900000e+002
Tlfsmo = 6.0000000e+001
ThetQH = 0.0000000e+000
Forfuv = #Y#
Forfww = #Y#
Sigcor = #N#
Trasol = #Cyclic-method#
Momsol = #Cyclic#
Commnt =
Commnt = no. discharges: 0
Commnt = no. observation points: 11
Filsta = #Calibrationpoints.obs#
Commnt = no. drogues: 0

```
Commnt =
Commnt =
Commnt =                no. cross sections: 0
Commnt =
SMhydr = #YYYYY#
SMderv = #YYYYYY#
SMproc = #YYYYYYYYYY#
PMhydr = #YYYYYY#
PMderv = #YYY#
PMproc = #YYYYYYYYYY#
SHhydr = #YYYY#
SHderv = #YYYYY#
SHproc = #YYYYYYYYYY#
SHflux = #YYYY#
PHhydr = #YYYYYY#
PHderv = #YYY#
PHproc = #YYYYYYYYYY#
PHflux = #YYYY#
Flmap  =  0.0000000e+000 1440  2.1594000e+005
Flhis  =  0.0000000e+000 60  2.1594000e+005
Flpp   =  0.0000000e+000 60  2.1594000e+005
Flrst  = 1440
Commnt =
Online = #N#
BdfMor = #Y#
BdfH   = #vanrijn84#
BdfEps = 1
BdfL   = #vanrijn84#
BdfRou = #vanrijn84#
BdfOut = #Y#
Commnt =
```

Vita

Dylan Blaskey was born and raised in Madison, Wisconsin. He obtained his Bachelor's degree in Bioproducts and Biosystems Engineering from the University of Minnesota in 2015. He joined the University of New Orleans Civil and Environmental Engineering department to study solutions to the coastal land loss issues of southern Louisiana.